STABILITY INVESTIGATION OF ETI COPPER MINE TAILINGS DAM USING FINITE ELEMENT ANALYSIS

A THESIS SUBMITTED TO
THE GRADUATE SCHOOL OF APPLIED AND NATURAL SCIENCES
OF
MIDDLE EAST TECHNICAL UNIVERSITY

BY

ESRA NUR TANRISEVEN

IN PARTIAL FULFILLMENT OF THE REQUIREMENTS
FOR
THE DEGREE OF MASTER OF SCIENCE
IN
MINING ENGINEERING

SEPTEMBER 2012

Approval of the thesis:

STABILITY INVESTIGATION OF ETI COPPER MINE TAILINGS DAM USING FINITE ELEMENT ANALYSIS

submitted by **ESRA NUR TANRISEVEN** in partial fulfillment of the requirements for the degree of **Master of Science in Mining Engineering Department, Middle East Technical University** by,

Prof. Dr. Canan Özgen _____
Dean, Graduate School of **Natural and Applied Sciences**

Prof. Dr. Ali İhsan Arol _____
Head of Department, **Mining Engineering**

Assoc. Prof. Dr. Hasan Aydın Bilgin
Supervisor, **Mining Engineering Dept., METU** _____

Prof. Dr. H. Şebnem Düzgün
Co-Supervisor, **Mining Engineering Dept., METU** _____

Examining Committee Members:

Prof. Dr. Nurkan Karahanoğlu _____
Geological Engineering Dept., METU

Assoc. Prof. Dr. Hasan Aydın Bilgin _____
Mining Engineering Dept., METU

Prof. Dr. H. Şebnem Düzgün _____
Mining Engineering Dept., METU

Prof. Dr. Bahtiyar Ünver _____
Mining Engineering Dept., Hacettepe University

Asisst. Prof. Dr. Nejan Huvaj Sarıhan _____
Civil Engineering Dept., METU

Date: 14.09.2012

I hereby declare that all information in this document has been obtained and presented in accordance with academic rules and ethical conduct. I also declare that, as required by these rules and conduct, I have fully cited and referenced all material and results that are not original to this work.

Name, Last Name: Esra Nur Tanrıseven

Signature :

ABSTRACT

STABILITY INVESTIGATION OF ETI COPPER MINE TAILINGS DAM USING FINITE ELEMENT ANALYSIS

TANRISEVEN, Esra Nur
M.Sc., Department of Mining Engineering
Supervisor: Assoc. Prof. Dr. Hasan Aydın Bilgin

September 2012, 109 pages

In mining industry, waste storage is a very prominent issue; in this respect, safety of storage structures is one of the leading problems in the industry. Most of the tailings dams require remedial measures, throughout their lifespan to increase their reliability. The objective of the study is to investigate stability problems of formerly constructed but newly raised Eti Copper Mine tailings dam and alternative dam geometries for future raises. Plenty of methods were developed to analyze the reliability of structures; limit equilibrium methods, finite element methods and finite difference methods are among them. In this case, stability of the dam was analyzed with finite element method under static loading conditions. In order to determine input parameters properly, disturbed samples obtained at the field investigations were used. For this purpose, several laboratory experiments were conducted to determine natural moisture content, grain size distribution, specific gravity, Atterberg limits, maximum dry density and shear strength parameters of tailings and embankment material.

Keywords: Tailings Dam, Dam Stability, Computer Aided Design, Finite Element Analysis

ÖZ

SONLU ELEMANLAR ANALİZİ İLE ETİ BAKIR MADENİ ATIK BARAJININ STABİLİTESİNİN DEĞERLENDİRİLMESİ

TANRISEVEN, Esra Nur
Yüksek Lisans, Maden Mühendisliği Bölümü
Tez Yöneticisi: Doç. Dr. Hasan Aydın Bilgin

Eylül 2012, 109 sayfa

Madencilik endüstrisinde atık depolama çok önemli bir konudur, bu bağlamda depolama yapılarının güvenliği endüstride önde gelen sorunlardandır. Güvenilirliliğini arttırmak için, kullanım süreleri boyunca pek çok atık barajının iyileştirici önlemlere ihtiyacı olmaktadır. Bu çalışma önceden inşa edilmiş son zamanlarda yükseltilmiş olan Eti Bakır madeni atık barajının şu andaki halinin ve ileride yapılacak yükseltmeler için üretilmiş seçeneklerin stabilite problemlerini incelemek amacıyla yapılmıştır. Yapıların güvenliğini analiz etmek için pek çok yöntem geliştirilmiştir, limit-denge, sonlu elemanlar ve sonlu farklar analiz yöntemleri bunlar arasındadır. Bu vakada barajın duraylılığı sonlu elemanlar yöntemiyle statik koşullar altında analiz edilmiştir. Modelin girdi parametrelerini uygun bir şekilde belirlenmek amacıyla, saha çalışmalarının sonucunda elde edilmiş örselenmiş örnekler kullanılmştır. Bu amaçla çeşitli laboratuvar deneyleri yapılarak atık malzemesi ve baraj malzemesi için doğal nem içeriği, tane boyu dağılımı, özgül ağırlık, atterberg limitleri, maksimum kuru birim hacim ağırlık ve makaslama dayanımı parametreleri belirlenmiştir.

Anahtar Kelimeler: Atık Barajı, Baraj duraylılığı, Bilgisayar-Destekli Tasarım, Sonlu Elemanlar Analizi

To My Family…

ACKNOWLEDGEMENTS

First of all, I would like to express my sincere appreciation and gratitude to my supervisor dear Assoc. Prof. Dr. H. Aydın Bilgin and co-advisor Prof. Dr. Şebnem Düzgün for their invaluable supervision, kind support, and continuous guidance in preparation of this thesis. I also present my special thanks to the examining committee members, Prof. Dr. Nurkan Karahanoğlu, Prof. Dr. Bahtiyar Ünver, Assist. Prof. Dr. Nejan Huvaj Sarıhan for serving on the M.Sc. thesis committee.

I must offer acknowledgement to Ulaş Nacar, Kamber Bölgen, Ali Bal in METU Soil Mechanics Laboratory and Hakan Uysal in Rock Mechanics Laboratory for their help and invaluable guidance. Most of all I feel thankful for Birol Fidan who provided vehicles at the sampling stage.

I would also like to thank to my friends and colleagues for their support and help, Ahmet Güneş Yardımcı, Doğukan Güner, Hilal Soydan, Onur Gölbaşı, Başar Mutlu, Hakkı Ketizmen, Ömer Erdem, Mustafa Çırak, Deniz Tuncay, Oğuzhan Tanrıseven, Burak Yurt, Ahmet Kenan Yurt.

Finally, I feel grateful to my family and I want to dedicate this dissertation to my family and my husband. Most of all, I would like to express my sincere gratitude to my mother Günsel Gayretli, my father Ahmet Gayretli, my sisters Büşra and Nisa Gayretli, and my husband Bilgehan Tanrıseven for their enduring love, unconditional support and encouragement, which have been the real inspiration during my studies.

TABLE OF CONTENTS

LIST OF TABLES

TABLES

LIST OF FIGURES

FIGURES

NOMENCLATURE

ASTM	**:**	American Society for Testing and Minerals
c	**:**	Cohesion (kPa)
$\mathbf{G_s}$	**:**	Specific Gravity
LL	**:**	Liquid Limit
PI	**:**	Plasticity Index
PL	**:**	Plastic Limit
UCS	**:**	Uniaxial Compressive Strength (kPa)
$\emptyset$	**:**	Internal Friction Angle
γ	**:**	Unit Weight
$\mathbf{W_c}$	**:**	Water Content
$\gamma_{d,max}$	**:**	Maximum Dry Unit Weight (kN/m^3)
$\mathbf{W_{opt}}$	**:**	Optimum Water Content
ρ	**:**	Density
ψ	**:**	Angle of Dilation
SSR	**:**	Shear Strength Reduction
SRF	**:**	Strength Reduction Factor
FEM	**:**	Finite Element Method
SF	**:**	Safety Factor
E	**:**	Modulus of Elasticity
υ	**:**	Poisson's ratio

CHAPTER 1

INTRODUCTION

1.1 General Remarks

Most of the mining activities, particularly activities of metallic ores, collect the waste materials in dams in order to diminish its adverse effects on the environment. Dams contain tailings with high water content. Tailings dams have two main purposes; these are to provide a large volume to store vast amounts of waste material and to provide an area where the waste material is compacted (Oyanguren et al., 2008). Their stability and safety is essential for sustainability of the mine environment and natural resources near the mine. In order to maintain sustainability of the dam, stability analysis and regular monitoring are necessary.

1.2 Statement of the Problem

Tailings dams are exposed to a number of external actions caused by their operation and interaction with tailings, foundation and atmosphere. Stability of tailings dams during the operation and after the closure of the mine is very important in terms of environmental aspects.

Rico et al. (2008) declared that, a series of characteristics make tailings dam more vulnerable to failure than water storage dams, namely: "(1) use of locally derived fills (soil, coarse waste, overburden and tailings) for the construction of the embankment; (2) multi-stage raising of dam to deal with the increase in stored material volume; (3) deficiency for policies on specific design criteria; (4) need for continuous monitoring and control during construction and operation of the dam; (5) the high remediation cost following the closure of the mine."

The dam experienced piping through embankment, because of heavy rain on July, 2009. Thus, increasing water level affects the stability of the dam. Effect of slope geometry, changing water level and slime-sand boundary on the stability is the main problem. Changing water level and wrong estimation of slime-sand boundary may result in failures.

1.3 Objectives and Scope of the Study

The main objectives of the research study presented in this thesis are:

1. To determine the material properties of dam-foundation-slurry system by laboratory tests for Eti copper mine tailings dam,
2. To determine the location of phreatic surface within the dam
3. To examine the long-term stability of the dam under static loading conditions with PHASE 2 v.8.01,
4. To analyze the long-term stability of alternative geometries for future raises of tailings dam under static loading conditions with PHASE 2 v.8.01.

1.4 Research Methodology

In order to accomplish the objectives, the following approach was adopted:

1. A literature survey was performed to understand the associated aspects such as; geotechnical properties of tailings, embankment, foundation material, construction methods of tailings dams, failure modes of tailings dams, pore pressures that develop during construction stage of a tailings embankment, conditions of stability analysis for tailings embankments, choice of a numerical tool for stability analysis.
2. The finite element program PHASE 2 v.8.01 was utilized as a numerical modeling tool for stability analysis of the tailings dam.
3. The Eti Copper Mine tailings dam (located in Kastamonu) was studied as a case study; because of data availability.
4. Representative samples of soil materials were taken from dam body and slurry, and rock material were obtained from host rock. Laboratory experiments were performed on selected samples to determine engineering properties of the materials. Design values for finite element modeling were chosen from the test results.

5. The slope stability of the dam was analyzed with a two-dimensional finite element program PHASE 2 v.8.01.
6. The factor of safety was computed for possible field loading conditions using finite element method. The calculated factor of safety values were compared to approved safe design values. According to recommendations of Swedish tailings dams' safety guidelines document GruvRIDAS (2007) and U.S. Army Corps. of Engineers (2003), a safety factor of approximately 1.5 is required to be maintained for a safe slope.
7. Results have been discussed and conclusions have been drawn in the conclusions and recommendations part.

1.5 Outline of the Thesis

This thesis consists of the following parts:

1. Method of construction of tailings dams, failure modes of tailings dams, design considerations for long term stability of tailings dams, previous studies are given in chapter 2.
2. Generel information about the study area is given in chapter 3.
3. Determination of mechanical properties of foundation, tailings and dam body material is presented in chapter 4.
4. The Eti copper mine tailings dam was modeled with PHASE 2 v.8.01 finite element program. Stability analysis that was conducted both on the present condition of the dam and alternative dam geometries for future increases are given in chapter 5.
5. Conclusions and recommendations are presented in chapter 6.

CHAPTER 2

LITERATURE SURVEY

2.1 Introduction

In this chapter the following subjects are clarified, these are; types of tailings dams, construction methods, stability analysis, failure modes and a short summary of previous studies related to this topic.

2.2 Types of Tailings Dams

In this section mostly "U.S. Environmental Protection Agency (1994) was used as source. There are two main types of structures, which are used to keep tailings in impoundments, the embankment and the retention dams. Embankments are more widespread than retention dams. Retention dams (Figure 2.1) are constructed at full height at the start while embankments are builded in stages as the need for additional capacity emerges (U.S. Environmental Protection Agency, 1994). There are four main types of impoundments; these are valley, ring-dike, specially dug pit and in-pit. The selection of impoundment type mainly depends on site conditions, topography and economic considerations. Most of the tailings dams are in the form of the valley type.

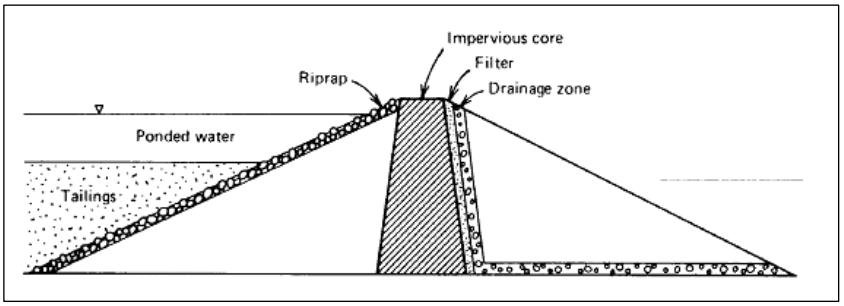

Figure 2.1 Retention Type Dam (Vick, 1990)

2.2.1 Valley Type Impoundment

This type of embankments are economically favourable, since it make use of natural indentations to retain tailings. Another advantage is the reduced dam size, because of the utilization of sides of valley or other depression to enclose tailings. Moreover, tailings in valley type dams reveal less relief for air dispersion. All these advantages make this type of dams the most commonly used one. According to topographical properties of selected valley, the dam body can be constructed perpendicular, parallel or both perpendicular and parallel to valley base declination direction (U.S. Environmental Protection Agency, 1994). Valley type dams could be in single or multiple form in accordance with required reservoir volume. In multiple form, a series of connected embankments contain the tailings.

Valley type dams have several variations. The cross-valley type is the most commonly used one because of its applicability to nearly any topographical depression in single or multiple form (U.S. Environmental Protection Agency, 1994). Dam is builded by joining two valley walls, constraining the tailings in the valley. This arrangement requires the least fill material. Figure 2.2 indicates single and multiple cross-valley dam configurations.

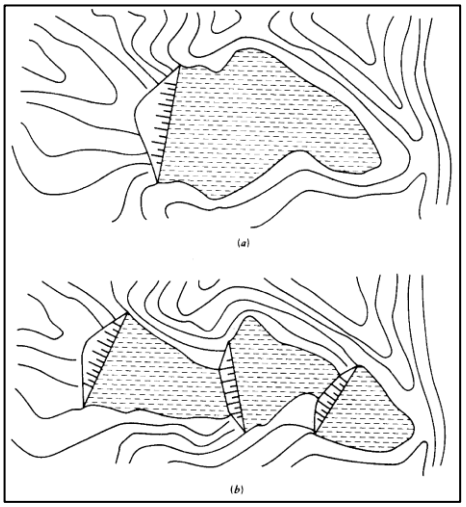

Figure 2.2 Single (a) and Multiple (b) Cross-Valley Dam Types (Vick, 1990)

There are two variations of this type, namely, the side-hill dam and the valley-bottom dam. These variations may be applied, if there is lack of essential valley topography or there is extremely large drainage basin (U.S. Environmental Protection Agency, 1994). The side hill design is a three sided dam builded against a hillside (Figure 2.3). This layout is favourable for hillsides with a grade less than 10%. The valley-bottom dam (Figure 2.4) is a combination of cross-valley and side-hill layouts. The valley-bottom design is employed, when drainage basin is too large for cross-valley type and the slope of the field is too steep for side-hill type.

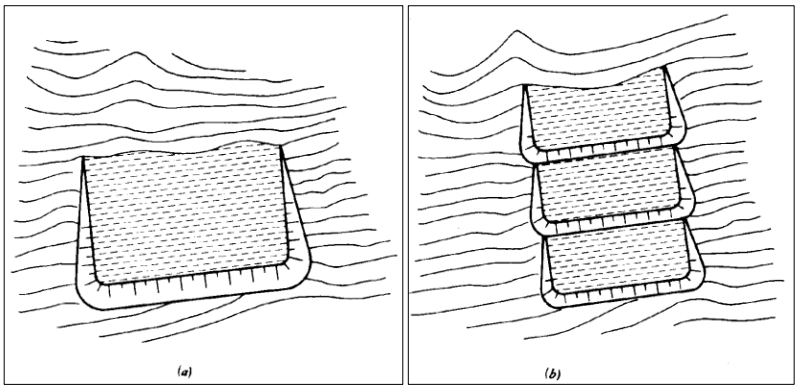

Figure 2.3 Single (a) and Multiple (b) Side-Hill Dams (Vick, 1990)

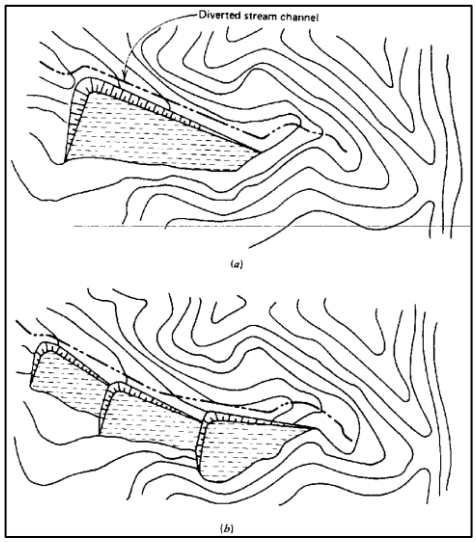

Figure 2.4 Single (a) and Multiple (b) Valley-Bottom Dams (Vick, 1990)

The valley type dams are susceptible to overtopping by flooding, erosion at the intersection of the dam and valley walls, and liquefaction because of precipitation runoff and excessive surface water inflow from drainage basin (U.S. Environmental Protection Agency, 1994).

The durability of a valley dam generally depends on hydrostatic pressure level within embankment. An abnormal, sudden rise in the hydrostatic pressure beyond design levels may generate a failure (U.S. Environmental Protection Agency, 1994). For the sustainability of the structure, inflow control is an important factor. Sufficient internal drainage improve the stability of the structure against liquefaction and increase the consolidation of tailings.

2.2.2 Ring-Dike Type Impoundment

The ring-dike layout could be convenient, when topographic depressions are unavailable. The configuration can be constructed in single or multiple forms (Figure 2.5). This type of dam layout needs large amount of fill material for construction, because it requires fill on all sides (U.S. Environmental Protection Agency, 1994).

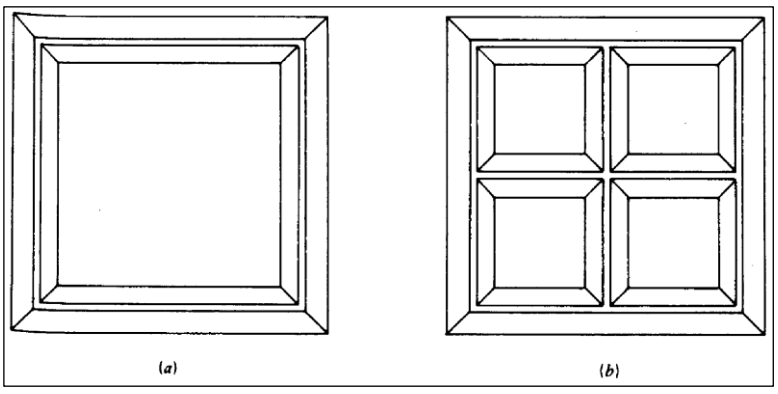

Figure 2.5 Single (a) and Multiple (b) Ring-Dike Dam Configurations (Vick, 1990)

Also this design is generaly simpler than valley dam design, because of the low height of dikes. The regular geometry of this type facilitates the usage of liners. Ring-dike type

dams give better water control rather than valley type dams, which are located in a drainage basin (U.S. Environmental Protection Agency, 1994). Reduced surface runoff and flood impacts, results in smaller dam and less complicated water control precautions. It can be concluded that ring-dike configuration gives a better seepage control than most of other layouts (U.S. Environmental Protection Agency, 1994).

Besides its advantages, this type has also some drawbacks. First of all, it is hard to find a flat terrain for the construction, and increased length of the embankment walls increases failure possibility (U.S. Environmental Protection Agency, 1994). Other disadvantages are high construction cost and considerable wind erosion of the tailings. Figure 2.6 shows a ring-dike type impoundment.

Figure 2.6 Ring-dike type impoundment (Steiner, 2006)

2.2.3 Specially Dug Pit Type Impoundment

For this type impoundments a pit is excavated specifically for tailings disposal. This type composed of four or more cells with impermeable liners. The material dug out from pit is used for dam construction (U.S. Environmental Protection Agency, 1994). This dam design possesses some of the same advantages with ring-dike design.

2.2.4 In-pit Type Impoundment

This method is less widespread than ring-dike and valley configurations. The tailings materials is disposed into a previously mined out pit, therefore construction cost is eliminated (Figure 2.7). Impermeable pit walls eliminates most of the failure causes, such as piping and liquefaction, however pit slope stability has to be checked (U.S. Environmental Protection Agency, 1994).

Figure 2.7 The El Valle tailings impoundment (Spain) at startup of tailings disposal operations (In pit type tailings impoundment) (Breitenbach, 2010)

2.3 Tailings Dam Construction Methods

Dams that are constructed of earth and rock materials are commonly known as fill-type dams or embankment dams. Narita (2000) stated that, there are two major features for the embankment dam construction.

"1. Precise conditions are not necessitated for the foundation of embankment dams. Embankment dams can be constructed as well on the pervious foundations and alluvial deposit, whereas hard rock foundation is necessary for concrete dams.

2. Construction of embankment dams is more economical than concrete dams, since they can be constructed in the city border and construction materials can be supplied near the dam site."

Embankment dams can be constructed using upstream, downstream or centerline methods. Each of the structures are constructed successively, subsequent stages of the dam are formed on the previous one. Because the small quantity of construction material is needed at one time, the choices available for construction material are a lot. For instance; tailings, waste rock and natural soil can be used for construction in any combination whereas retention dams are generally constructed of natural soil (Vick, 1990).

2.3.1 Upstream Method

Upstream method of construction is the most widely used and economical method. The construction starts with a starter dike at the downstream toe (Figure 2.8). Tailings material is discharged from the crest peripherally by using spigots or cyclones (U.S. Environmental Protection Agency, 1994). As a result, accumulation of tailings composes a dike and beach area. The beach becomes the foundation of the following dike. In some cases, the dikes are constructed and the discharge is used to form the beach and to reduce the permeability of the upstream face. Dikes may be built with either borrow fill, or with beach tailings excavated from the beach (U.S. Environmental Protection Agency, 1994). Before moving on to the next stage, compaction is conducted on the constructed dike.

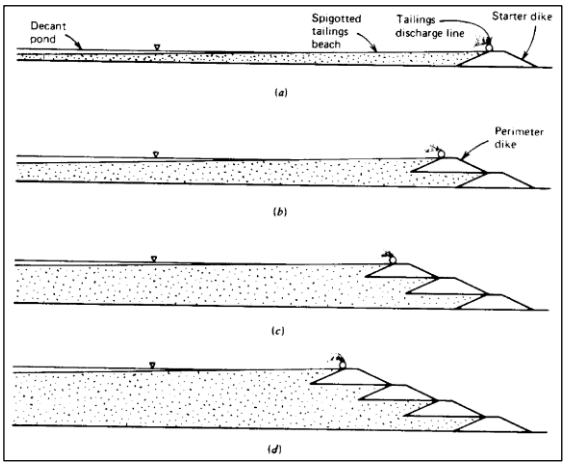

Figure 2.8 Upstream embankment construction (Vick, 1990)

The only criteria for the application of upstream method of construction is that the tailings accumulation must constitute a stiff foundation for the next dike. Vick (1990) stated a general rule for upstream construction method, the tailings should contain sand between 40-60%. Thus, upstream method can not be used for tailings with very low sand content. Brawner et al (1973), stated that, "If a tractor can not be operated on the first 100 to 200 ft of beach, the grind is too fine for upstream construction methods."

Besides particle size distribution, phreatic surface level, storage capacity, liquefaction susceptibility and dam raising rate also limits the applicability of upstream method (U.S. Environmental Protection Agency, 1994). Vick (1990) described four factors affecting phreatic surface level; these are permeability of the foundation material with respect to the tailings material, the degree of particle size segregation, ponded water level with regard to embankment crest, and lateral permeability within the deposit. If a tailings dam is expected to receive high amounts of water, it should be constructed with a method other than upstream construction method (U.S. Environmental Protection Agency, 1994). An increase in phreatic surface and complete saturation of the outer shell may result in failure by sliding or piping, this potential may be lessened by an outer rock fill. Embankments constructed with this method generally show low specific gravity with high water content, which may result in liquefaction in case of a seismic activity (U.S. Environmental Protection Agency, 1994). It can be concluded that, upstream construction is not suitable for areas where a risk for seismic activity exists.

The rate of embankment construction could build excess pore pressures within the dam, which may result in a shear failure (Brawner, 1973). Phreatic surface level, downstream slope of the dam and strength of the tailings material within the shearing zone may generate failure (U.S. Environmental Protection Agency, 1994). Horizontal drainage zones may be utilized to control pore pressure within the embankment.

2.3.2 Downstream Method

Downstream construction commences with a starter dike as in the upstream construction method and constructed of compacted borrow materials, on the other hand, pervious sands and gravels can be used for construction with sands and clays to minimize

seepage. In the downstream method, subsequent stages of the dam are constructed on top of the downstream slope of the previous section, the centerline of the top of the dam shifts toward downstream side (Figure 2.9).

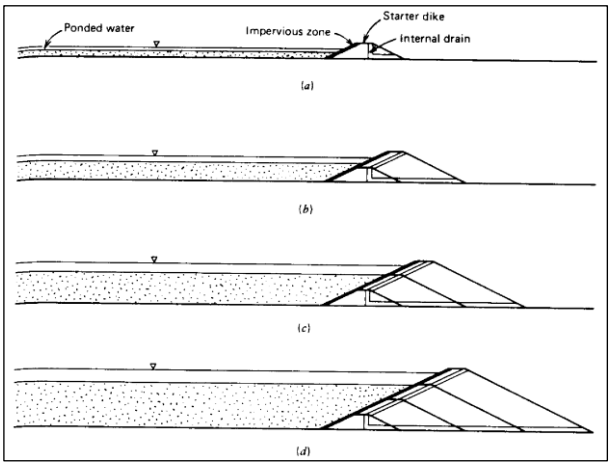

Figure 2.9 Downstream embankment construction (Vick, 1990)

Various depositional techniques may be utilized with this construction method, peripheral spigotting is the most common one (U.S. Environmental Protection Agency, 1994). If the amount of coarse tailings is inadequate to construct the dam, local borrow materails could be included for part of the dam. If coarse rock is used, an impervious membrane or filter is needed to prevent piping through the dam. If a wide tailings beach is constituted by spigotting and the embankment is composed of permeable tailings, the phreatic surface may be controlled without internal drains and impervious zones (U.S. Environmental Protection Agency, 1994). Drainage system helps to control phreatic surface and minimizes the build-up of pore water pressure which results in the reduction of shear strength (U.S. Environmental Protection Agency, 1994). This construction method is well adapted to conditions where large volume of tailings may be stored, as a result of the ability to include drains in the design.

The downstream construction method gives a better stability than upstream construction because of the ease of compaction, the incorporation of phreatic surface control measures and the foundation strength is not depend on the tailings deposit (U.S.

Environmental Protection Agency, 1994). An important disadvantage of this method is the large volume of borrow material required to raise the dam, which may result in increasing cost, if tailings can not provide sufficient material (U.S. Environmental Protection Agency, 1994).

2.3.3 Centerline Method

Centerline construction method begins with a starter dike and tailings are spigotted from the dam crest to constitute a beach. Subsequent stages of the dam are constructed on both downstream and beach side, the centerline is kept as fill (Figure 2.10). The tailings at the downstream slope side should be compacted to preclude shear failure.

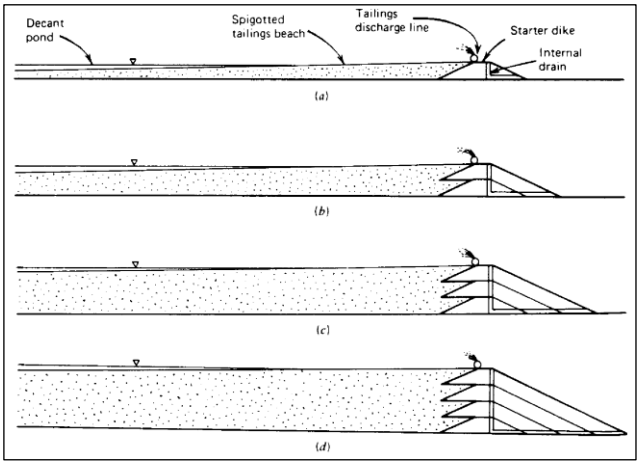

Figure 2.10 Centerline embankment construction (Vick, 1990)

Drainage zones may be included in the design as in the downstream method. A wide beach is not compulsory and this method could be used with tailings that contain low amount of sand (U.S. Environmental Protection Agency, 1994). If rapid drainage is necessary to support the construction equipment, coarse gradation of the tailings required. This type of embankment is not suitable for permanent storage huge volumes of water, whereas short-term storage of water caused by mill shutdown or heavy precipitation will not adversely affect the embankment stability (U.S. Environmental Protection Agency, 1994).

In case that the embankment material is well compacted and good internal drainage is provided, this embankment type is durable to seismic activity (U.S. Environmental Protection Agency, 1994). Even the tailings material near the upstream slope liquefies, the downstream and central parts of the dam may remain stable due to drainage and compaction characteristics (U.S. Environmental Protection Agency, 1994).

A comparison of the construction methods is given in Table 2.1.

Table 2.1 Comparison of Embankment Types (Vick, 1990)

Embankment Type	Mill Tailings Requirements	Discharge Requirements	Water-Storage Suitability	Seismic Resistance	Raising Rate Restrictions	Embankment Fill Requirements	Relative Embankment Cost	Use of Low Permeability Cores
Water retention	Suitable for any type of tailings	Any discharge procedure suitable	Good	Good	Entire embankment constructed initially	Natural soil borrow	High	Possible
Upstream	At least 60% sand in whole tailings. Low pulp density for grain-size segregation.	Peripheral discharge, well-controlled beach necessary	Not suitable for significant water storage	Poor in high seismic areas	Less than 15-30 ft/yr most desirable. Over 50 ft/yr can be hazardous	Native soil, sand tailings, waste rock	Low	Not possible
Downstream	Suitable for any type of tailings	Varies according to design detail	Good	Good	None	Sand tailings, waste rock, native soils	High	Possible (inclined cone)
Centerline	Sands or low-plasticity slimes	Peripheral discharge of at least nominal beach necessary	Not recommended for permanent storage. Temporary flood storage can be designed.	Acceptable	Height restrictions for individuals raises may apply	Sand tailings, waste rock, native soil	Moderate	Possible (Central cone)

2.4 Stability Analysis of Tailings Embankments

In order to evaluate the slope stability, design and loading conditions which affects the slope during its life have to be established. There are three critical loading conditions that must be considered for the satbility analysis; (1) at the end of construction, (2) staged construction, (3) steady state seepage.

2.4.1 End of Construction Analysis

Stability analysis of an embankment during construction and at the end of construction is performed using drained strength parameters in free-draining soils and undrained strength parameters in slow draining soils. In order to determine degree of drainage that may develop during construction period, consolidation analysis could be used (U.S. Army Corps. of Engineers, 2003). Soils with permeability values greater than 10^{-4}cm/sec usually drains fully throughout construction; however, soils with permeability less than 10^{-7} cm/sec is undrained at the end of construction (U.S. Army Corps. of Engineers, 2003).

In case of an incomplete but partial drainage of soil during construction, stability is analyzed assuming fully drained and completely undrained conditions, and the worst condition should be used for design basis (U.S. Army Corps. of Engineers, 2003). For undrained conditions, degree of saturation and density of the soil, and imposed loads control the pore pressures. Pore pressures for undrained conditions can be estimated from laboratory test results or empirical rules, however in most cases it is troublesome (U.S. Army Corps. of Engineers, 2003). For this reason, stability for undrained conditions is generally analyzed using total stresses rather than effective stresses for slow draining soils. However, for free draining soils stability is analyzed with effective stress parameters.

For embankments constructed on soft clay foundation, staged construction could be necessary (U.S. Army Corps. of Engineers, 2003). Consolidated-undrained triaxial tests can be used to state the strength parameters for partial consolidation during staged construction.

Successive raising of the dam results in compression of the fill and increase in pore pressure. Pore pressure may be critical at any intermediate stage, but it has the highest value at full height of the dam. Increase in pore pressure may be dangerous for either upstream or downstream slope (Singh & Varshney, 1995).

Construction pore pressure is affected by several factors, such as compaction moisture content, rate of construction and soil type. Compressibility of the soil increases the construction pore pressures. Because of the high compressibility of clayey soils, high pore pressures may develop within the embankment. However, in silts and silty sands of low plasticity low pore pressures may develop due to their low compressibility (Singh & Varshney, 1995).

Pore water pressure of low permeability soils is set to zero for total stress analysis. For free draining soils, pore water pressures should be determined for the stability analysis during and at the end of construction period. Pore water pressure can be determined by the water levels within and adjacent to the slope. U.S. Army Corps. of Engineers (2003) stated that pore pressures can be estimated using the following techniques:

"1. Steady-state seepage analysis techniques such as flow nets or finite element analyses for nonhydrostatic conditions.

2. Hydrostatic pressure computations for conditions of no flow."

2.4.2 Staged Construction Analysis

Staged construction analysis is applicable to all types of embankments constructed on soft foundations. Nevertheless, this analysis commonly used for rapidly constructed upstream embankments (Zardari, 2011). During staged construction, slow loading helps significant load induced pore pressure dissipation. Upstream embankments raised at a rate less than 4.5-9 m/year, it is assumed that the excess pore pressure dissipates sufficiently and staged construction analysis is not taken into consideration (Zardari, 2011).

When a raise is added to the embankment, it may generate excess pore pressures in the first raise in addition to initial pore pressures due to seepage (Zardari, 2011). Some

portion of excess pore pressures of the first raise dissipates before the addition of the second raise. However, complete pore pressure dissipation will not occur; some residual pore pressures will remain. When the second raise is added to the embankment, there exist residual pore pressures from the previous raise together with excess pore pressures due to second raise.

Tailings dams are constructed in stages in order to provide enough time for consolidation and pore water dissipation, which improves the stability of the tailings embankment and the foundation. The construction stage of a tailings dam is critical for the dam stability. During construction of an embankment, positive excess pore water pressure may develop in slimes or in the foundation soil. The stability of upstream embankments can be improved by the utilization of vertical drains and by berms located at the downstream side (Ladd, 1991).

Due to the postulation that potential dam failure occur gradually and shear induced pore pressures dissipate completely, the staged construction stability analysis is considered as the consolidated drained case. Therefore, this is an effective stress analysis (ESA) case, the factor of safety computed with this method is unrealistic and higher, because most of the failures during staged construction occur in undrained conditions (Ladd, 1991). On the other hand, if the failure occurs immediately without dissipation of shear induced pore pressures, staged construction is assumed as consolidated undrained case and undrained strength analysis (USA) is done. The factor of safety obtained from undrained strength analysis can be reliable, because the undrained shear strength is less than drained shear strength for normally consolidated soils (Ladd, 1991).

2.4.3 Long-Term Stability Analysis

Long-term analysis is performed when there is no rapid change in external loading and the embankment reach its maximum height. Moreover, pore pressures and stresses within the dam body are in equilibrium and steady state seepage conditions exist under full reservoir level, therefore, the soil under phreatic surface develops positive pore pressures (Zardari, 2011). In other words, this type of stability analysis is performed when there is sufficient time after the construction of the dam for the development of

hydrostatic conditions. Hydrostatic condition is a special type of steady-state seepage, in which no flow exists (U.S. Army Corps. of Engineers, 2003). Internal stresses and pore pressures are assumed to be in equilibrium for slowly raised embankments due to staged construction. Another assumption is that steady state seepage condition develops when the embankment attain maximum height. All of these assumptions provide the lowest prediction of long-term pore pressures (Vick, 1990).

The maximum capacity of the dam is the ultimate water level that can be maintained long enough to introduce a steady-state seepage condition. The surcharge pool is a temporary pool, which is higher than the storage pool. It adds a load to the driving force, however often could not persist long enough to establish steady-state seepage condition (U.S. Army Corps. of Engineers, 2003). A steady state seepage condition is dangerous for downstream slope, because the seepage forces act towards the downstream slope (Singh & Varshney, 1995). The stability conditions of the downstream side should be analyzed at maximum surcharge pool level. Stability analysis of surcharge pool condition should be performed using drained strength parameters (c' and ∅'), assuming the possibility of steady-state seepage at the surcharge pool level (U.S. Army Corps. of Engineers, 2003).

In long-term condition, all soils are fully drained without regarding their permeability. Long-term stability is analyzed by using drained strength in terms of effective shear strength parameters, with pore pressures appropriate for the long-term condition. The pore pressure values used in the analyses must represent the field conditions and steady state seepage in the long-term condition. U.S. Army Corps. of Engineers (2003) stated that pore pressures can be estimated from;

"1. Field measurements in existing slopes.
2. Past experience and judgment.
3. Hydrostatic pressure computations for no flow conditions.
4. Steady-state seepage analyses by making use of flow nets and finite element analyses."

There are two different notions to take into account the shear induced pore pressures at failure in long-term analysis. Johnson (1975) stated that neglecting the shear induced

pore pressures may result in high shear strength. However, Kealy & Soderberg (1969) and Wahler (1974) claimed that the effective stress parameters, without taking into consideration the shear induced pore pressures at failure, can be used in long term analysis.

The characteristics of very loose tailings deposits could be similar to the characteristics of natural sensitive clay deposits (Zardari, 2011). A small initial slide in a slope of sensitive clay may result in rapid change in the loading conditions at the toe of the slope and may produce a series of slides resulting in slope failure (Bishop & Bjerrum, 1960).

2.5 Failure Modes of Tailings Embankments

There are a number of common failure modes, to which embankment dams are susceptible. These failure modes include circular failure, foundation failure, erosion, overtopping, piping and liquefaction. Most of the dam failures stem from loss of freeboard or overtopping of the reservoir water due to flooding. Table 2.2 gives the summary of failure modes, causes and remedial measures.

2.5.1 Circular Failure

Circular failure occurs when the embankment fill material lose shear strength along a circular slip surface. Failure surface seems as a segment of a circle, slope failures may range from local sloughing of tailings along the face of an embankment to massive circular failures extending over the entire structure (U.S. Environmental Protection Agency, 1994). For an unstable slope, the shear stress that tends to induce movement exceeds the resisting shear strength along a potential failure surface. Instability takes place when the shear stress on the slip surface is equal to shear strength (Vick, 1990). Rotational failure may take place because of the following conditions such as; inadequate control of pore pressure, overstressing of soil, change in the water table, changes in the permeability of foundation soil, embankment disturbance by vibration, settlement of foundation material (CANMET, 1977).

Table 2.2 Failure modes of tailings embankments, causes and remedial measures (ICOLD, 1996)

Failure Mode	Cause	Remedy
Overtopping	• Inadequate hydrological or hydraulic design • Loss of freeboard due to crest settlement	• Gabions, mine pit waste or surrounding borrow material may be quickly imported to aid the strength of embankment • Opening of emergency pumps and spillways
Slope instability	• Overstressing of foundation soil and dam fill • Inadequate control of pore pressure	• Soil reinforcement and strengthening measures • Installing a drainage trench at the toe of downstream face and/or horizontal bore drains. Filters can prevent the entry of fill material into the drain.
Internal erosion	• Inadequate control of seepage • Bad filter and drain design • Poor design or construction control resulting in cracks or leakage through conduits	• Raising downstream embankments with drainage blanket • Installation of horizontal bores to relieve pressure • Installation of deep trenches towards downstream face
External erosion	• Inadequate slope and toe protection	• Vegetation of the downstream face • Placing crushed mine waste on the downstream embankment face • Construction of berms on downstream face • Placing rock fill such as mine pit waste adjacent to the toe
Earthquake action	• Steep slopes • Liquefaction of embankment and foundation soil	• Filling of cracks with a suitable material
Damage to decant system	• Excessive settlement • Chemical attack on concrete/steel	• Opening of emergency pumps or spillways

2.5.2 Foundation Failure

Foundation failures are common failure modes among earthfill structures. Where a weak soil or rock layer presents at shallow depth in the foundation below the embankment, movement takes place along a failure plane if the structure produces stresses more than the strength of the soil in the weak layer (CANMET, 1977). Figure 2.11 shows the foundation failure that took place in Los Frailes mine (Spain) in 24 April 1998, which resulted in 6.8 million m^3 toxic material release (ICOLD and UNEP, 2001).

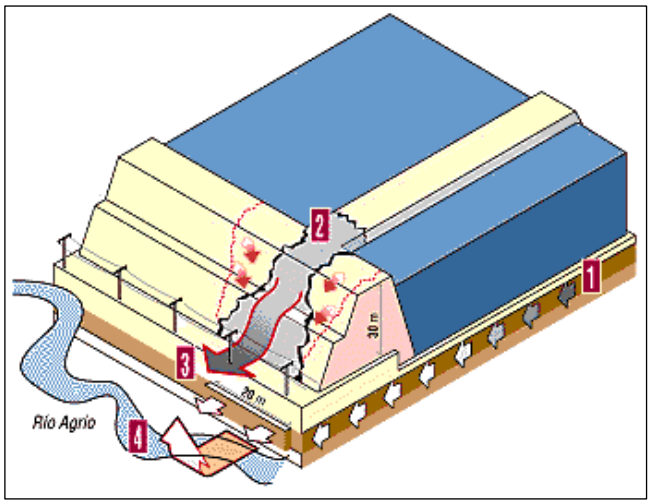

Figure 2.11 Schematic view of the foundation failure of tailings dam in Los Frailes Mine (Spain) (www.wise-uranium.org, 2008)

2.5.3 Erosion

In areas that receive high precipitation, some types of protection measures are required against erosion. Tailings dams may be vulnerable to erosion in two main areas, embankment abutments and face (U.S. Environmental Protection Agency, 1994).

Generally, this type of failure stems from erroneous design and maintenance, and it may be prevented with proper storm water diversion methods. Erosion of embankment faces may spring from fracture in tailings lines installed on the embankment crest (U.S. Environmental Protection Agency, 1994). Storm water flow concentrating along the

contact between the embankment and abutment may result in erosion (CANMET, 1977). Maintenance and alternating tailings lines may prevent erosion. Figure 2.12 shows erosion of embankment face of Cerro Negro tailings dam (Chile) in 10 March 2003, which resulted in 80,000 m^3 tailings release (www.tailings.info, 2012).

Figure 2.12 Erosion of embankment face of Cerro Negro tailings dam near Santiago, Chile (www.tailings.info, 2012)

2.5.4 Overtopping

The most widespread causes of failure is overtopping by flooding. Overtopping generally results from the volume of surface water flows or storm water flows exceeds the capacity of the impoundment. In other words, inadequate hydrological or hydraulic design and loss of freeboard due to crest settlement may result in overtopping (ICOLD, 1996).

A rapid increase in pore pressure related to large storm water inflow may end up with the liquefaction of unconsolidated impounded sands and slimes (U.S. Environmental Protection Agency, 1994). Moreover, the friction stem from rapid flow over an unprotected embankment crest may wash away a channel in the fill material, allowing consistent release to occur, because tailings embankments are mostly constructed of highly erodible materials (U.S. Environmental Protection Agency, 1994). This type of

sustained high flow over the embankment crest may result in a major embankment failure within minutes (CANMET, 1977). Figure 2.13 shows overtopping failure of Merriespruit tailings dam (Virginia, South Africa) in 22 February 1994, which resulted in 500,000 m^3 slurry flow over 2 km (ICOLD and UNEP, 2001).

Figure 2.13 Overtopping failure of Merriespruit tailings dam in Virginia, South Africa (www.tailings.info, 2012)

2.5.5 Piping

Piping expresses internal erosion along a seepage pathway within dam and foundation which ends up with the generation of a channel permitting concentrated flow. Erosion usually initiates at the downstream toe and proceeds toward the reservoir, by forming channels or pipes under the dam. These pipes or channels proceed through paths of maximum permeability and may not develop until many after construction (Durham University, Geo-Engineering Web site). Piping may stem from seepage from the embankment face with sufficient velocity to erode the embankment face (Figure 2.14). The resulting void space develops progressive erosion extending towards the source of the seepage. In the worst case, the seepage may create a channel from the embankment to the embankment face (CANMET, 1977). Thus, excessive piping may culminate in local or general failure of the foundation or embankment.

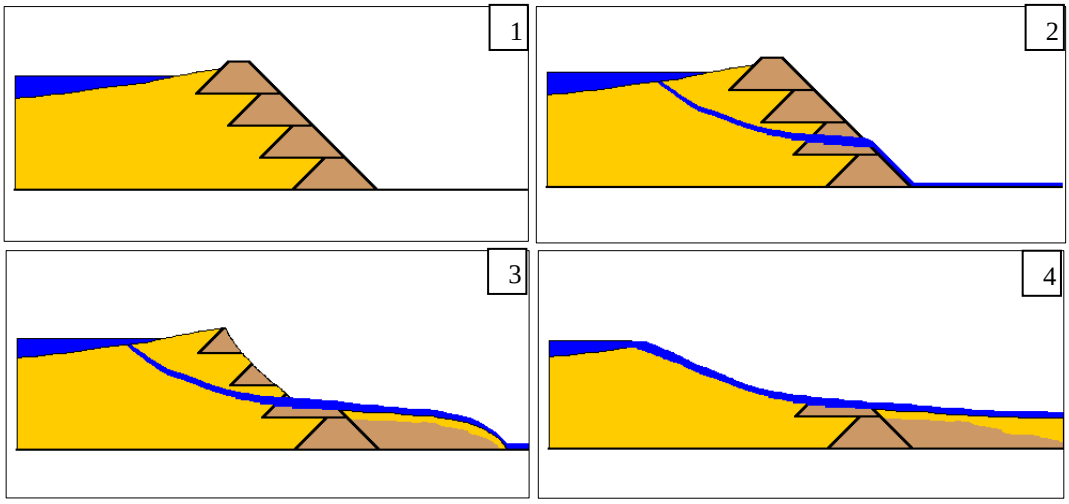

Figure 2.14 Stages of piping; 1) stable state, 2) and 3) piping through the dam body, 4) dam failure (www.wise-uranium.org, 2008)

2.5.6 Liquefaction

Liquefaction is an incident in which the stiffness and strength of a soil is reduced by earthquake shaking or other types of rapid loading. Liquefaction is one of the most common failure modes of cross-valley dams (U.S. Environmental Protection Agency, 1994). Liquefaction occurs when the soil is saturated, in other words, spaces between soil particles are completely filled with water (The Soil Liquefaction web site, 2000). This water exerts a pressure on the soil particles, which influences the particle packing. Just before an earthquake, the water pressure is relatively low. Nevertheless, earthquake shaking may end up with increase in water pressure to the point where soil particles can move easily with respect to each other (The Soil Liquefaction web site, 2000). Figure 2.15 shows the stages of seismic liquefaction. Not only earthquake shaking but also activities related to construction such as blasting may also trigger an increase in water pressure. When liquefaction takes place, the soil strength decreases and, the ability of the soil to support the foundation is reduced. Because tailings deposits are composed of unconsolidated, saturated deposits of grains with similar size, they are vulnerable to temporal suspension of grains in water (Vick, 1990). Liquefied tailings may behave like a viscous fluid, so that they may pour out from narrow openings and flow significant distances (CANMET, 1977).

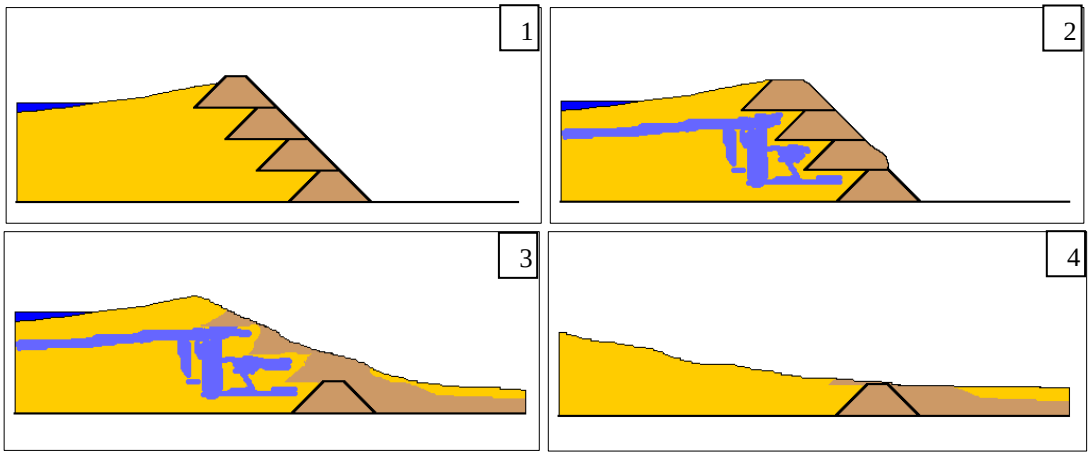

Figure 2.15 Stages of a seismic liquefaction failure; 1) stable state, 2) liquefaction, 3),4) dam failure (www.wise-uranium.org, 2008)

U.S. Environmental Protection Agency (1994) stated that factors affecting liquefaction potential include:

"1. Soil type - Uniform grain size materials, mostly in the fine sand sizes, are the most susceptible to liquefaction.

2. Relative density or compactness - The more compact or dense material is more resistant to liquefaction.

3. Confining pressure at the time of dynamic loading - Applying overloads to loose deposits may provide an opportunity to prevent liquefaction.

4. Ground Shaking Intensity and duration - Liquefaction may occur due to an earthquake, or other types of seismic action.

5. Location of the water table - A high water table is harmful. For this reason, a tailings deposit constructed on a pervious foundation or a dam with a phreatic line kept low by providing sufficient internal drainage may reduce liquefaction potential (Vick, 1990)."

By compacting the fill materials at the construction stage, maintaining a low pond level, incorporating drainage facilities and confining pressures can be controlled to reduce possibility of liquefaction (U.S. Environmental Protection Agency, 1994). If the tailings dam is composed of fine sands, compaction of dam material increases their density and reduces their susceptibility to liquefaction. Compaction of the dam material to obtain relative densities more than or equal to 60% provides satisfactory protection (CANMET,

1977). The embankment may be stable against liquefaction failure; provided the phreatic surface is maintained below the embankment surface or embankment materials possess a relative density of 60% or greater (U.S. Environmental Protection Agency, 1994).

2.6 Evaluation of Tailings Dam Failures

The analysis of tailings dam incidents provides crucial information about factors of dam stability, including in situ characteristics, selection of embankment construction type, along with risk factors identification.There are a number of studies have been conducted to summarise causes of major tailings dam failures all over the world. International Commission on Large Dams (ICOLD) performed the most comprehensive and recent research (221 tailings dam failures), with regard to previous investigations of the U.S. Commission on Large Dams (USCOLD). In order to gain information about the causes of tailings dam instabilities, the investigation of Rico et al. (2008) was examined. This study includes the compilation of 147 tailings dam disasters in a database.

Rico et al. (2008) selected seven quantitative and qualitative parameters from the database: dam type, type of construction, state of activity, storage volume, dam height, failure causes and type of failure in order to perform the statistical analysis.

In tailings dam failure cause analysis, 11 failure causes were spotted (Figure 2.16), and each of them was assigned to a unique category, which contributed mostly to the dam failure. In most of the failures (39%), the dam failure resulted from a combination of different causes. For instance, failure attributed to meteorological events may also be associated with seepage, overtopping, foundation failure. Most of the incidents are related to meteorological events (e.g. unusual rainfall and snow), responsible for 25% of worldwide cases and 35% in Europe (Rico et al., 2008). Seismic liquefaction causes no failure in Europe, whereas it is in second order (14%) for rest of the world.

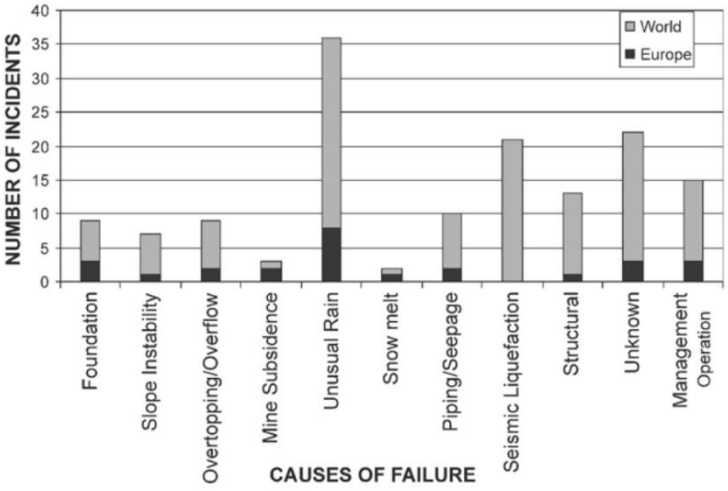

Figure 2.16 Distribution of the number of failures according to causes in the world and in Europe (Rico, Benito, Salgueiro, Diez-Herrero, & Pereira, 2008)

In Figure 2.17, the construction types are presented along with the state of activity of the dam. The graph shows most of the failures worldwide occured in upstream type active dams. In Europe, dams constructed with upstream and downstream construction methods had dam incidents with similar percentages (47 and 40%, respectively) (Rico et al., 2008).

Out of all failure causes, 83% occured in active dams, 15% in inactive and abandoned dams and only 2% of failures occurred in inactive but maintained dams. In active dams, the most frequent causes are related to natural dangers, followed by management operation and structural failures (Rico et al., 2008).

The type of construction affects the stability of the dam, dams constructed with upstream construction (UPS) are 76% of the cases in the world and 47% of failures in Europe. Downstream (DOWN) and centerline (CTL) constructed tailings dams represent 15% and 5% of global cases, respectively.

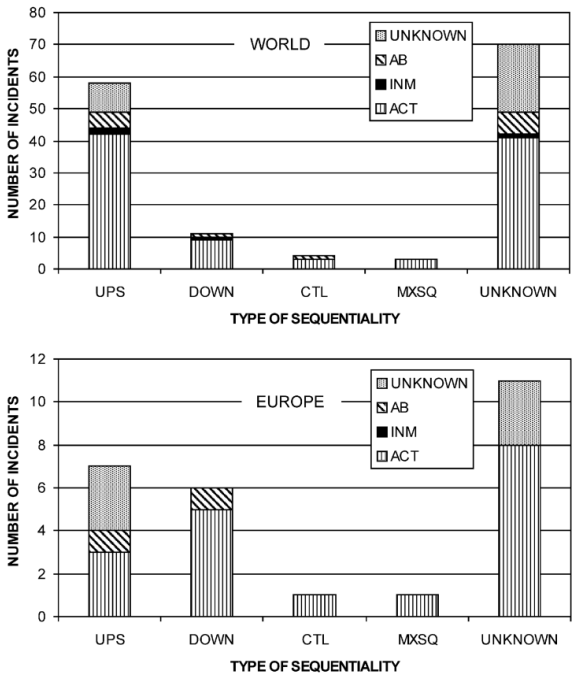

Figure 2.17 Distribution of the number of failures according to dam construction type and state of activity in the world and in Europe. Active; abandoned or inactive but maintained dam at the time of failure (Rico et al., 2008)

2.7 Previous Studies

There are small amount of studies in the literature about the stability of tailings dam. Hence, the literature survey was extended to stability analysis of embankment dams, earth-fill and rock-fill dams. The main reason is that the tailings dams are being constructed typically as earth-fill dams. Moreover, the same laboratory tests are conducted on the materials and similar approaches are developed for stability analyses of both types. The previous works related to the research is summarized in the following paragraphs.

Oyanguren et al. (2008) analyzed the stability of the Llerin rock fill dams in Spain with Barto-Kjaernsli's shear criterion. The required parameters for this criterion were obtained from in situ direct shear test, to lessen the deflections generated in laboratory tests. A specially designed shear box was used in the tests. Friction for rock fill materials was assumed variable and changing with normal stress value on shear plane. Samples

were subjected to a constant normal stress and an increasing tangential stresses upon failure. Moreover, to determine the cohesion and internal friction angle of the material, varying normal stress values were applied. For the stability analysis slope with maximum inclination was detected. So as to model the behavior of the dam-foundation-sludge system, shear criteria and required parameters for each of the materials were considered separately. For foundation materials simple compression strength, indirect tensile strength and tilt-test were applied. For dam materials granulometric analysis, Los Angeles wear resistance and in situ direct shear tests were done. In order to characterize the foundation rock mass Bieniawski's classification were managed. Because of the liquefaction possibility, friction and cohesion of the sludge were assumed as null. Finally, SLOPE program was used to model the dam and to obtain a safety factor for the dam. Five slip surfaces were inspected, and as a result the dam is found as safe with a safety factor larger than 1.4 for all cases. Oyanguren et al. (2008) concluded that the structure is safe in long term even under the seismic risk conditions.

Liang et al. (1999) studied the reliability-based approach for slope stability analysis. The stability of King Talal embankment dam was analyzed. For this purpose a computer program RESLOP had been developed in FORTRAN 77 language and verified by using a slope failure case in Chicago. RESLOP program based on a reliability-based approach for the evaluation of slope instability, which taking into account the uncertainties in parameters. Factor of safety probabilistic method was performed with Fellenius limit equilibrium method. In order to perform reliability analysis of a slope, a performance function, g(x), was described by using modified Fellenius method that defines the stability of the region. Moreover, to assess the uncertainties in the input parameters the reliability index, β, is calculated. Triaxial compression tests and direct shear tests were done to find soil strength parameters. Liang et al. (1999) used two criteria in order to state critical slip surfaces for the dam. First one defines critical surface with minimum safety factor, and the second one relying on minimum reliability index. Three loading conditions were studied for the analysis; end of construction (total stress analysis), rapid drawdown (effective stress analysis), and steady state seepage (effective stress analysis). Finally, it was found that the upstream face under rapid drawdown loading conditions is the most critical case with minimum mean safety factor and reliability index, which is below the required value.

Babu et al. (2007) focused on the failure of several dams in Gujarat region as a result of the earthquake in 2001. For this purpose failed sections of Chang, Tappar, Kaswati and Rudramata dams were back-analyzed by managing pseudo-static limit equilibrium approach. Moreover, rehabilitated sections of the dams after the earthquake were analyzed. The main cause of the failures in the field was thought to be the liquefaction of the saturated liquefiable alluvium layer beneath the foundation soil, which had resulted in smaller safety factors. For this reason, dam sections were back analyzed with and without considering the existence of liquefiable layer. For evaluation, deterministic and probabilistic analyses were carried out for both static and pseudo-static loading conditions. At four dam locations after the remedial measures were taken, liquefaction potential of the soil had been assessed with the aid of standard penetration test (SPT) and the soil had been found as reliable against liquefaction. Shear strength parameters of dam material were found with laboratory tri-axial tests. In order to analyze the failed dam sections, SLIDE (2005) software was utilized. Failed dam sections were analyzed with deterministic and probabilistic approaches for pseudo-static loading conditions. Rehabilitated dam sections were examined with deterministic and probabilistic analysis for both static and pseudo-static loading conditions. As a result, it was found that old dam sections had not been safe, but the rehabilitated sections were safe with respect to approaches.

In a study a Rico et al. (2008) inspected a worldwide database of historic dam failures and performed a regression analysis so as to find the relationship between tailings dam geometric parameters (dam height, tailings volume) and the hydraulic characteristics of tailings flood. Regression analysis showed a good correlation exists between them. The resulting correlation between them could be interpreted to predict the spilled tailings volume, tailings run out distance and outflow peak discharge.

Zandarín et al. (2009) studied the role of capillary water in the stability of a tailings dam from nickel industry in Cuba, with the aim of gaining information about geotechnical attitude of dams. Coupled hydro-mechanical finite element method was used in order to model the dam behavior. With the aim of describing the mechanical behavior of tailings, foundation and embankment materials, Barcelona Basic Model (BBM) viscoplastic

formulation was managed. Mechanical parameters of tailings were found from oedometer, triaxial and Brazilian tensile tests. Mechanical properties of the dam material were assumed to be identical with the tailings', since both come from the same geological origin. Mechanical parameters of the embankment were predicted by considering the soil type and some index properties. Hydro-mechanical attitude of the dam was modeled with finite element code Code_Bright. With this model, sixteen years of continuous filling of dam were simulated. As a result of the model, it was found that porosity decreases faster at the perimeter than at the central zone. This was due to the favorable drainage conditions in the surroundings of the dam, greater permeability and lower water table levels, which lead to higher effective stress and faster consolidation process. Under heavy rains, phreatic levels in the dam rise quickly because of capillary water. On the contrary, after heavy rains phreatic levels fall slowly due to the low hydraulic conductivity. Then, the critical condition for the dam stability was obtained. After the rainstorms took place, safety factor of the slope fell from 2.5 to 1.1. As a result of this study it is founded that dam stability depends strongly on capillary phenomena. With the aid of this result, capillary water measurement stored in the unsaturated zone of the deposit was recommended in the scope of monitoring schedule of tailing storage facilities.

Huat et al (2006) studied a coupled hydrology/stability model to deal with the limitations brought about by standard methods that are used to investigate stability of tropical soil slopes. Dynamic hydrological condition was simulated as it is changing with rainfall. A finite element hydrology – limit equilibrium analysis model was developed. Shear strength parameters for unsaturated soils were defined with extended Mohr Coulomb failure criterion. In order to investigate the hydrological response in the slope stability analysis Seep/W and Slope/W programs were used developed by Geo-slope International Ltd.,Canada. Firstly, a homogenous slope model was developed with Seep/W and output of this model was later used as input in Slope/W program incorporating Bishop's method for stability analysis. Consequently, model was applied to various conditions and the results were summarized in the form of design charts.

Dillon et al. (2004) presented the methods used to design the tailings dam in Lisheen Underground Lead-Zinc Mine (Ireland) and construction studies. In order to define the

ground conditions geotechnical drilling, CPT, SPT and falling head permeability tests were done as part of the field investigations. The engineering properties were determined by field and laboratory testing. Gathered parameters were used to analyze the stability of the tailings dam and the dam was found as stable under pseudo-static conditions. Furthermore, peat consolidation, phreatic conditions and embankment crest movement were monitored. Moreover, during construction stages micro-gravity survey were carried out to investigate the bedrock. After the completion of the construction resistivity monitoring had been carried out for six months to measure consolidation of the peat.

Mendoza et al. (2009) studied a methodology to enhance the environmental safety according to the parameters used in their construction and management. In this study an alternative model was designed to evaluate the environmental risk. In this method it was not needed to gather the historical data as in traditional methods. In order to that, geotechnical stability, erosion of slope, sealing of the dam, overtopping probability, volume of stored material and pollution load of the stored material were analyzed. These parameters were obtained in different units, and then transformed into homogeneous units by using rating curves. In the cases analyzed, the methodology is validated and an environmental risk index value was obtained. Values lower than this established value indicated a safe dam.

Chakraborty et al. (2009) investigates the behavior of tailings dam under seismic and conditions. The analysis was performed using various softwares like FLAC3D, TALREN 4, SEEP/W and SLOPE/W. For the FLAC3D model the Mohr-Coulomb plasticity model is used. The phreatic surface developed from the FLAC3D seepage analysis is very similar to the phreatic surface obtained in SEEP/W analysis.
It was concluded that from the results of seepage analysis the finite difference method based FLAC3D and finite element method based SEEP/W give similar results.

Day et al. (1998) performed stability assessment during construction and drainage design of Thika Dam using “The Imperial College Finite Element Program (ICFEP)”. The stability of the dam was evaluated using fully coupled deformation/consolidation two-dimensional finite element analysis and behaviour of the fill was represented by a form of the Modified Cam Clay constitutive model. Finite element analysis was used to

determine required amount of drainage in different zones within the embankment to maintain embankment stability during construction. The analysis were performed for five different drainage options.

Al-Homoud et al. (2004) developed a probabilistic 3-D slope stability analysis model (PTDSSAM) to assess stabilities of foundations and embankment dams under staged construction conditions taking into account uncertainty, spatial variabilities and correlations of shear strength parameters, in addition the uncertainties in pore water pressure. The overall stability of the dam and foundation were evaluated using both effective stress analysis (ESA) and undrained strength analysis (USA) . The stability of Karameh dam was analyzed during staged construction using deterministic and probabilistic analysis, and detailed sensitivity analyses were carried out with respect to different input parameters. As a result, USA gives lower safety factors than ESA.

Psarropoulos & Tsompanakis (2008) investigated the behaviour and the stability of tailings dams under static and dynamic loading conditions. The three most commonly used method of construction of tailings dams were examined; upstream, downstream, centerline. In order to explore the sensitivity of slope stability to slope inclination and to confirm the accuracy of SSR method, the finite element code PLAXIS and Bishop simplified method were used. As a result of this study it was obtained that downstream method leads to more stable dams and numerical analysis is more conservative than limit equilibrium analysis. In pseudostatic analysis two-dimensional numerical simulations were performed using QUAD4M finite element code. The soil conditions below the dam, the geomechanical material properties and the ground motion characteristics were examined. Results showed that site conditions and material nonlinearity affect the dynamic instability.

Saad & Mitri (2011) performed transient coupled nonlinear finite-element analyses by utilizing ABAQUS to examine the hydromechanical behavior of the upstream tailings dam during staged construction including the transient partially saturated flow within the embankment, the two-dimensional consolidation and nonlinear material behaviour of the tailings. The tailings impoundment was separated into three zones based on their particle size by following the method of Shulz (1979). The zones are sand-sized tailings retained

on the 0.063 mm sieve, the beach composed of coarse to fine grained tailings and the slimes passing the 0.063 mm sieve. The Drucker-Prager cap model was used to model the tailings in the beach and slime zones. The embankment dykes zone and upper foundation layer were modeled by the linear elastic-perfectly plastic Drucker-Prager model and modified Cam clay model, respectively. The results of the study were the permeability of the beached tailings influences the stability of the embankment and internal drainage medium is insufficient in lowering the phreatic surface in embankments with low-permeability beached tailings materials.

Weishui et al.(n.d.) analyzed the stability of tailings dam under seismic action. The seepage field was examined within the tailings pond. Based on the hydraulic head distribution and velocity in the dam, seismic analysis was carried out for the tailings pond in steady state flow condition. Three seismic intensity values were input and factor of safety values were obtained for the dam under seismic action. The safety factor decreased 0.3-0.4 with increasing seismic intensity.

Moreover, Li et al. (2009) focused on numerical finite element upper and lower bound limit analysis by making use of the strength reduction method to generate stability charts for three-dimensional homogeneous and inhomogeneous undrained slopes.

CHAPTER 3

GENERAL INFORMATION ABOUT THE STUDY AREA

3.1 Characteristics of the Tailings Dam Area

The study area, Küre is located in Kastamonu. Küre is 60 km to Kastamonu and 30 km to İnebolu. Settlements in the vicinity of the mine area are İnebolu, Seydiler, Ağlı, Devrekani, Doğanyurt, Azdavay. The area of Kastamonu is 860 km^2, and the population is 20,522. The Küre district covers an area of 541 km^2 (Turkey's State Institute for Statistics) and the town lies at an elevation of 1,500 m. satellite image of the mine area is given in Figure 3.1 and closer view of the tailings dam is given in and Figure 3.2.

Figure 3.1 Satellite image of the mine area (Google Earth, 2011)

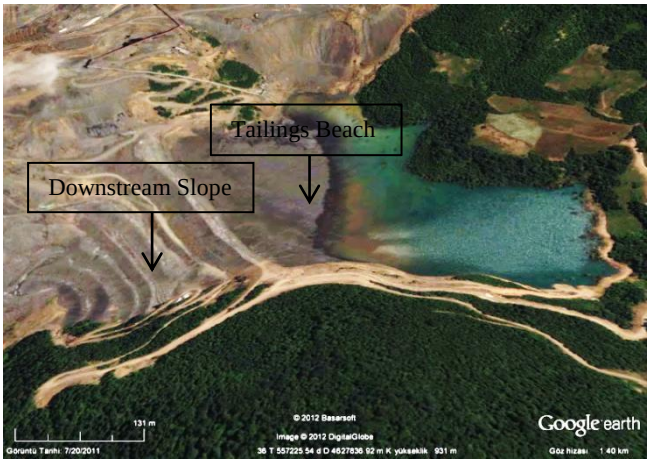

Figure 3.2 Side view of the tailings dam (Google Earth, 2011)

The general topography of the region is mountainous and hilly. Topographic contours of the hills over the area are; Kızana hill (1,268m), Kızancak hill (1,139m), Karacakaya hill (1,279m), Toykondu hill (1,279 m), Bakibaba hill (1,304 m) (Vardar et al., 2010).

Küre Mountains show carstic property that is regional structure. Rainfall and water erosion forms caves and canyons (Vardar et al., 2010). Deep valleys with limestone-dominated caves might be observed over the area. Hiraçayırıözü stream and linked watercourses have been corroded. The major rivers over the area are İkizciler, Düzdere, Çatak and Zımana (Vardar et al., 2010).

Küre is in the region that is transition of black sea climate and terrestrial climate. Because of that, the weather is snowy and cold in winter, and mild in summer. Fog is observed in every season. In Kastamonu district climatic conditions changes with altitude from coastal region to inner parts. In winters, coasts are mild and rainy, however because the inner parts has an altitude over 1,000 m it is cold and snowy (Vardar et al., 2010). As a result, from outer to inner parts, the characteristics of Black Sea climate are replaced with characteristics of harsh Terrestrial climate. The average temperature is 5^{o}C in winters, and 30^{o}C in summers (General Directorate of Meteorology, 1975-2008). The coldest months are January and February and the hottest ones are July and August. The climate of the area is typical black sea climate with a mean annual rainfall of 40.52 kg/m^2 (General Directorate of Meteorology, 1975-2008).

Figure 3.3 shows earthquake zones in Kastamonu, and Küre takes place in the third degree earthquake zone. The seismicity of the region is affected by North Anatolian fault zone. According to latest studies the velocity was decided as 1-1.3 cm/y (Deprem Araştırma Dairesi). North Anatolian fault zone moves towards west.

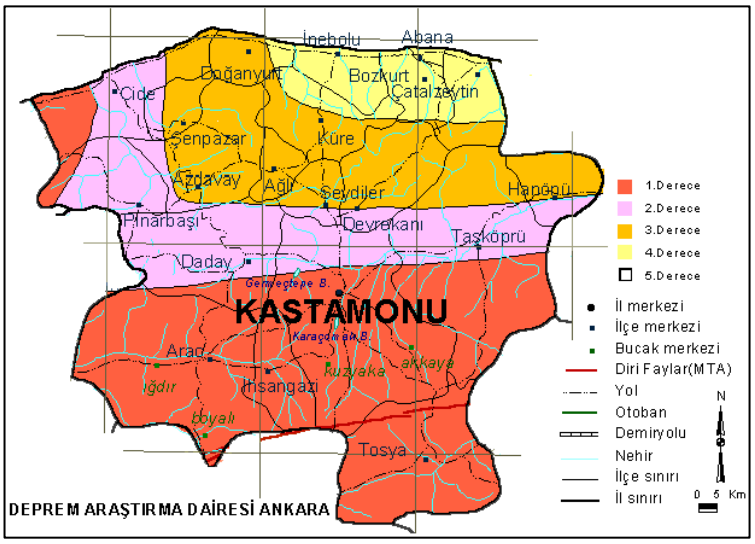

Figure 3.3 Eatrhquake zones in Kastamonu (Deprem Araştırma Dairesi)

3.2 General Information about Tailings Dam

The main ore minerals in the reserve are pyrite and chalcopyrite. The mine is operated by Eti Copper Incorporated Company and has the third largest copper reserve in Turkey (Vardar et al., 2010). Firstly, Etibank took the concession of the area in 1955, then Aşıköy field was started to operate. Between 1955 and 1957 underground production was done. In 1957 Küre Incorporated Company was founded and then the mine was devolved to Etibank in 1959. In Bakibaba field the operations were performed by MTA between 1923 and 1963. In 1968, this field was revolved to KBİ. In 1991, Etibank again took the ownership. Finally, Cengiz Holding incorporated the mine in 2004, still operates the mine.

There are a lot of streams and springs in the study area. The Eti copper mine tailings dam is constructed on Hiraçayırıözü stream (Vardar et al., 2010). Düzdere is in the

drainage basin of tailings dam. Water resources of the mine are Çatak dam, İkizciler pump station, and Düzdere pump station (Vardar et al., 2010). Construction purpose of Çatak dam was identified as to provide industrial water to Eti copper mine according to information from DSİ (Vardar et al., 2010). However, in summers, the water in the dam becomes insufficient, and water discharged from tailings dam is again pumped to processing facility (Vardar et al., 2010). Aşıköy and Toykondu ore deposits include 10.4 million tons of ore with 1.99% Cu and 35.13% S grades (Vardar et al., 2010). Basic ore minerals are pyrite and chalcopyrite. Annually, 900,000 tons of solid and 2,000,000 tons of liquid waste comprises at the concentrator facility (Vardar et al., 2010). The pulp material coming from the concentrator is stored in the tailings dam.

According to the report prepared by Vardar et al. (2010), the following information was obtained. The dam is located on jointed partially pervious andesite that is foundation material. Tailings dam is firstly constructed in the form of earth-rockfill dam between 847-884 m altitudes with INTES project, within the period operated by ETİBANK. Afterwards, the dam was raised to ETİBANK 1.stage (890m) and ETİBANK 2.stage (906 m), because the reservoir was full and dam became instable. The dam body reached to 946 m before the privatization, and today it has reached to 976 m. Current tailings level in the dam is 968.25 m. Base level of the dam is 850 m and current height of the dam is 126 m. Figure 3.4 shows the former and the latter conditions after construction.

Figure 3.4 A view of the dam on a) September, 2010, and b) July 30, 2011

The dam experienced piping through embankment, because of heavy rain. Figure 3.5

shows the piping event, which took part on July 19, 2009. As a result of this incident, it was decided to strengthen the dam. With the studies made in 2011, the embankment face was strengthened; moreover, the capacity of the dam was increased by increasing dam height.

Figure 3.5 Piping through dam because of heavy rain (July 19, 2009)

After heavy rain in 2009 the surface runoff water accumulated in the dam, which resulted in sudden increase in ponded water level. As a result of this situation, water diversion channels were constructed. Some part of flowing surface water, which depends on precipitation, is collected behind the upstream part of the dam in order to feed and backup the plant, and the excessive part is poured to Hiraçayırıözü stream with diversion channels (Figure 3.6). The water at the suction point is collected in tank at the pump station. The purpose of the tank is to pump the water back to the plant. These pumps are used in summers, in order to meet the water need of the facility. The remaining part of the water is discharged to stream course, after pH balancing. Two discharge pipes are placed in case of water rise in the dam in excessive rainfall conditions.

Figure 3.6 Diversion channels behind the dam

CHAPTER 4

GEOMECHNICAL LABORATORY EXPERIMENTS

4.1 Material Sampling

In order to define engineering properties of embankment material, tailings and foundation, disturbed samples are taken from the site. For this purpose, trenches were opened at 4 different places of the dam with the aid of an excavator in order to obtain disturbed samples from dam body. As dam body contains large amounts of gravel (approximately 51%), undisturbed samples could not be taken (Figure 4.1, Figure 4.2).

Figure 4.1 View of dam body material

Figure 4.2 The uppermost face of the dam

Figure 4.3 View of tailings material

The tailings material does not constitute a stable form, thus undisturbed samples could not be obtained and only disturbed samples could be taken from the site (Figure 4.3, Figure 4.4).

Figure 4.4 Getting disturbed samples from tailings material

In order to define the properties of foundation material, rock blocks were taken from host rock next to the dam (Figure 4.5).

Figure 4.5 Host rock next to the dam

4.2 Laboratory Experiments on Soil Samples

4.2.1 Index and Geomechanical Properties of Dam Body Material

The following experiments were conducted on disturbed samples taken from 4 different places of the dam; moisture content, specific gravity, particle size analysis, Atterberg limits test, standard compaction test, direct shear test.

4.2.1.1 **Moisture Content and Specific Gravity**

Table 4.1 shows the moisture content and specific gravity values for the dam body samples. Average moisture content of the samples was found as 9.71% (ranges from 7.82% to 12.59%). This water content is probably lower than existing in the field, since it was measured after transportation to Ankara. Specific gravity of the samples changes between 2.84 and 2.93, average specific gravity of the dam body was found as 2.883.

Table 4.1 Specific gravity and moisture content values of samples

	1st Sample	2nd Sample	3rd Sample	4th Sample	Average
Specific Gravity	2.927	2.878	2.892	2.836	2.883
Moisture Content, %	9.75	8.67	7.82	12.59	9.71

4.2.1.2 **Particle Size Analysis**

The percentages of clay, silt, sand and gravel size particles present in a soil can be obtained from the particle size analysis.The particle size distribution of soil larger than 75 μm (remain on the No. 200 sieve) is determined by the method of sieving, whereas the particle size distribution of soil smaller than 75 μm is determined by the method of sedimentation, using a hydrometer.

A series of sieves was used to seperate the portion retained on the No.200 (75 μm) sieve into a series of fractions using the 2 in. (50 mm), 1½ in. (37.5 mm), 1 in. (25.0 mm), ¾

in. (19.0 mm), 1⁄2 in. (12.5 mm), 3⁄8 in. (9.5 mm), 1⁄4 in. (6.3 mm), No.4 (4.75 mm), No.10 (2.0 mm), No.30 (0.6 mm), No.50 (0.3 mm), No.70 (0.212 mm), No.100 (0.15 mm) and No.200 (75 μm) sieves.

The sedimentation method is based on Stokes' law which gives the velocity at which particles settle in a suspension; settling velocity increases with increasing particle size. The Stokes' law is not applicable to particles smaller than 0.2 μm, settlement of which is controlled by Brownian movement.

Particle size distribution of disturbed samples taken from the dam body was determined by sieving and hydrometer testing according to ASTM D422 – 63, 2007 standards. Obtained particle size distribution curves are given in Figure 4.6. With reference to the curves, it was concluded that the dam body is mostly composed of gravel (51%), and sand (35%) sized particles, moreover it contains (14%) clay sized particles. Particle sizes of the samples are given in Table 4.2.

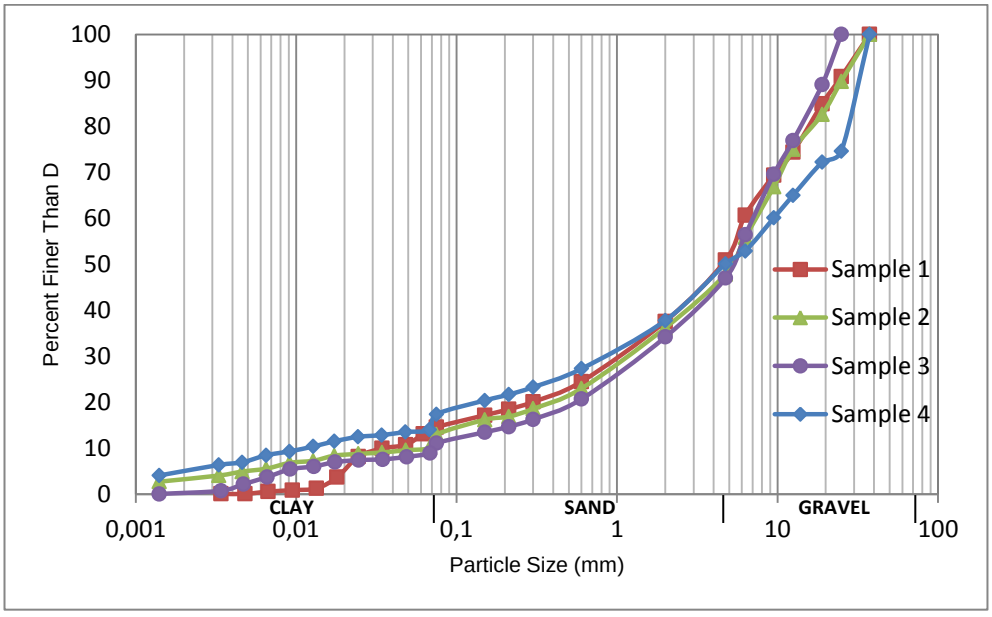

Figure 4.6 Particle size analysis of dam body samples

Table 4.2 Particle contents of samples

	1st Sample	2nd Sample	3rd Sample	4th Sample
Gravel %	49.1	52.1	53	49.9
Sand %	36.3	34.9	35.9	32.7
Clay %	14.57	12.95	11.06	17.42

4.2.1.3 **Atterberg Limits and Soil Classification**

This experiment covers the determination of the liquid limit, plastic limit, and the plasticity index of dam body material. The Atterberg limits test was done according to ASTM D4318 – 10 standards. These limits differentiate the boundaries of the several consistency states of plastic soils. This test performed only on soils that passes through 425-μm (No.40) sieve.

Liquid limit (LL) is the water content of a soil in percent at the boundary between the semiliquid and plastic states. With the results the relationship between the water content, and the corresponding number of drops, was plotted on a semilogarithmic graph with the water content as ordinates, and the number of drops as abscissas. A best line was drawn through the plotted points, the water content corresponding to 25-drops on this line is the liquid limit of the soil.

Plastic limit (PL) is the water content of a soil in percent at the boundary between the plastic and semi-solid states. The soil mass was rolled between the palm or fingers with sufficient pressure into a thread of uniform diameter of 3.2 mm throughout its length. The water content of the soil at this state is the plastic limit of it.

Plasticity index (PI) is the range of moisture content over which a soil behaves plastically. It is the difference between the liquid limit and the plastic limit. Fine sized part of the dam body material has an average liquid limit of 29 %, plastic limit of 18 % and plasticity index of 10 %, detailed results are given in Table 4.3.

Particle size distribution and Atterberg limits were evaluated according to the Unified Soil Classification System ASTM D 2487 – 11 in order to classify the soil. Dam body samples has coarse material fraction more than 50 % and contains sand more than 15 % and fine particles more than 12%. In order to determine if fine particles are clay or silt, the LL and PI of the soil is inspected on the plasticity chart given in Figure 4.7. Fine particles were found as clay, because the points of all samples fall above the "A line" and plasticity index is greater than 7. Therefore, the dam body sample was classified as clayey gravel (GC) with sand and cobbles.

Table 4.3 Atterberg limits of samples taken from dam body

	1st Sample	2nd Sample	3rd Sample	4th Sample
LL	30	26	28	30
PL	19	18	18	18
PI	11	8	10	12
	CL	CL	CL	CL

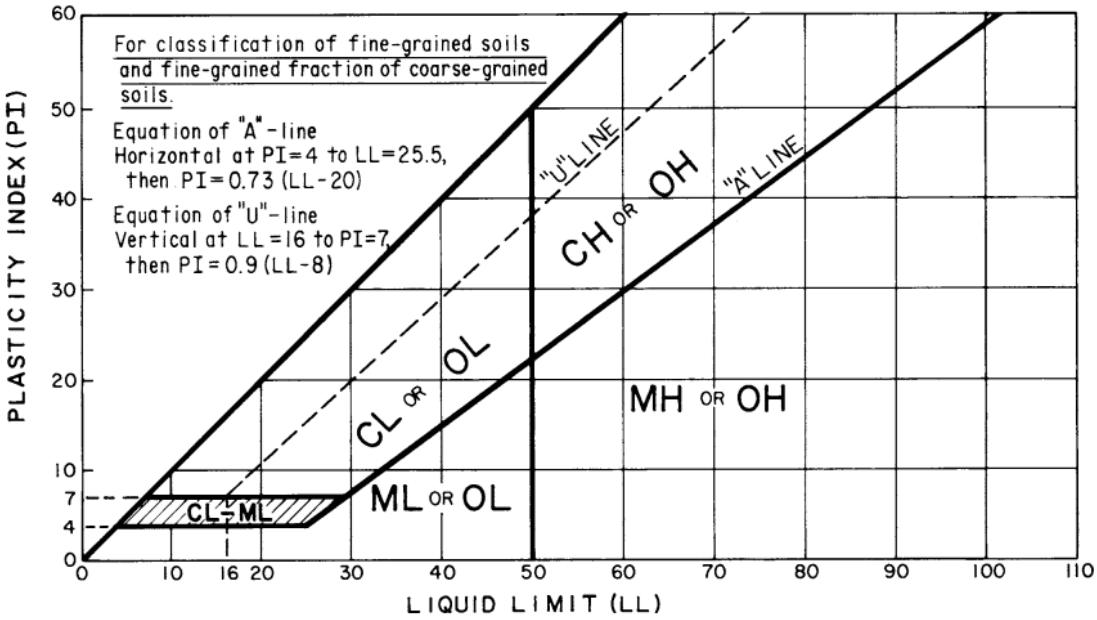

Figure 4.7 Plasticity chart (ASTM, D2487 – 11)

U.S. Army Corps. of Engineers (2003) stated that the soil liquefaction phenomenon, or significant soil strength and stiffness reduction as a result of shear-induced increase in pore water pressure, is one of the major causes of earthquake damage to embankments and slopes. Liquefaction instances have been mostly linked to saturated loose sandy or silty soils. Coulter and Migliaccio (1966); Chang (1978) and Youd et al. (1984) indicated loose gravelly soils are also vulnerable to liquefaction. Cohesive soils with more than 20% of particles finer than 0.005 mm, or with PI value equal to or greater than 14, or with LL value equal to or greater than 34 are generally considered not susceptible to liquefaction. With the aid of these information, it is concluded that the dam body is vulnerable to soil liquefaction.

4.2.1.4 **Standard Compaction Test**

In the construction of earth dams or other types of engineering structures, loose soils are compacted to a denser state. Compaction increases the unit weight and strength properties of soils. Moreover, compaction increases stability of embankment slopes. The degree of compaction is measured in terms of dry unit weight.

Laboratory compaction method was used to determine the correlation between moisture content and dry density of soils taken from different regions of the dam. In standard compaction testing, a compactive effort of 600 kN-m/m^3 is applied by the equipment. This method can only be applied to soils that have 30% or less by mass of soil retained on the $^3/_4$ –in. (19.0 mm) sieve and have not been previously compacted. The tests were done according to ASTM D698-07 standards. Three methods (method A,B,C) are provided for this test and method C is suitable for the material specification. 6 in. (152.4 mm) diameter mold was used. Soil material passing through $^3/_4$ –in. (19.0 mm) sieve was prepared at selected water content and placed in three layers into the mold; each layer was compacted by applying 56 blows. The procedure was repeated for a sufficient number of specified water contents to achieve a relationship between dry density and moisture content. Unified compaction curve for all samples is given in Figure 4.8.

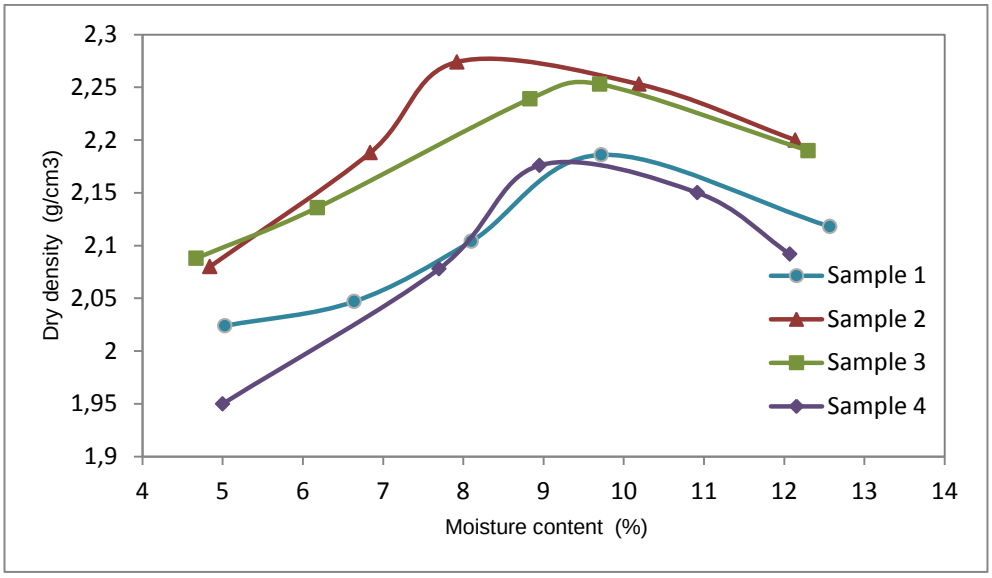

Figure 4.8 Standard proctor compaction curves for all samples

The maximum dry density value and the optimum moisture content at which the soil is compacted to this maximum dry density value were obtained from the compaction curve, and the obtained values are given in Table 4.4. The maximum dry density is corresponding to 100 percent compaction for the given soil under the given compactive effort.

Table 4.4 Optimum water content and max. dry density values

	1st Sample	**2nd Sample**	**3rd Sample**	**4th Sample**
Optimum Water Content , %	9,839	8,453	9,540	9,430
Max. Dry Density (g/cm^3)	2,187	2,277	2,252	2,180

4.2.1.5 **Direct Shear Test**

The shear strength of a soil is the resistance of the soil to interparticle movement. This resistance is derived from cohesion and friction. Cohesion is the attraction of one particle to another. Internal friction is the resistance to movement. The shear strength of a

granular soil is defined by equation 4.1. This equation is referred as the Mohr-Coulomb failure criteria. For saturated soils, the stress carried by the soil solids is the effective stress and equation 4.1 is modified to equation 4.2.

$$\tau = c + \sigma \tan \emptyset \tag{4.1}$$

$$\tau = c + \ \sigma - u \ \tan \emptyset = c' + \sigma' \tan \emptyset' \tag{4.2}$$

Where u is the pore water pressure, c' is the effective cohesion, and σ' is the effective stress on the failure plane at the failure.

The cohesion (c) and angle of internal friction (∅) depends on the stress history of the soil, current stress state, and the type of test. There are two types of shear strength test, drained and undrained. The drained shear strength represents the long-term condition where there is no increase in pore water pressure due to the applied load. The undrained shear strength represents the short-term conditions, or construction, where the water pressure does not have time to dissipate. (http:/www.dot.state.mn.us)

Coarse granular soils are generally used as fill material for earth-retraining structures and embankments due to their good drainage and compaction properties and high strength. Bauer & Zhao (1993) stated that the shear strength testing of coarse soils can be a problem because most testing equipment is of small size with respect to particle size in the soil. A 6x6 cm direct shearbox is not suitable for testing of coarse granular materials. Nakao and Fityus (2008) stated that to obtain reasonable shear strength parameters for coarse granular soils, the size of the shear box must be many times the size of the largest particle.

In order to determine effective cohesion (c') and effective internal friction angle (∅') values belonging to dam body as input parameters of the slope stability analysis, direct shear tests were conducted on the disturbed samples. The consolidated-drained test procedure was performed with regard to ASTM D3080M – 11 standards to measure the effective shear strength parameters. The consolidated-drained test is used to represent the long-term loading and drained conditions in the field. Complete drainage is allowed

during axial loading and shearing stages. Specimens are sheared by increasing horizontal shear load, slowly. The shear load is applied to the lower part of the box, while the upper part is restrained against horizontal movement. The soil is sheared slow enough, to drain the soil completely and to inhibit excess pore water pressures.

Undisturbed sampling was impossible for the embankment material and do not have special particle arrangements. In this case, the behavior of the material of a certain composition is primarily ruled by its density, which can be reconstituted in laboratory.In direct shear test, soil specimen is prepared with a specified compaction value. The required compaction amount is generally denoted between 90% and 95%. Das (1983) stated that in most specifications for earthwork, it is desirable to achieve a compacted field dry unit weight of 90-95 % of the maximum dry unit weight obtained in the laboratory by either modified or standard compaction test. Rolston et al. (2009) indicated the compaction requirement as 90% of the standard density. However, in Küre case no compaction was applied to the dam material at the construction stage. Therefore, a systematic approach was developed for specimen preparation. Initially placed material in the field, compacts maximum under the weight of upper layers. This compaction decreases towards to the upper parts of the dam. The tailings dam was divided into three main zones; it was assumed that each zone had a dry density of 70%, 80%, and 90% of the standard compaction test results according to its depth from surface. Samples at field moisture contents were created by adding water. The specimens were prepared by compacting the soil in three lifts within the shearbox, so that each lift had the same relative compression. The soil samples have 70%, 80%, 90% compaction values.

A 30x30cm square shear box was used (Figure 4.9) and the sample was reconstituted in the laboratory with 15 cm depth and according to proctor test results. ASTM D3080M – 11 standards the minimum specimen width to thickness ratio is designated as 2:1. In ASTM standard, it is stated that the minimum specimen width for square specimens must not be more than 10 times the maximum particle size and the minimum initial specimen thickness must be more than 6 times the maximum particle diameter. According to these information, maximum particle size was determined as 15/6=2.5 cm. Therefore, before testing commenced, the sample was screened to remove all particles greater than 2.5 cm.

The samples were tested under 360, 580 and 830 kPa. Normal stresses required for testing were estimated by dividing the applied load by the area of the shear box. Loads represent the weight of the rock overburden consistent with the depth of the sample in the embankment.

Figure 4.9 Direct shear box (30x30cm)

Tests were performed in a water bath and the sample was completely submerged in water to make sure that the samples had no cohesion. In order to measure drained strength parameters, the sample is firstly consolidated under normal load for 20 hours, before shearing it at a rate that is slow enough to ensure that significant excess pore pressures are not created within the sample.

In order to inspect the effect of compaction on shear strength the sample is tested under the same normal stress (580 kPa) and shearing rate. The results are given in Figure 4.10. The sample was compacted at a dry density 80% of maximum dry density obtained from proctor was failed at 466.650 kPa, whereas the sample with 90% dry density was broke down at 470.188 kPa. Therefore, it can be concluded that compaction assumption made in this study does not affect the stability analysis results much.

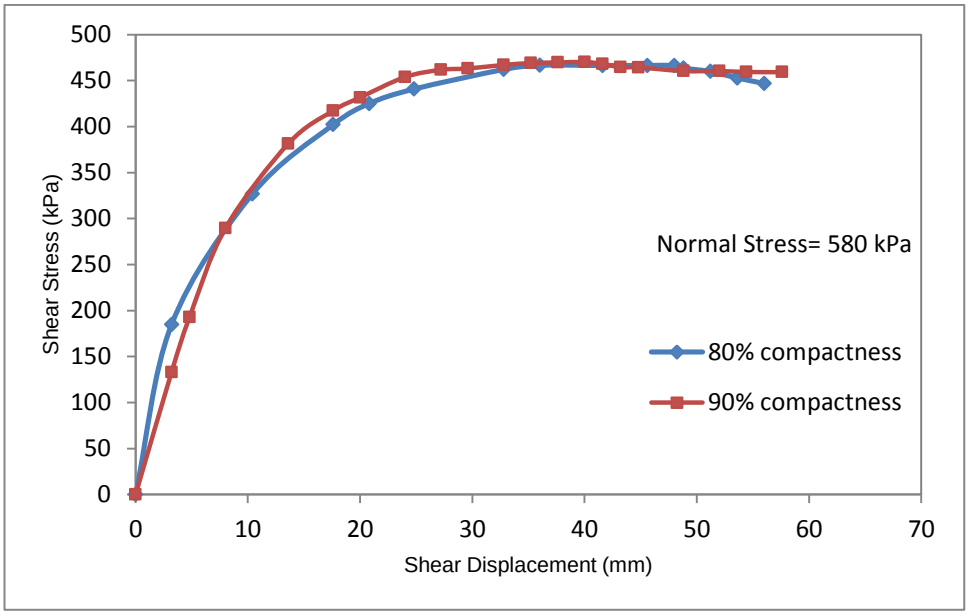

Figure 4.10 Shear Displacement vs. Shear Stress relationship for different compaction values

Based on discussions in Jewell & Wroth (1987) and Bauer & Zhao (1993), Mowafy (1986), Bauer et al. (1990b) it is generally accepted that a shearing rate of around 1 mm/min is appropriate for the shearing of granular backfills. The samples were sheared at a constant rate of 0.8 mm/min, which is suitable for this given information and shearing rate obtained from consolidation curves.

Peak shear strength and ultimate shear strength were obtained from shear stress versus shear strain plots (Figure 4.11). Effective internal friction angle and cohesion were determined by plotting the effective stresses at failure from Consolidated-Drained tests, both linear trendlines were drawn through the points. Mohr Coulomb failure criteria was used to represent the behaviour of the dam body material. In deterministic approach a single value should be selected for design from the scatter of test results (Wolff, 1985). Cohesion is the ordinate of the envelope and internal friction angle is the slope of the envelope.

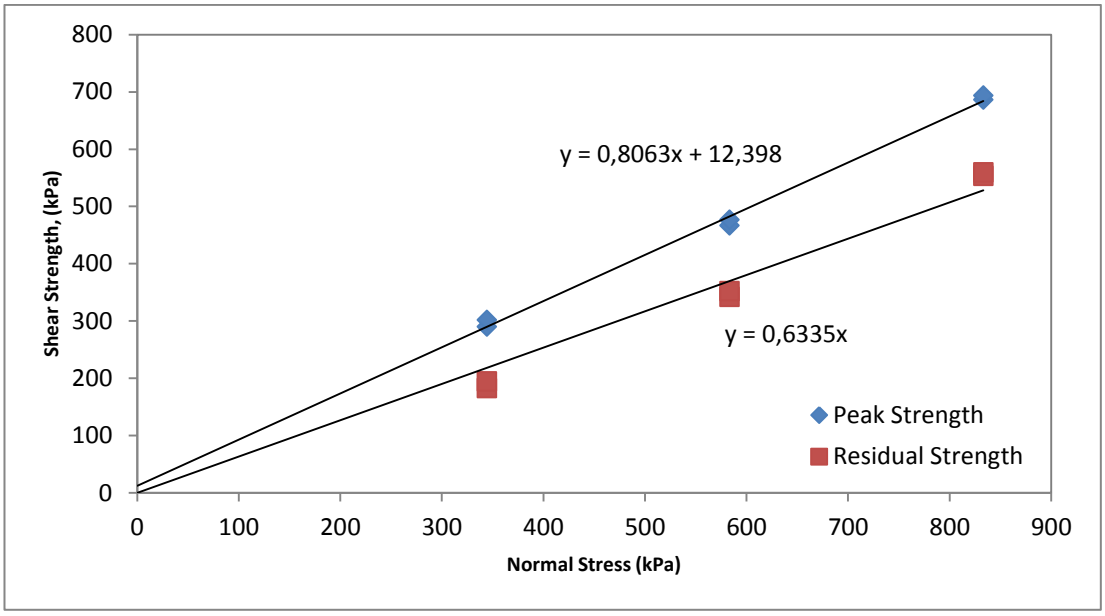

Figure 4.11 Failure envelopes for embankment material

Table 4.5 shows peak and ultimate cohesion and internal friction angle values for dam body. Typical friction-angle values for medium-dense sand is given in the range of 32º to 38º, while typical friction-angle values for medium-dense sandy gravel can range from 34º to 48º (Das, 1983). Moreover, for sand-sized material typical values of peak and ultimate internal friction angles are 28º to 60º (Holtz & Kovacs, 2003) and 26º to 35º (Das, 1983), respectively. The lower values are applied to round; loose sand and the higher values are for angular, dense sand.

Table 4.5 Peak and ultimate strength parameters of embankment material

	Peak	**Ultimate**
Effective Internal Friction Angle, Ø′ (º)	38.88	32.35
Effective Cohesion, c' (kPa)	12.4	0

4.2.2 Index and Geomechanical Properties of Tailings Material

The following experiments were conducted on disturbed samples taken from 2 different places of the tailings beach; moisture content, specific gravity, particle size analysis, Atterberg limits test, standard compaction test, one-dimensional consolidation test and direct shear test.

4.2.2.1 **Moisture Content and Specific Gravity**

Table 4.6shows the moisture content and specific gravity values for the tailings samples. Average moisture content of the samples was found as 36.57% (ranges from 35.11% to 38.03%). Specific gravity of the samples changes between 3.61 and 3.91, average specific gravity of the dam body was found as 3.76.

Table 4.6 Specific gravity and moisture content values of tailings samples

	1st T. Sample	**2nd T. Sample**	**Average**
Specific Gravity	3.91	3.61	3.76
Moisture Content, %	38.03	35.11	36.57

4.2.2.2 **Particle Size Analysis**

Particle size distribution of disturbed samples taken from tailings material was determined by the method of sieving and sedimentation according to ASTM D422 – 63 standards. Obtained particle size distribution curves are given in Figure 4.16. In accordance with this curves, tailings material was found to include sand (3.89 %) and fine size particles (96.11 %).

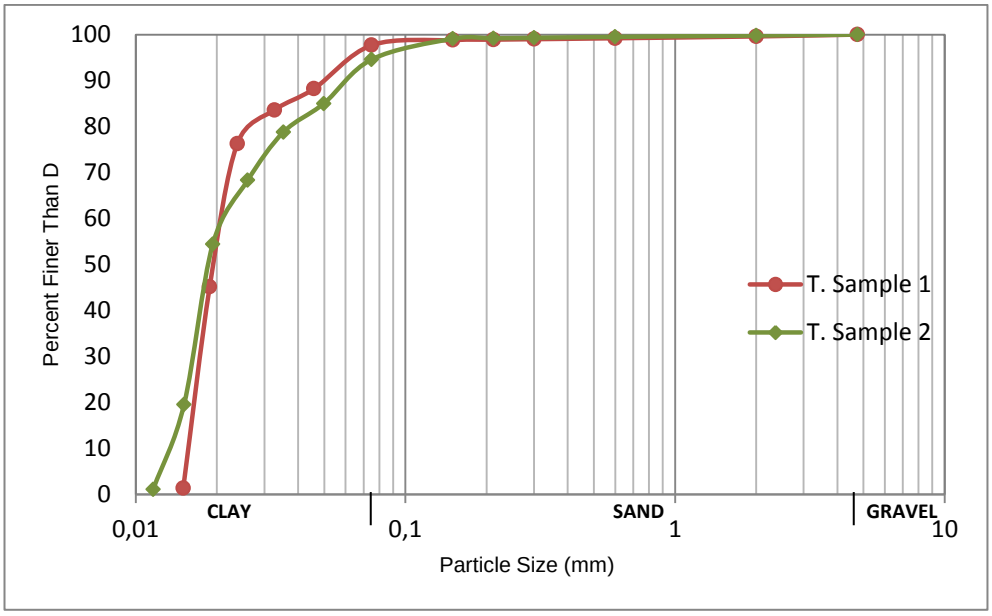

Figure 4.12 Particle size analysis of tailing samples

4.2.2.3 **Atterberg Limits and Soil Classification**

In order to determine the classification of the tailings material, Atterberg limits tests were conducted on 2 samples. According to test results, tailings material has an average liquid limit of 23%, plastic limit of 17% and plasticity index of 6%, detailed results are given in Table 4.7.

Table 4.7 Atterberg limits of samples taken from tailings material

	1st T. Sample	**2nd T. Sample**
LL	22	23
PL	15	18
PI	7	5
	CL-ML	CL-ML

Particle size distribution and Atterberg limits were evaluated according to the Unified Soil Classification System ASTM D2487 – 11, in order to classify the soil the chart given in Figure 4.7 was used. Soil was classified as a silty clay, CL-ML, because the position of the plasticity index versus liquid limit plot falls above the "A line" and the plasticity index is in the range of 4 to 7.

4.2.2.4 **Standard Compaction Test**

For tailings material, method A is suitable for the material specification that is less than 25% by mass of the material is retained on the No.4 (4.75 mm) sieve. 4 in. (101.6 mm) diameter mold was used. 6 in. (152.4 mm) diameter mold was used. Soil material passing through No.4 (4.75 mm) sieve was prepared at selected water content and placed in three layers into the mold; each layer was compacted by applying 25 rammer blows (ASTM, D698-07). The procedure is repeated for a sufficient number of specified water contents to achieve a relationship between dry density and moisture content. Figure 4.13 shows the obtained graphs from the experiment.

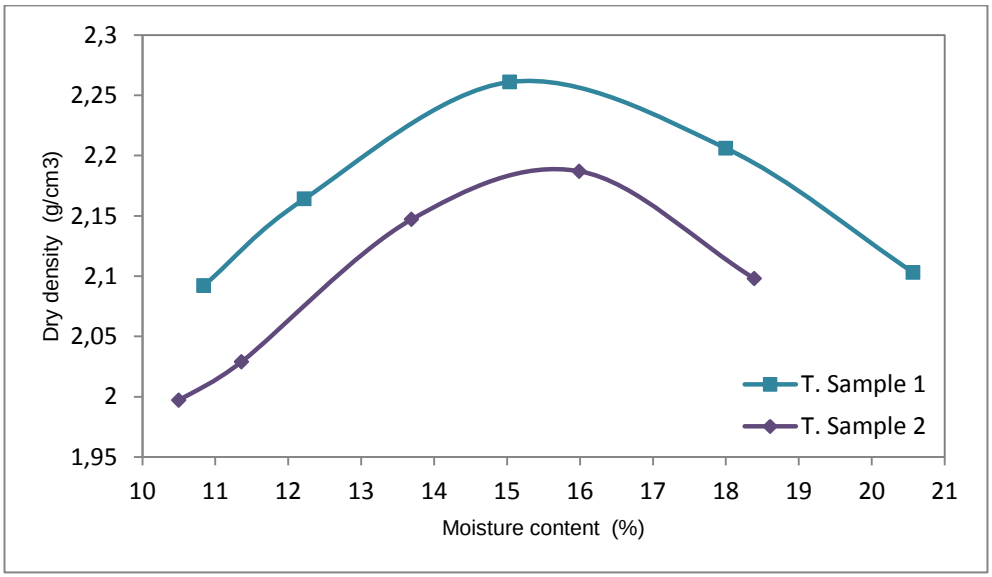

Figure 4.13 Standard proctor compaction curves for tailings samples

The maximum dry density value and the water content at which the soil is compacted to this maximum dry density value were obtained from the compaction curve, and the obtained values are given in Table 4.8. The maximum dry density is corresponding to 100 percent compaction for the given soil under the given compactive effort.

Table 4.8 Optimum water content and max. dry density values

	1st T. Sample	**2nd T. Sample**
Optimum Water Content , %	15.3	15.632
Max. Dry Density (g/cm^3)	2.263	2.19

4.2.2.5 **One-Dimensional Consolidation Test**

One-Dimensional consolidation tests were conducted in order to obtain modulus of elasticity, bulk density, moisture content of tailings material, under expected effective stresses at various depths existing in the field. Consolidation of loose tailings under their own weights is represented. Experiments were done according to ASTM D2435-M11 standards that provide information about consolidation magnitude of tailings when it is constrained laterally and drained axially while subjected to load increments (ASTM, D2435-M11). Test method A was performed by applying constant load increment for 24 hr and doubling the load at the end of 24 hr. Samples prepared at their natural moisture contents were loaded under 0.125, 0.25, 0.5, 1, 2, 4, 6 kg/cm^2 respectively at each loading step. Time-deformation readings were used to obtain void ratio and water content within the specimen, equation 4.3, 4.4, 4.5, 4.6 were used for these purposes, the results are shown in Table 4.6.

$$\rho_d = \frac{M_s/V_t}{1+w} \tag{4.3}$$

ρ_d: Dry density of soil (g/cm^3)

M_s: Mass of specimen (g)

V_t: Total volume of the specimen (cm3)

w: Water content of the specimen (%)

$$\rho = \frac{G_s\,(1+w)}{1+e}\,\rho_w \tag{4.4}$$

ρ: Bulk density of soil specimen

G_s: Specific gravity of soil particles

e: Void ratio

ρ_w: Density of water

$$\frac{\Delta H}{H_0} = \frac{\Delta e}{1+e_0} \tag{4.5}$$

$$e_0 = e_f + \Delta e \tag{4.6}$$

ΔH: Change in thickness of the specimen

H_0: Initial thickness of the specimen

Δe: Change in void ratio

e_0: Initial void ratio

e_f: Final void ratio

Vick (1983) stated that slimes of copper tailings generally have low to moderate plasticity and shows high in-place void ratios among 0.7 to 1.3. Volpe (1979) specified a range between 0.6 and 1.4 for copper tailings void ratio. The specimens were prepared with 1.36 and 1.224 void ratios respectively. Therefore, the initial specimen void ratio is suitable. Table 4.9 shows the void ratios during one-dimensional consolidation test.

Table 4.9 Void ratios of tailings samples during the consolidation

	e_0	$e_{0.5\ kg/cm^2}$	$e_{1\ kg/cm^2}$	$e_{2\ kg/cm^2}$	$e_{4\ kg/cm^2}$	$e_{6\ kg/cm^2}$
1st T. Sample	1.36	1.268	1.217	1.151	1.084	1.0256
2nd T. Sample	1.224	1.112	1.075	1.031	0.989	0.954
Average	1.292	1.19	1.146	1.091	1.0365	0.9898

According to consolidation test results, oedometer modulus was obtained for both samples. Modulus of elasticity of tailings material was derived from equations 4.7, 4.8, 4.9. Poisson's ratio was assumed as 0.3 according to Table A.5.

$$m_v = \frac{\Delta e}{1 + e_0} \frac{1}{\Delta \sigma'} \tag{4.7}$$

$$E_{oed} = \frac{1}{m_v} \tag{4.8}$$

$$E_{oed} = \frac{E_s}{1 + \upsilon} \frac{1 - \upsilon}{1 - 2\upsilon} \tag{4.9}$$

m_v: Coefficient of volume compressibility (cm2/kg)

$\Delta\sigma'$: Increase in effective stress (kg/cm^2)

E_{oed}: Oedometer modulus (kg/cm^2)

E_s: Modulus of elasticity (kg/cm^2)

υ: Poisson's ratio

The relationship between applied load and oedometer modulus is given in Figure 4.14. It shows good agreement with the results of a study with similar mixture percentages (Figure 4.15).

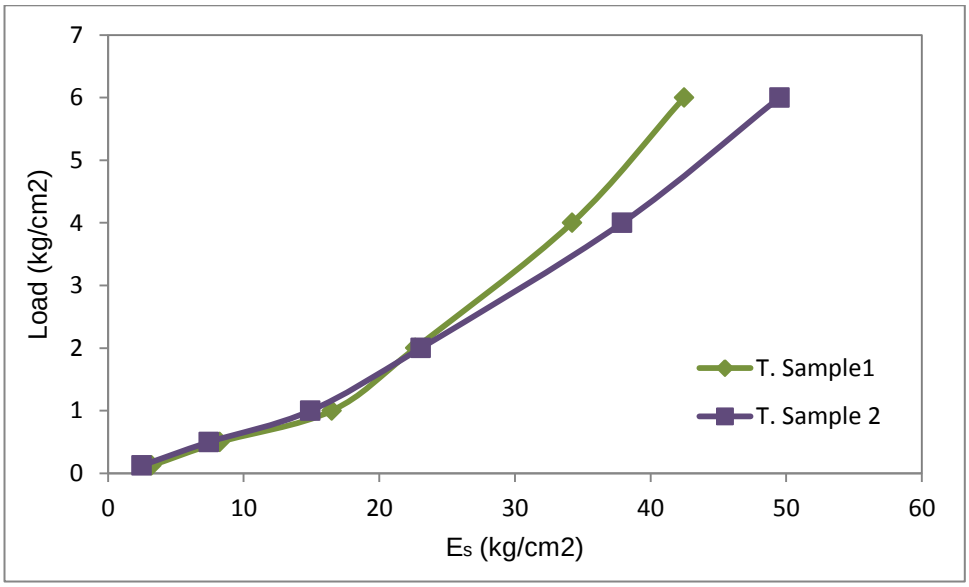

Figure 4.14 Variation of oedometer modulus E_s values with respect to loading conditions

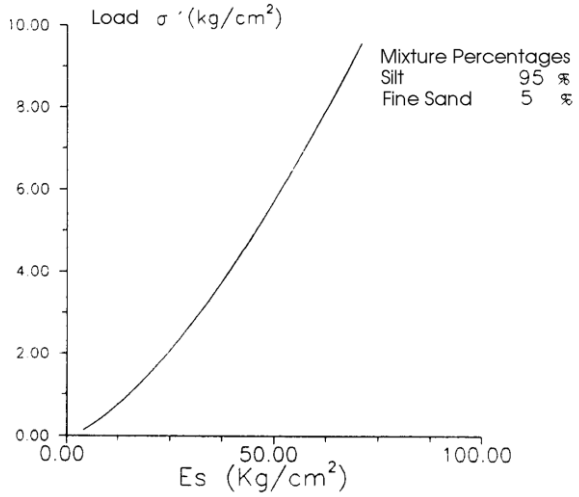

Figure 4.15 Variation of oedometer modulus with respect to loading values for 95% silt and 5% sand condition (Grammatikopoulos et al.)

Modulus of elasticity values were determined according to the depth it presents. In this respect tailings material was divided into three layers, Table 4.10 shows the obtained values.

Table 4.10 Modulus of Elasticity values for layers of tailings material

Layers	Modulus of Elasticity (kPa)
1	13531.62
2	9386.96
3	4510.54

4.2.2.6 **Direct Shear Test**

Consolidated-drained direct shear test was performed on disturbed samples in accordance with ASTM D3080M – 11 standards, so as to define the input parameters for tailing dam stability analysis, cohesion (c') and internal friction angle (Ø'). Disturbed soil specimens were reconstituted in the laboratory into the (6x6x2) cm shearbox in order to obtain samples with natural water contents and unit weights. Samples with

different moisture content and bulk density prepared according to the data obtained from one-dimensional consolidation test. Tests were held under three different stress levels; 180, 360, and 530 kPa normal pressures.

For the sake of drainage throughout the test, an appropriate shearing velocity must be chosen. The rate of shear displacement generally affects peak strength more than residual strength (Thiel, 2012). The strain rate must be slow enough to give representative results of long term shear conditions. In order to determine the shearing rate samples with the same properties were tested under the same normal loads and different shearing rates, namely 0.0122 mm/min and 0.122 mm/min. Figure 4.16 shows the relationship between shear strength and shear displacement for both velocities. Because of the tailings material is mostly composed of silt, there is no problem in drainage and the same shear strength value was obtained for both of the velocities. This means all the shearing rates in this range is suitable for the experiments, therefore 0.122 mm/min rate was selected.

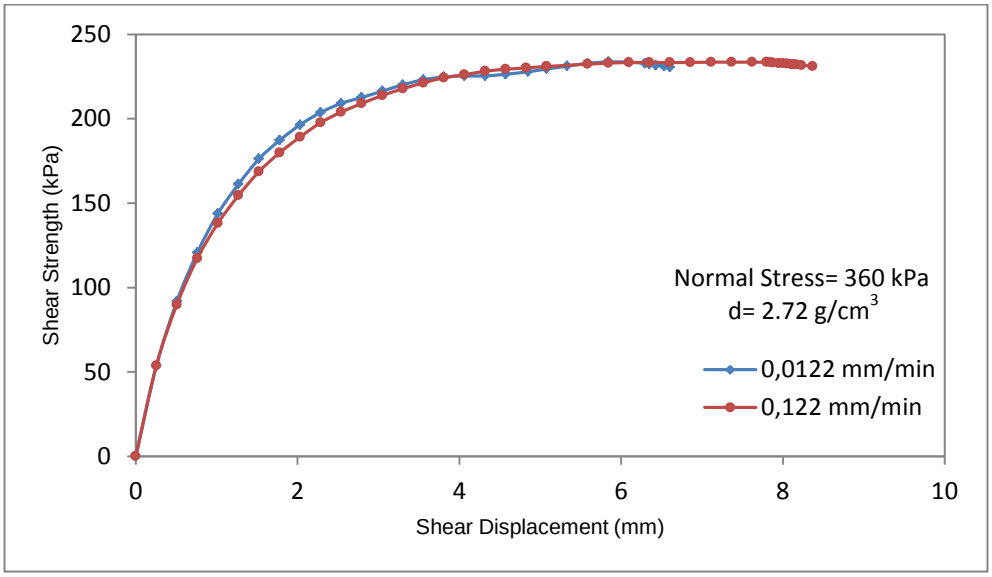

Figure 4.16 Shear strength versus shear displacement relationship for T.sample 1 for different shearing rates

Peak and residual failure envelopes for soil specimens from direct shear test data is plotted in Figure 4.17. Peak and residual strength parameters of tailings material are

given in Table 4.11. Peak friction angle and residual friction angle are nearly the same; however, cohesion values are very different.

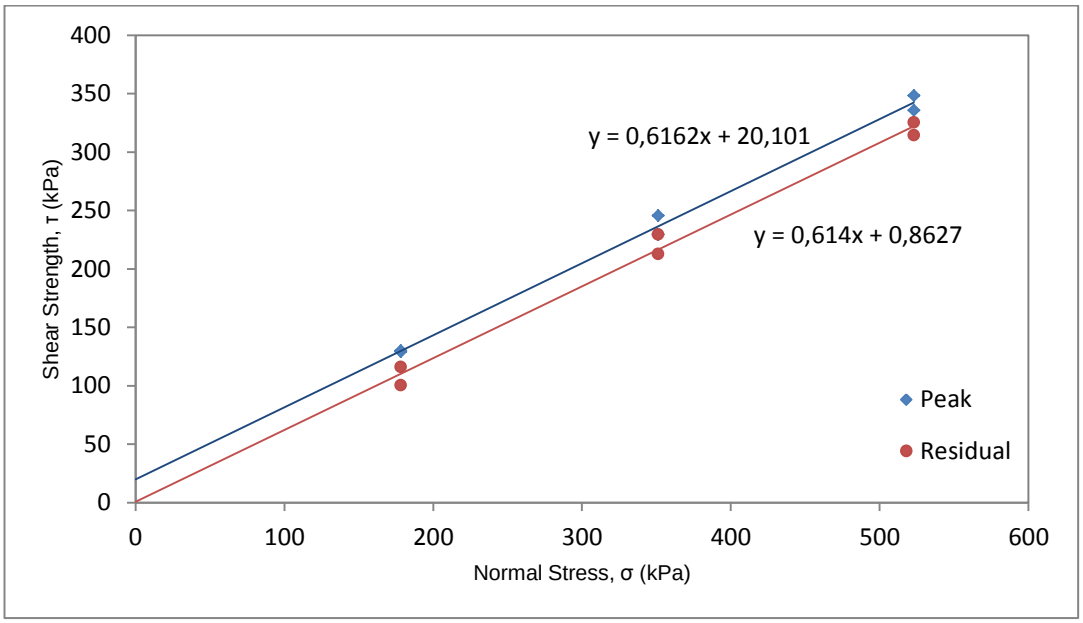

Figure 4.17 Failure envelopes for tailings samples

Table 4.11 Peak and residual strength parameters of tailings material

	Peak	**Residual**
Effective Internal Friction Angle, $\emptyset'$ (^{o})	31.64	31.55
Effective Cohesion, c' (kPa)	20.101	0.8627

In literature, it is stated that, tailing materials are generally cohesive and their internal friction angle is between 30^o-36^o (CANMET, 1977). The obtained internal friction angle values are consistent with these values, and with the values stated in Table 4.12 and Table 4.13.

Table 4.12 Internal friction angle and cohesion values (Shamsai et al., 2007)

Material	Initial void ratio (e_0)	Friction angle $\emptyset$ (^{o})	Cohesion, C_{cu} (kg/cm^2)	Source
Copper tailings, all types	-	13-18	0-0.98	(Volpe, 1979)
Copper beach sands	0.7	19-20	0.34-0.44	(Wahler, 1974)
Copper slimes	0.6	14	0.64	(Wahler, 1974)
Copper slimes	0.9-1.3	14-24	0-0.2	(Wahler, 1974)
Copper whole tailings	0.5-1.1	8-29	0.30-0.97	(Shamsai et al., 2007)
Copper slimes	0.5-1.1	24-37	0.08-0.21	(Shamsai et al., 2007)

Table 4.13 Typical values of drained friction angle $\emptyset'$ of tailings (Zardari, 2011)

Material	$\emptyset'$ (^{o})	Effective Stress Range (kPa)	Source
Copper sands	34	0-816	(Mittal & Morgenstern, 1975)
Copper sands	33-37	0-672	(Volpe, 1975)
Copper slimes	33-37	0-672	(Volpe, 1975)
Gold slimes	28-40.5	960	(Blight & Steffen, 1979)

4.3 Laboratory Experiments on Rock Samples

In order to obtain the characteristics of foundation material below the dam, several laboratory experiments were performed on rock samples. These are; density-porosity test, uniaxial compressive strength test and triaxial compressive strength test.

4.3.1 Density-Porosity Test

Density is the mass per unit volume of rock and it is often related to the porosity of the rock. It is also defined by unit weight and specific gravity. Density is a physical property

and it is influenced by the specific gravity of the composition minerals and the compaction of the minerals. Density and porosity affects the strength of rock material. The rock with low density and high porosity usually has low strength. Porosity gives information about how densely the material is packed. It is the ratio of the pore volume to the total volume of material; therefore, porosity is a fraction between 0 and 1. There is an indirect proportionality between density and porosity of rock. That is, the higher the density of a rock, the lower the porosity of rock.

In order to determine density and porosity of foundation material 34 regular and 26 irregular rock specimens were tested. Average porosity of the rock is 3.385% and average unit weight of the rock is 26.65 kN/m^3.

4.3.2 Uniaxial and Triaxial Compressive Strength Test

These experiments were performed in accordance with (ASTM D7012–10, 2010) standards to designate the strength properties of intact rock core specimens in uniaxial and triaxial compression. The uniaxial compressive strength tests provide data about the uniaxial strength, shear strength, internal friction angle, cohesion, Young's modulus and Poisson's ratio. In ASTM Standards, acceptable specimen length to diameter ratio is determined as between 2.0-2.5. Specimens with a length to diameter ratio less than 2.0:1 are undesirable.

Deformation controlled uniaxial compressive strength test was conducted on 5 rock specimens and UCS of the rock was obtained as 85.2 MPa. Modulus of elasticity (E) and Poisson's ratio (υ) were obtained as 20.652 GPa and 0.423, respectively.
Triaxial testing was conducted on 6 specimens, as a result of the tests cohesion (c) and internal friction angle (∅) were found as 14.66 MPa and 55.23^o, respectively.

CHAPTER 5

TAILINGS DAM STABILITY ANALYSIS

5.1 Finite Element Method

In the slope stability assessment, the factor of safety is of primary importance in order to determine how close the slopes to failure. The factor of safety is the ratio of actual soil shear strength to the required minimum shear strength to prevent failure or the factor by which the shear strength is reduced to result in slope failure (Duncan, 1996).

Traditional limit equilibrium analyses are the most commonly used technique; however the Finite Element Method (FEM) has become an alternative method, recently (Hammah et al., (n.d.)). The main assumption of limit equilibrium methods is that failure occurs through sliding of a block or mass along a slip surface (Rocscience Inc., 2004). The popularity of limit-equilibrium methods comes from their simplicity, ability to evaluate the sensitivity of stability to input parameters. Limit-equilibrium methods utilize minimum input data. Resulted factor of safety values for excavations and slopes usually ensure that deformations are within reasonable range. Despite its benefits, the limit equilibrium approach has some prominent deficiencies. The technique ignores stress-strain behavior of rocks and soils. As well, it makes arbitrary assumptions to provide statically determinate condition.

Finite Element Method is a powerful tool to analyze stresses and displacements in the embankment and foundation (Hammah et al., (n.d.)). The Shear Strength Reduction (SSR) method allows the FEM to calculate factor of safety for slopes. Despite of the benefits of SSR technique, it has not found widespread application for slope stability analysis because of limited information about the technique (Hammah et al., (n.d.)).

FEM can take into account staged construction and variation of material properties in

embankment material and foundation. The SSR method provides several advantages such as prediction of stresses, deformation of support elements at failure, and visualization of development of failure mechanisms (Hammah et al., (n.d.)). The SSR method is particularly useful when several different failure modes are possible, because this method automatically finds the critical mechanism. Dawson et al. (1999), Griffiths et al. (1999) and Hammah et al. (2004) utilized the SSR technique to calculate factors of safety for slopes.

Hammah et al.(n.d.) inspected the effects of Young's modulus (E), Poisson's ratio (υ), angle of dilation (ψ), and two models of post-peak material behavior. These parameters are absent from limit-equilibrium analysis and this study helps to identify the assumptions in limit equilibrium analysis. The first assumption of the limit equilibrium analysis is the elastic-perfectly plastic strength model, which supposes that the post-peak strength is the same as peak strength. The authors tested the impact of Poisson's ratio and Young's modulus. These parameters significantly influence the deformation magnitude; however, they had minimum effect on factor of safety values (Hammah et al., (n.d.)). Hammah et al. (n.d.) and Griffiths & Lane (1999) indicated that the angle of dilation does not have significant effect on slope stability due to low confinement environment. Material stiffness parameters affect deformation patterns and failure mechanisms that may differ significantly from limit equilibrium solution (Hammah et al.(n.d.)).

In SSR analysis, instability of the model or non-convergence determines if a slope has failed or not. The convergence of a FEM is characterized by three factors; (i) the stopping criterion, (ii) the tolerance value of the stopping criterion, and (iii) the number of iterations before a solution is converged.

In the SSR method slope materials are assumed as elasto-plastic material and material shear strength parameters are progressively reduced until failure occurs (Rocscience Inc., 2004). For Mohr-Coulomb material shear strength is lessened by factor of safety (F) is determined from the following equation (Rocscience Inc., 2004).

$$\frac{\tau}{F} = \frac{c'}{F} + \frac{\tan \emptyset'}{F} \qquad (5.1)$$

The basic algorithm of SSR method for Mohr-Coulomb materials is given by (Rocscience Inc., 2004) as follows.

Step 1: Develop a finite element model and find the maximum total deformation in the slope.
Step 2: Increase the value of safety factor by F and calculate the factored material properties with the above formula. Enter the new strength parameters into the model and compute to find the maximum total deformation.
Step 3: Repeat step 2 until the slope fails. The slope factor of safety is the F value after which failure occurs.

There are various constitutive models available in PHASE 2 v.8.01, these are Mohr-Coulomb, Hoek-Brown, Drucker-Prager, Generalized Hoek-Brown, Cam-Clay and Modified Cam-Clay. The selection of a model depends on the mechanical properties and history of the soil and stress changes that will take place in the future (Wood, 1990). Formerly, Mohr-Coulomb model (Olalla & Cuellar, 2001 and Gens & Alonso, 2006) and Modified Cam-Clay model (Priscu, 1999) were employed for numerical analysis of tailings dams. These models were utilized by considering that they were applicable to the tailings material (Zardari, 2011). Soils are complex materials showing anisotropic, non-linear and time-dependent behavior for different stress levels.

5.1.1 Advantages of Finite Element Method

Finite element SSR method presents a number of benefits over traditional limit-equilibrium analysis. Firstly, it eliminates the assumptions on failure mechanisms such as type, shape, and location of failure surfaces. However, the SSR technique establishes the critical failure mechanism automatically. Another advantage of SSR method is that it eliminates the assumptions about the locations and inclinations of inter-slice forces. Moreover, by entering the correct deformation properties of materials, the finite element method can estimate the deformations at the stress levels within the slope (Rocscience Inc., 2004). Additionally, the finite element method can model construction sequences, for example, staged construction of an embankment can be modeled in stages, moreover,

can be applied with complex slope configurations and soil deposits. Finally, SSR method can be more easily applied to 3D slope modeling the limit-equilibrium methods (Rocscience Inc., 2004).

The method can be utilized to clarify seepage induced failures, field soil properties, brittle soil behaviors, and engineering applications such as geotextiles, drains, soil nailing, retaining walls (Swan & Seo, 1999). FEM can give information about the strains within the body at working stress levels and can monitor overall shear failure (Griffiths D. V., 1999)

5.2 Determination of Characteristics of Tailings, and Embankment Material

Tailings material is discharged peripherally through spigots to the tailings dam, which are located at multiple points with regular intervals along the embankment crest. This type of discharging is used to achieve a uniform tailings flow, which will create uniform beaches (U.S. Environmental Protection Agency, 1994). Spigotting constitutes a gently sloping beach, where the coarsest fraction settles down near the discharge point and the particles becomes finer away from the discharge points. Figure 5.1 shows the working principle of the dam.

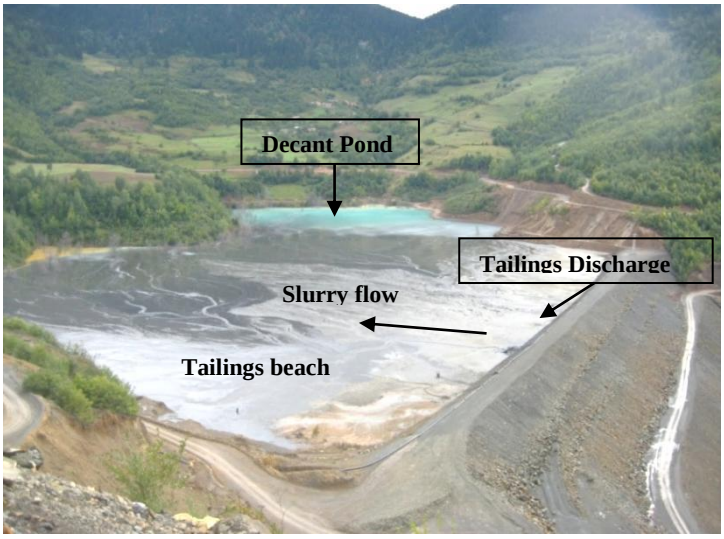

Figure 5.1 Working principle of the dam.

As a result of this variable gradation; permeability, shear strength and the density of the settled particles decreases with increasing distance from the discharge point (U.S. Environmental Protection Agency, 1994). This variable gradation could reduce the phreatic surface within the embankment. However, observations of actual permeability, particle size and shear strength distribution shows that this ideal gradation cannot be achieved in practice (Vick, 1990). Figure 5.2 shows the difference in soil characteristics with respect to the distance from spilling location. Moreover, beaches provide structural stability to the main embankment meanwhile create a long seepage path from the pond to the dam (Lighthall et al., 1989).

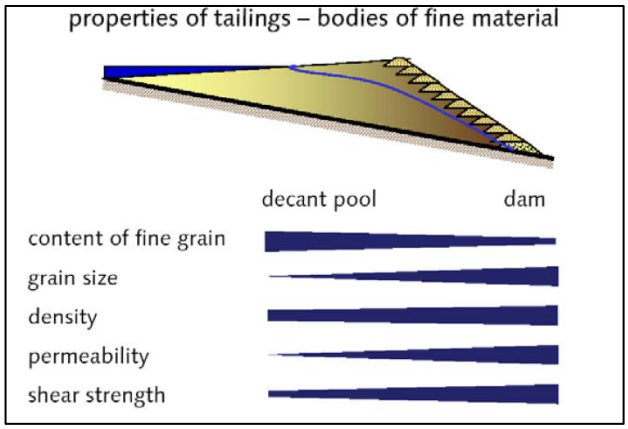

Figure 5.2 Behaviour of soil characteristic quantities in dependency of the spilling location (Witt et al., 2004)

The saturation line within a tailings dam is of significant importance in dam safety and the analysis of seepage field is a crucial problem in stability analysis of earthfill dams. The phreatic surface and pore-water pressure are determined with the help of finite element method.

The grain size distribution of the tailings near the embankment is very important for the permeability during the precipitation of the fine material of the slurry. The difference in permeability of embankment material and tailings has a considerable effect on the location of phreatic surface (Figure 5.3).

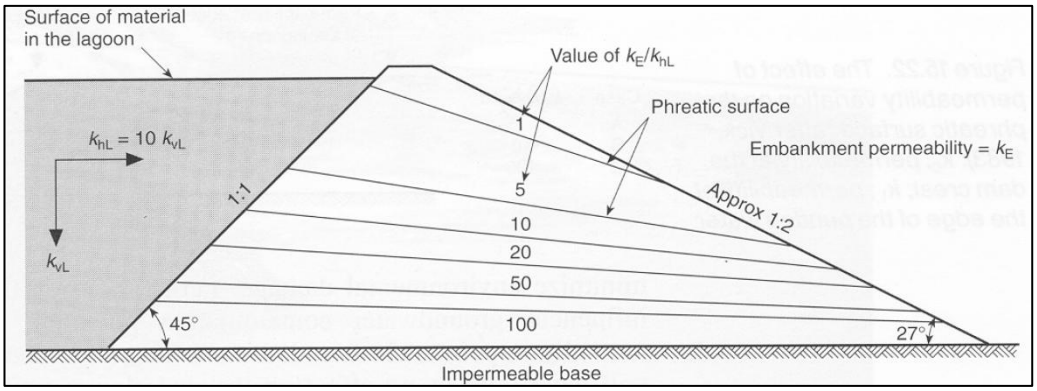

Figure 5.3 The location of phreatic surface within an embankment (Vick, 1990)

Generally tailings is composed of two parts; finer than 0.074 mm (no.200 sieve) and coarser than 0.074 mm, which are called tailings slimes and sand tailings respectively (Shamsai et al., 2007). Therefore, the tailings dam can be subdivided into three groups; the fine material, transmission zone and the coarse embankment material (Figure 5.4, Figure 5.5). Hydraulic conductivity of the sandy coarse material and the fine material can vary by more than 3 orders of magnitude (Witt et al., 2004). Volpe (1979) recommends that the variation in average permeability with distance is not significant, only about a factor of 10.

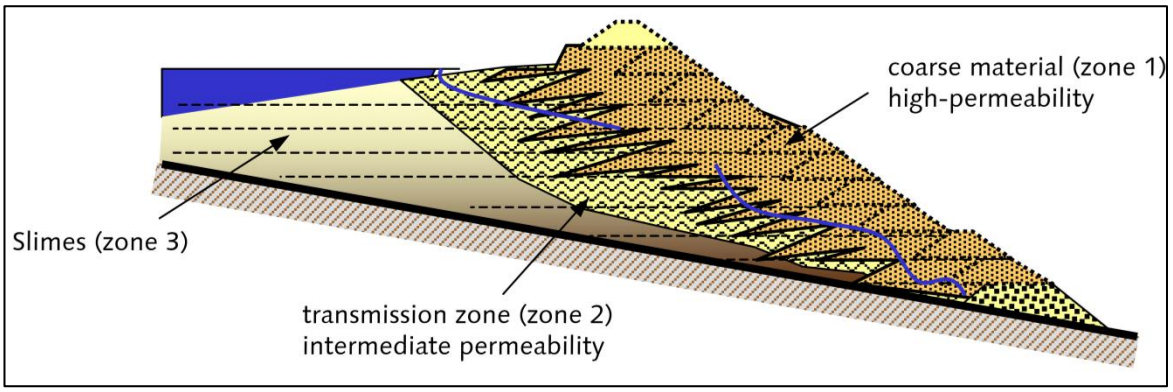

Figure 5.4 Conceptual model of permeability variation and phreatic surface within a tailings deposit (Witt et al., 2004)

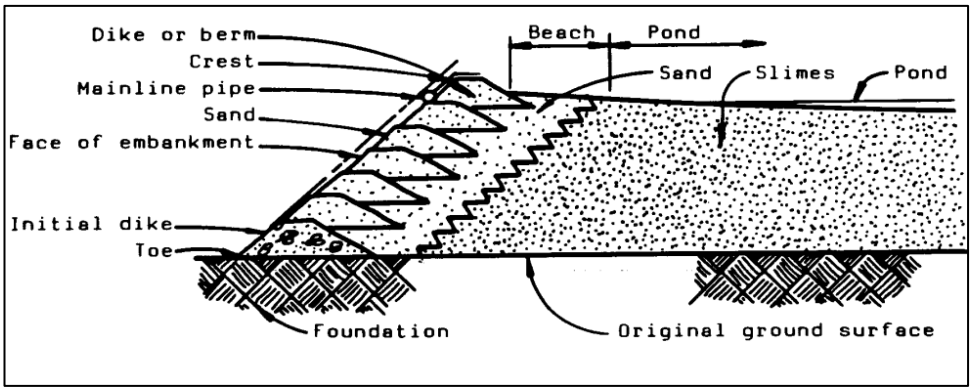

Figure 5.5 Schematic view of sand and slime boundary in tailings impoundment (IDAHO Department of Lands, 2012)

Because of their layered nature, tailings deposits exhibit considerable variation in permeability between horizontal and vertical directions, k_h/k_v is in the range of 2-10 for rather uniform beach sand deposits and for underwater –deposited slimes zones (Vick, 1983). Transition zones are likely to have high anisotropy ratios because of interlayering of coarse and fine particles, and the k_h/k_v ratio is 100 or more (Vick,1983). Bagarello (2009) stated that, this ratio reaches to 2 for sandy-loam soil. This k_h/k_v value was used for tailings material. Whereas the permeability of embankment material is assumed to be less anisotropic, and a ratio of k_v/k_h =0.8 is adopted (Saad & Mitri, 2011). The hydraulic conductivity decreases with increasing distance from the discharge point. This is because of the material becomes finer away from the discharge point.

The saturated hydraulic conductivity of copper tailings and copper slimes were chosen according to Figure 5.6, with the aid of information on Table 4.9. Vick (1990) stated that the ratio of permeability of coarser part (K_o) and finer part (K_s) is generally in range of 1-100 for mine tailings. The hydraulic conductivity of tailings in the slime zone is assumed one order of magnitude lower than the tailings in the beach zone; address to Abadjiev (1976), Vick (1983), and Witt (2004) (Saad & Mitri, 2011). During the analyses, saturated hydraulic conductivity of rock-fill part was assumed as the same with the hydraulic conductivity of coarse tailings, because of the intrusion of tailings material into the dam. Table 5.1 shows determined average hydraulic conductivity values for the model that are consistent with the values in Table 5.2

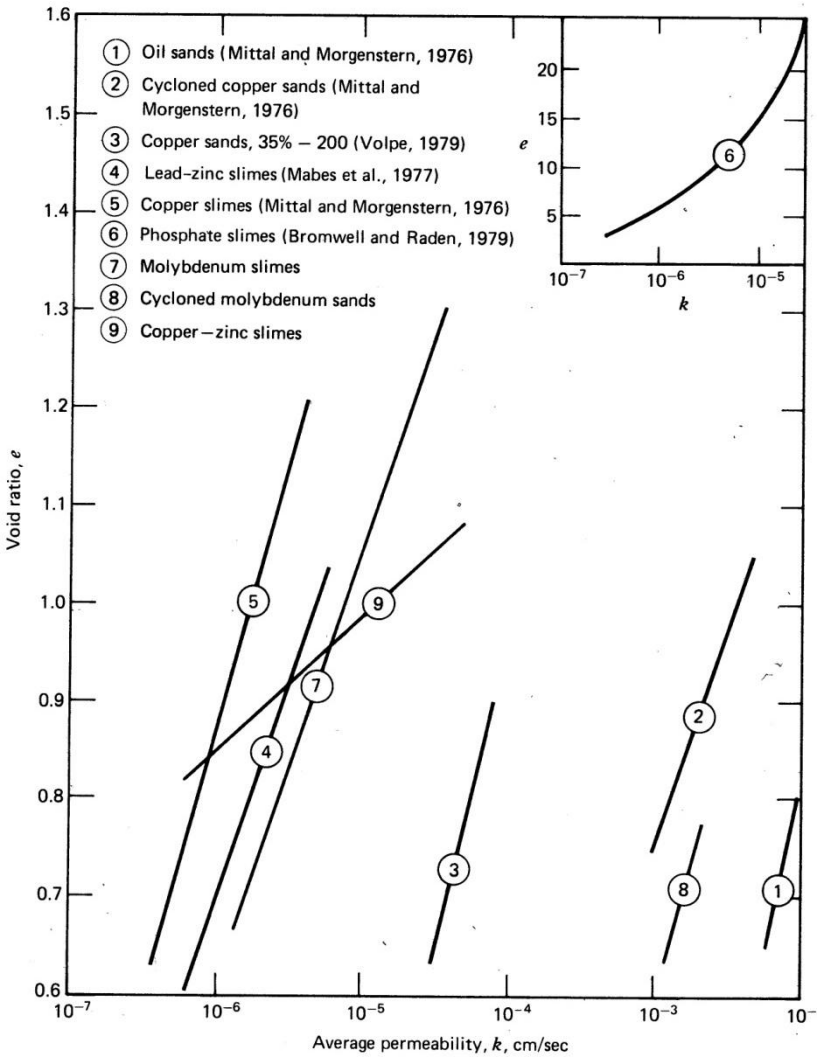

Figure 5.6 Variation in hydraulic conductivity as a function of void ratio (Vick, 1983)

Table 5.1 Average hydraulic conductivity values for beach sands and slime zone

Layers	Hydraulic Conductivity of slimes (cm/sec)	Hydraulic Conductivity of beach sand (cm/sec)	Hydraulic Conductivity of rockfill (cm/sec)
1	5.95×10^{-8}	5.95×10^{-7}	5.95×10^{-7}
2	8.95×10^{-8}	8.95×10^{-7}	8.95×10^{-7}
3	3.37×10^{-7}	3.37×10^{-6}	3.37×10^{-6}

Table 5.2 Typical permeability coefficients for various materials (modified from Hough (1957))

	Particle Size Range (mm)		**Effective Size (mm)**	**Permeability Coefficient (cm/sec)**
	D_{max}	D_{min}	D_{15}	k
Clean, fine to coarse gravel	80	10		10
Fine, uniform gravel	8	1.8		5
Uniform, coarse sand	2	0.5	0.6	0.4
Uniform, medium sand	0.5	0.25	0.3	0.1
Uniform, fine sand	0.25	0.05	0.06	$40x10^{-4}$
Silty sand	2	0.005	0.01	10^{-4}
Uniform silt	0.05	0.005	0.006	$0.5x10^{-4}$
Sandy Clay	1.0	0.001	0.002	$0.05x10^{-4}$
Silty Clay	0.05	0.001	0.0015	$0.01x10^{-4}$
Clay (30-50% clay sizes)	0.05	0.001	0.0008	$0.001x10^{-4}$

Jointed andesite that is resting below the tailings dam, the average porosity of the andesite is found as 3.385%. According to Table 5.3, permeability coefficient of foundation material is found as 10^{-9} cm/sec.

Table 5.3 Typical permeability coefficients for rock and soil formations[a] (Hunt, 2005)

	k (cm/s)	Intact Rock	Porosity *n* (%)	Fractured Rock	Soil
Practically impermeable	10^{-10} to 10^{-7}	Massive low-porosity rocks	0.1–0.5 0.5–5.0		Homogeneous clay below zone of weathering
Low discharge, poordrainage	10^{-6} to 10^{-3} (Sandstone)	Weathered granite Schist	5.0–30.0	Clay-filled joints	Very fine sands, organic and inorganic silts, mixtures of sand and clay, glacial till stratified clay deposits
High discharge, free draining	10^{-2} 10^{-1} 1.0 10^{1} 10^{2}			Jointed rock Open-jointed rock Heavily fractured rock	Clean sand, clean sand and gravel mixtures Clean gravel

[a] After Hoek, E. and Bray, J.W., *Rock Slope Engineering*, Institute of Mining and Metallurgy, London, 1977.

The Mohr-Coulomb failure criteria was chosen for all materials (tailings, foundation, rockfill) in the model. The Mohr-Coulomb model is an elastic-plastic model, which contains five model parameters Poisson's ratio, modulus of elasticty, angle of dilation, internal friction angle and cohesion. These parameters except Poisson's ratio and angle of dilation were obtained from laboratory tests. In his research, Azadegan (2012) obtained nearly the same shear strength parameters for clayey gravel. Therefore, modulus of elasticity and poisson's ratio values for embankment were taken from his study, which are 150,000 kPa and 0.35, respectively. These values are also in agreement with the values given in Table A.1, Table A.2, Table A.3, Table A.4. The angle of dilation is assumed as zero; an acceptable assumption for loose soil which composes the major portion of the dam (Zardari, 2011). Although the stiffnes of soil increases with depth, this stress dependency was not included in the model.

The Mohr-Coulomb failure criteria is suitable for the stability analysis of dams, slopes and embankments. Nevertheless, the model does not show softening behaviour after peak strength. The soft soils such as normally consolidated clays, usually give a decreasing mean effective stress during shearing, whereas the the Mohr-Coulomb model shows a constant mean effective stress (Zardari, 2011).

5.3 2-D Finite Element Analysis of Eti Copper Mine Tailings Dam

5.3.1 Long Term Stability Analysis of Existing Dam

The recently increased tailings dam stability and alternative dam geometries that is planned to be increased were analyzed under static loading conditions. Besides, the effects of ponded water level and slime-sand boundary position on stability were also analyzed. Long-term stability analysis was evaluated with PHASE 2 v.8.01 for the tailings dam. Shear strength reduction method was used for the stability analysis for plane strain analysis. The middle section of the dam was analyzed with finite element method to evaluate the stability of the dam. The location of the cross section can be seen in Figure 5.7, the results of the analyses are given in following sections in detail. The embankment has approximately 126m height. For the modeling phase, both the embankment and the tailings part were divided into three layers according to their depth and construction date. Each of the layers of the embankment is almost 40m. For the tailings part, it was assumed that firstly accumulated tailings composes the first layer, the remaining part was divided into two equal layers.

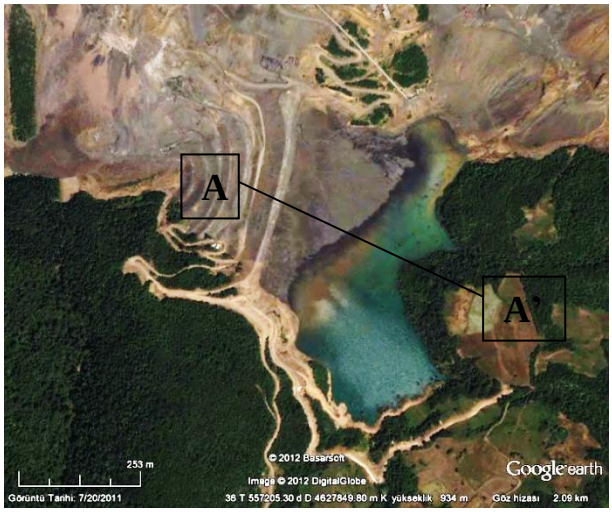

Figure 5.7 Analyzed cross-section of the dam (Google Earth, 2011)

It was assumed that the dam body is composed of only one type of material, because the dam is constructed of dump material of the mine. Therefore, material properties are uniform throughout the whole dam in the constructed model.

The Swedish safety guidelines document GruvRIDAS (2007) suggests a minimum safety factor of 1.5 for the stability of tailings dams at the end of construction and during normal operation conditions. Moreover, U.S. Army Corps. of Engineers (2003) recommends the same factor of safety value for the downstream slope for long term conditions (Table 5.4).

Table 5.4 Minimum required factors of safety: new earth and rock-fill dams (U.S. Army Corps. of Engineers, 2003)

Analysis Condition	**Required Minimum Factor of Safety**	**Slope**
End-of-Construction (including staged construction)	1.3	Upstream and Downstream
Long-term (Steady seepage, maximum storage pool, spillway crest or top of gates)	1.5	Downstream
Maximum surcharge pool	1.4	Downstream
Rapid drawdown	1.1-1.3	Upstream

Figure 5.8 shows the representation of the model, each of the layers in dam and tailings is indicated with different colors. Material properties that are used as input parameters in Phase 2 v.8.01 are given in Table 5.5 and Table 5.6. Unit weight, hydraulic conductivity and modulus of elasticity values were taken different for different layers and the rest of the properties were the same for the layers.

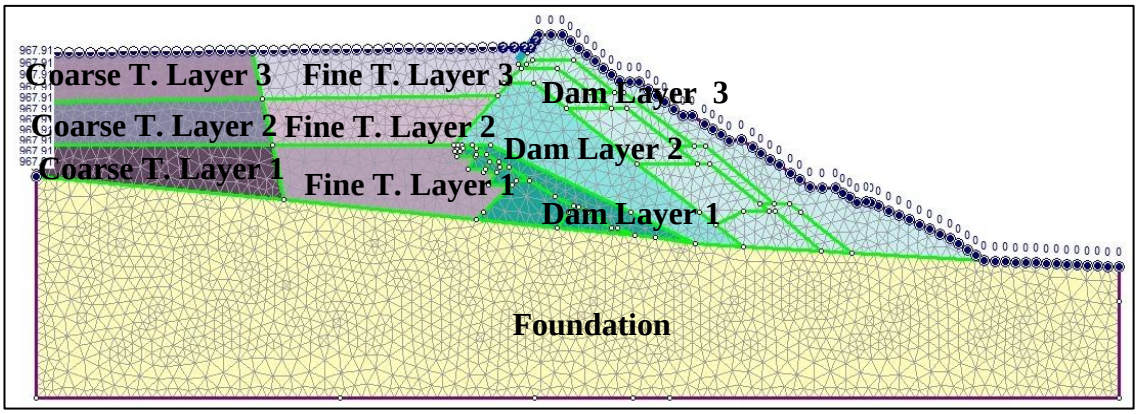

Figure 5.8 Representation of the model

Table 5.5 Material properties used in Phase 2 analysis

Paramaters	**Fine Tailings Layer-1**	**Fine Tailings Layer-2**	**Fine Tailings Layer-3**	**Coarse Tailings Layer-1**	**Coarse Tailings Layer-2**	**Coarse Tailings Layer-3**
Failure Criteria	Mohr-Coulomb	Mohr-Coulomb	Mohr-Coulomb	Mohr-Coulomb	Mohr-Coulomb	Mohr-Coulomb
c'_{peak} (kPa)	20.101	20.101	20.101	20.101	20.101	20.101
$\emptyset'_{peak}(^o)$	31.64	31.64	31.64	31.64	31.64	31.64
$c'_{residual}$ (kPa)	0.8627	0.8627	0.8627	0.8627	0.8627	0.8627
$\emptyset'_{residual}(^o)$	31.55	31.55	31.55	31.55	31.55	31.55
E (kPa)	13531.62	9386.96	4510.54	13531.62	9386.96	4510.54
υ	0.3	0.3	0.3	0.3	0.3	0.3
Unit weight (kN/m^3)	26.57	26.11	25.6	26.57	26.11	25.6
k_x (cm/sec)	1.19×10^{-7}	1.79×10^{-7}	6.74×10^{-7}	1.19×10^{-6}	1.79×10^{-6}	6.74×10^{-6}
k_y (cm/sec)	5.95×10^{-8}	8.95×10^{-8}	3.37×10^{-7}	5.95×10^{-7}	8.95×10^{-7}	3.37×10^{-6}

Table 5.6 Material properties used in Phase 2 analysis

Paramaters	Dam Layer-1	Dam Layer-2	Dam Layer-3	Foundation
Failure Criteria	Mohr-Coulomb	Mohr-Coulomb	Mohr-Coulomb	Mohr-Coulomb
c'_{peak} (kPa)	12.4	12.4	12.4	14660
$\emptyset'_{peak}$(°)	38.88	38.88	38.88	55.23
$c'_{ultimate}$ (kPa)	0	0	0	0
$\emptyset'_{ultimate}$(°)	32.35	32.35	32.35	0
E (kPa)	150000	150000	150000	20652
υ	0.35	0.35	0.35	0.423
Unit weight (kN/m^3)	21.42	19.04	16.65	26.65
k_x (cm/sec)	7.44×10^{-7}	1.12×10^{-6}	4.21×10^{-6}	10^{-9}
k_y (cm/sec)	5.95×10^{-7}	8.95×10^{-7}	3.37×10^{-6}	10^{-9}

A conceptual model was generated and some simplifications were done, such as same shear strength parameters were inputted for the all layers. The stability of the dam was analyzed for two positions of the slime-sand boundary; condition-1 (135m from embankment) and condition-2 (180m from embankment). As shown in Figure 5.9, identical boundary conditions were applied in the models. Base of the models were constrained both at horizontal and vertical directions, whereas only the horizontal displacement was constrained at the vertical boundaries. The surface of the slimes with ponded water on it, P=0 was assigned as boundary condition. While, the remaining part of the tailings surface was set as unknown. Because no leakage has been observed through dam body for the present condition of the dam, total head was assigned as 0 m on the downstream face of the impoundment. Besides, the dam experienced piping in 2009 because of sudden increase in ponded water level after heavy rain, to be on the safe side, the same analyses were performed with unknown boundary conditions on the downstream slope.

Ponded water load was also included in the stability analysis. The two slime-sand boundary conditions stated above were modeled for five different ponded water levels.

For these models, the ponded water load starts from 10m, 25m, 40m, 50m and 90m away from the embankment, see Figure 5.10. PHASE 2 v.8.01 program calculated the stress applied by ponded water load on slime surface automatically, according to the elevation difference between the start point and finish point of water load.

3 noded graded triangular elements were used in the model. A series of different mesh densities were tried, before determination of the current mesh density. 3262, 3385, 3466, 5288 and 5486 number of elements were used for the modeling, their outputs were compared and it was seen the results remain constant after 3466 number of elements. Thus, it was applied for the modeling. Figure 5.9 shows typical mesh used in the model, 3466 elements and 1861 nodes were used for mesh generation.

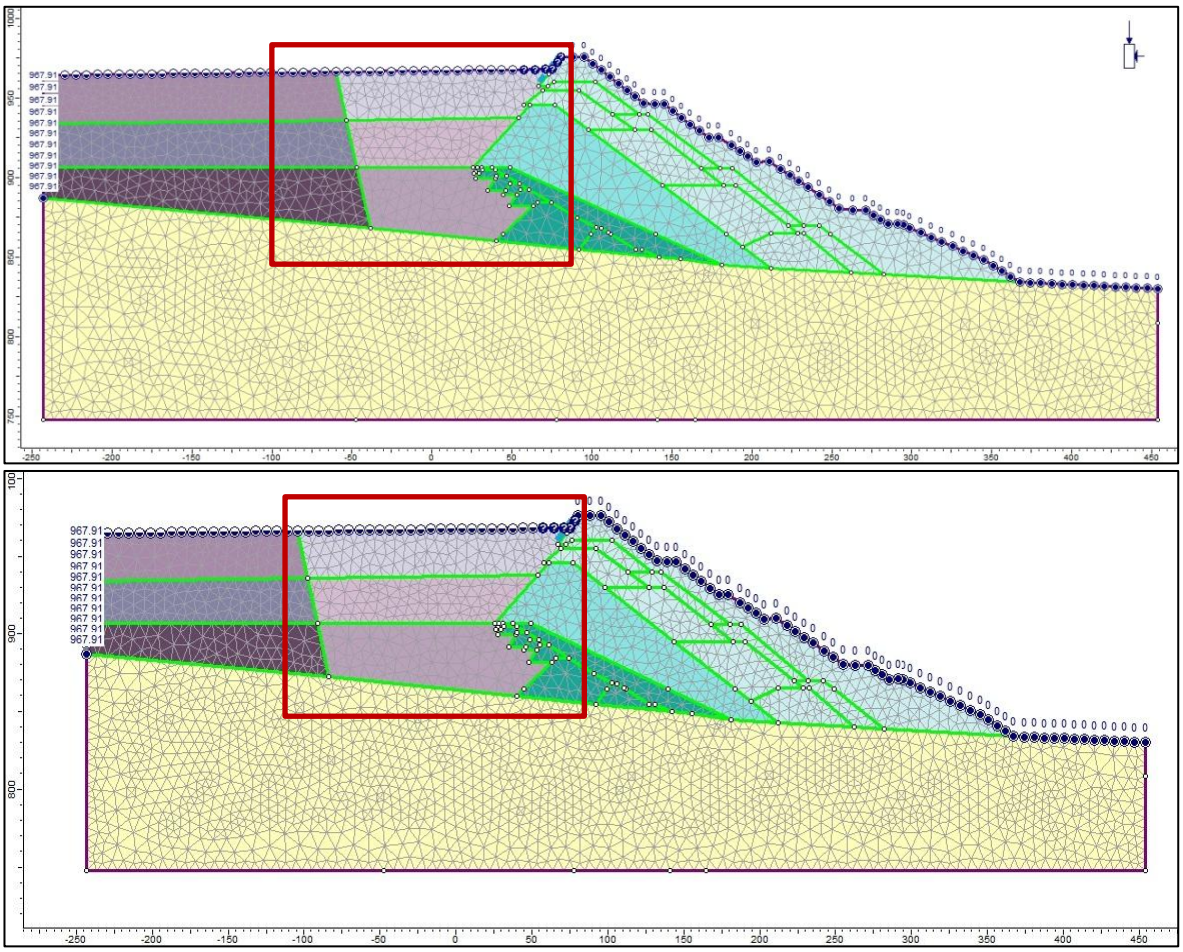

Figure 5.9 Models for different slime-sand boundary positions (condition-1 and -2) for no seepage condition on the downstream slope

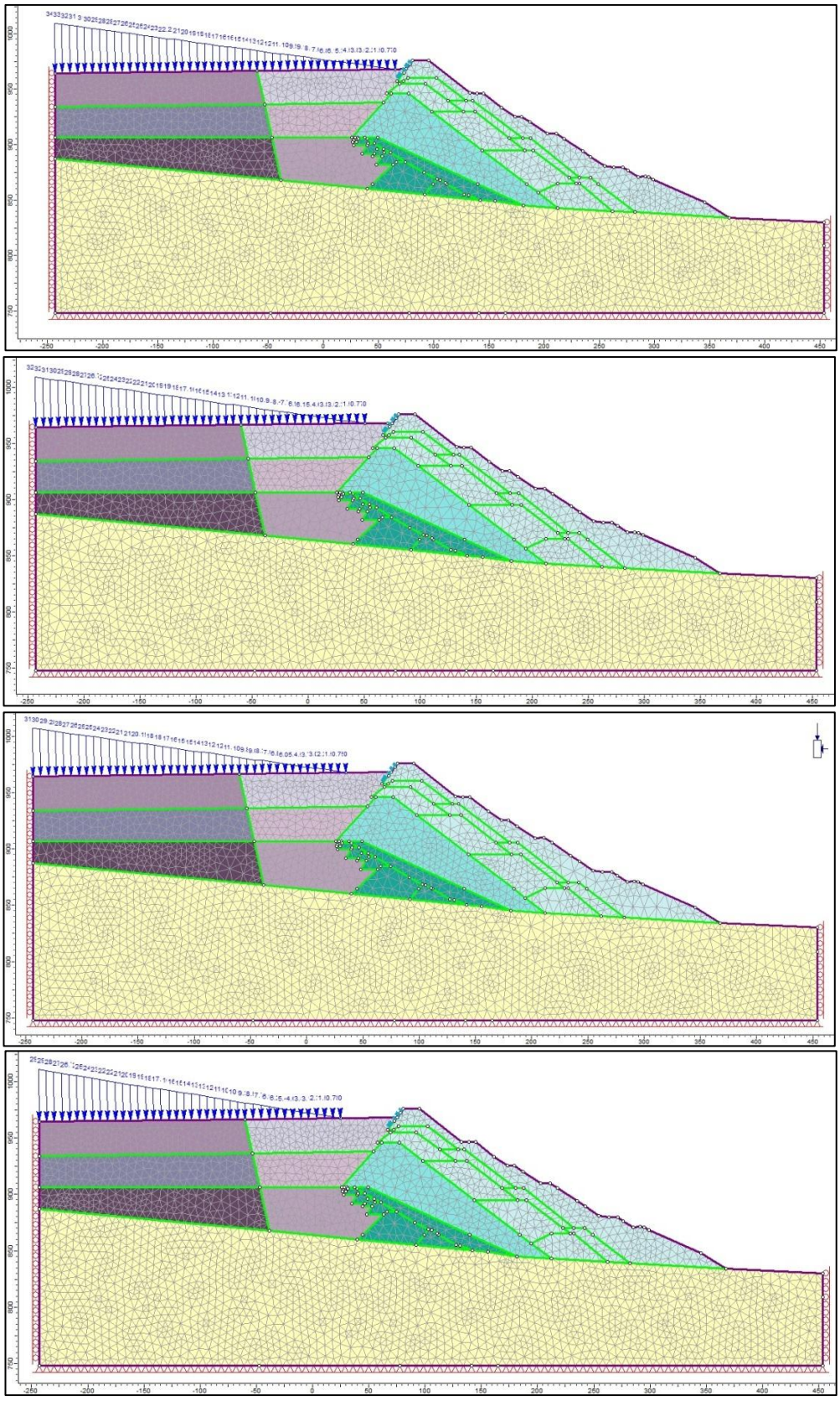

Figure 5.10 Models with different ponded water levels 10m, 25m, 40m and 50m

5.3.2 Stability Analysis of Alternative Dam Geometries for Future Increases

Eti Copper Mine enterprise plans to increase the dam height from 126m to 150m, in the future. For this case 10 alternative dam, geometries were generated, and stabilities were analyzed for the unique slime-sand boundary position and ponded water level. These are shown in Figure 5.11. The geometries were developed gradually from the first one. Initially, the toe was expanded for the 2nd model then the whole dam was widened for the 3rd one.

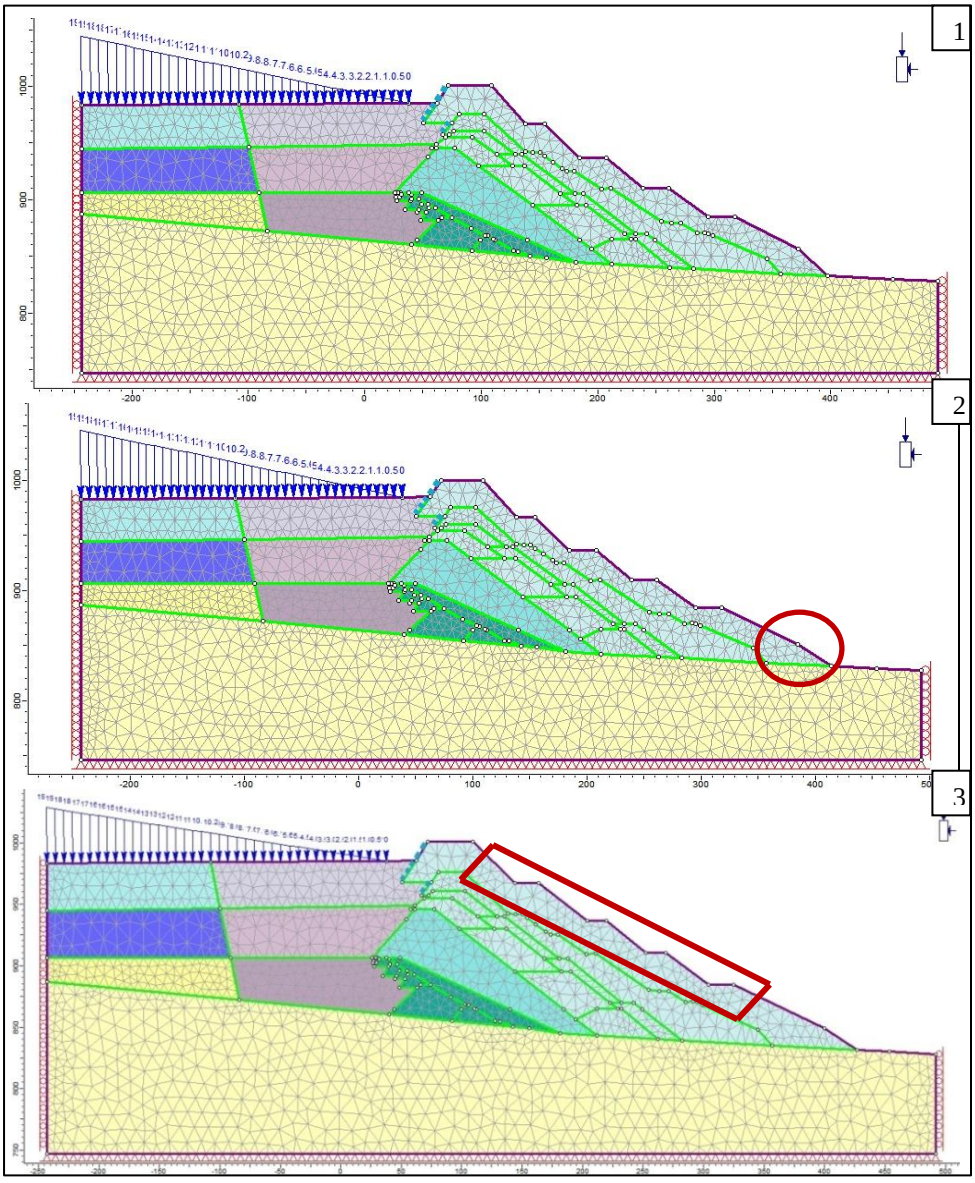

Figure 5.11 Alternative dam geometries for future increases

To create 4th geometry a berm was added to first face of the dam, and then, a berm was added to the toe for 5th model. Afterwards for the 6th model, a berm was created at the second face. In order to obtain the 7th , 8th, 9th model, toe of the 5th model was modified. The dam body in 9th model was expanded to obtain 10th model (Figure 5.11)

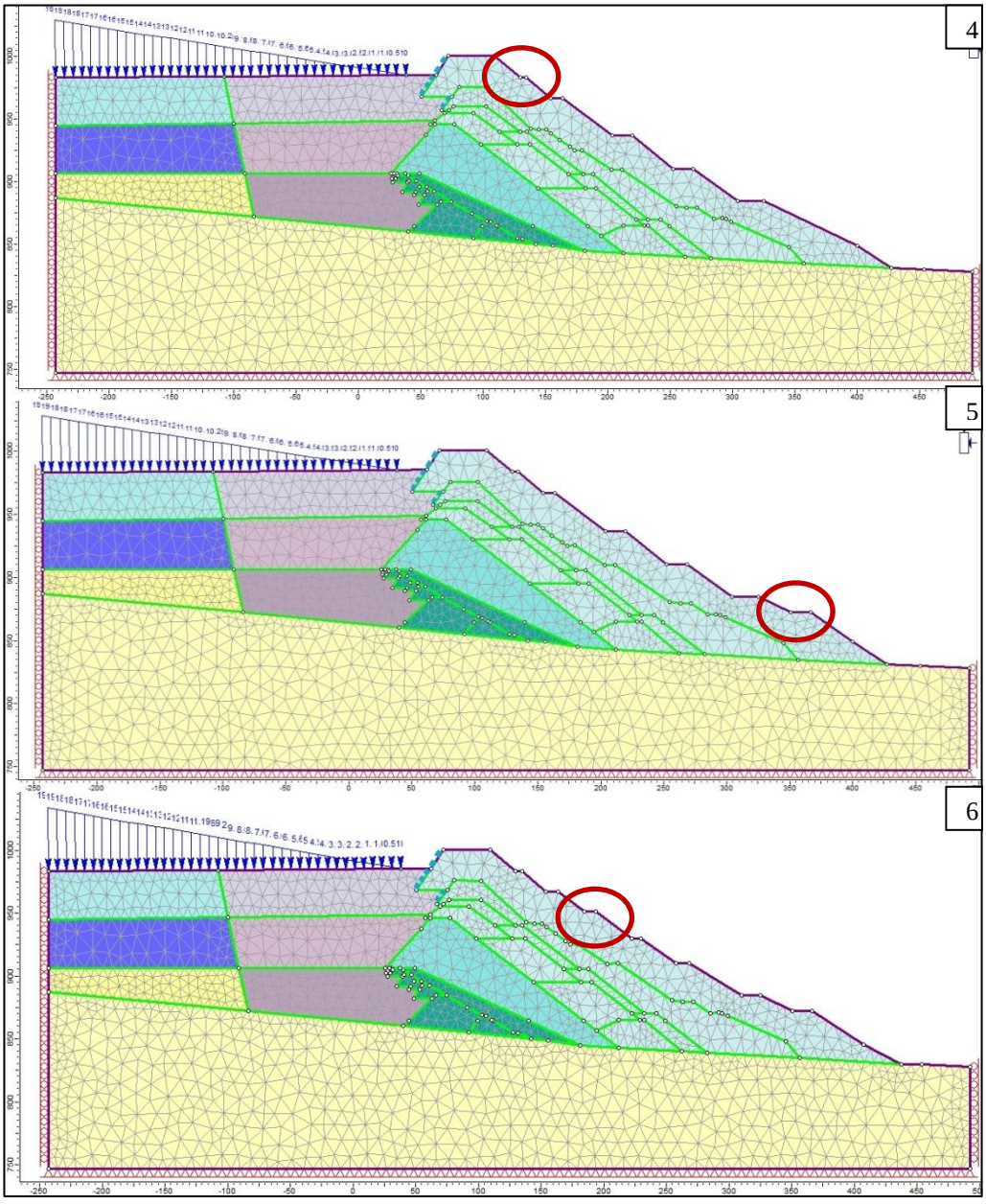

Figure 5.11 Alternative dam geometries for future increases (con't)

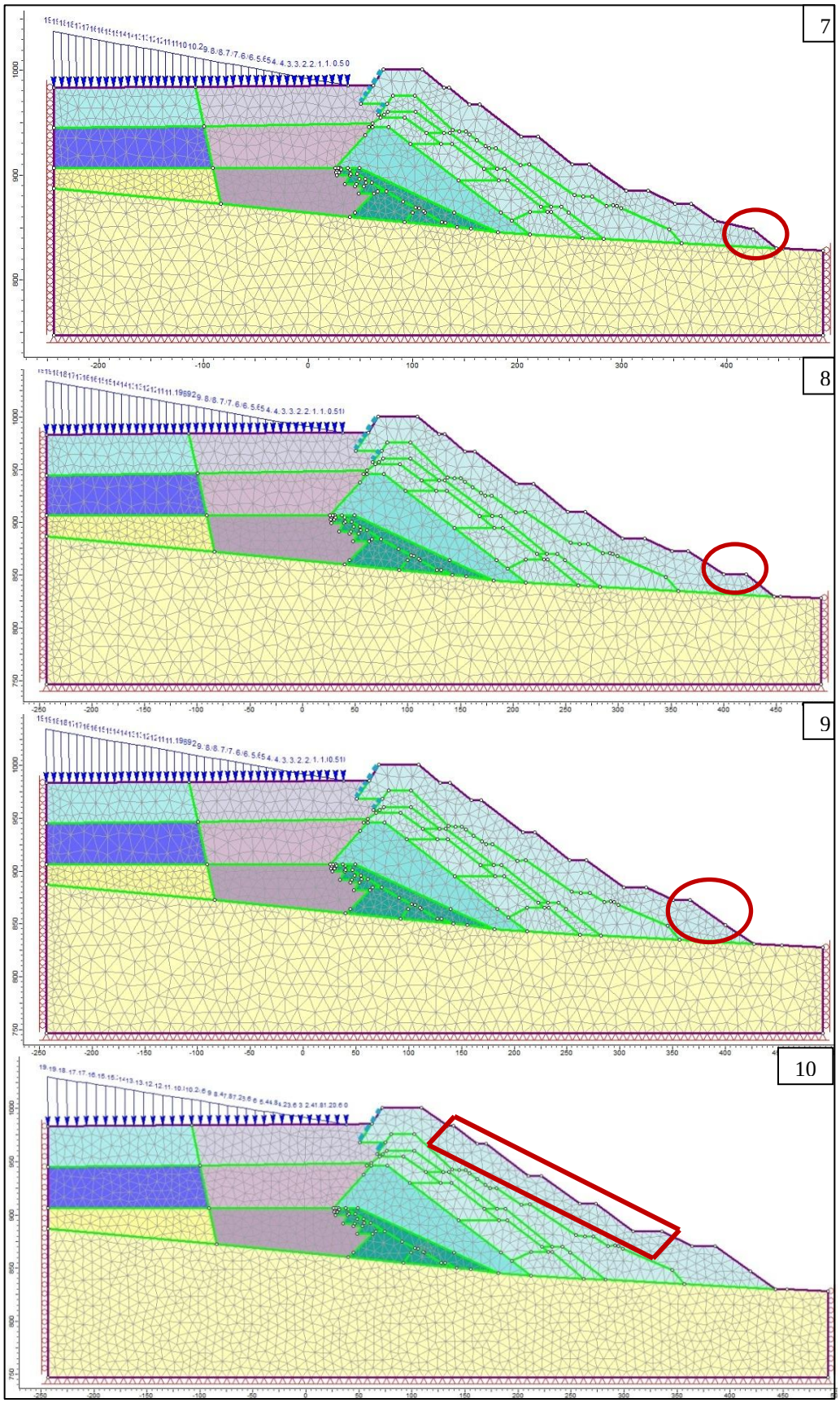

Figure 5.11 Alternative dam geometries for future increases (con't)

5.4 Results of the Analysis

5.4.1 Long Term Stability Analysis of Existing Dam

The figures through Figure 5.12 to Figure 5.16 illustrate the results of the model and Table 5.7 summarizes the results. Position of water table lowers with increasing distance of ponded water from embankment. The outputs show that the minimum safety factor is obtained for the situation at which ponded water starts 10m away from the embankment. Otherwise, nearly the same results were obtained. The maximum safety factor (SF) for condition-1 is obtained for 40 m from embankment with 0.11m total displacement and for condition-2 90 m from embankment with 0.12 m total displacement. Therefore, it can be stated that, the maximum safety factor is obtained when the water load on the beach sand part is approximately 90-95 m. Nevertheless, even for this situation the results are still unsatisfactory. According to Table 5.8, safety factors between 1.0 and 1.2 are classified as questionable safety that is valid for total head=0 condition. For unknown boundary condition on the downstream face, the maximum safety factor is 0.85, which means that the embankment is unsafe. Numerical values of maximum shear strain as illustrated through Figure 5.12 to Figure 5.16 can also be seen in Table 5.9. Total displacement values for the analyses are given in Table 5.10.

Table 5.7 SF values of the models

	Safety Factor Values			
	Condition-1 (135m)		**Condition-2 (180m)**	
Slime-Sand Boundary	**Boundary Conditions for Downstream Face**			
Ponded-water starts from	**Total head=0m**	**Unknown**	**Total head=0m**	**Unknown**
10 m	1.08	0.77	1.13	0.78
25 m	1.2	0.83	1.2	0.8
40 m	1.22	0.85	1.21	0.68
50 m	1.2	0.78	1.2	0.72
90 m	1.2	0.78	1.22	0.85

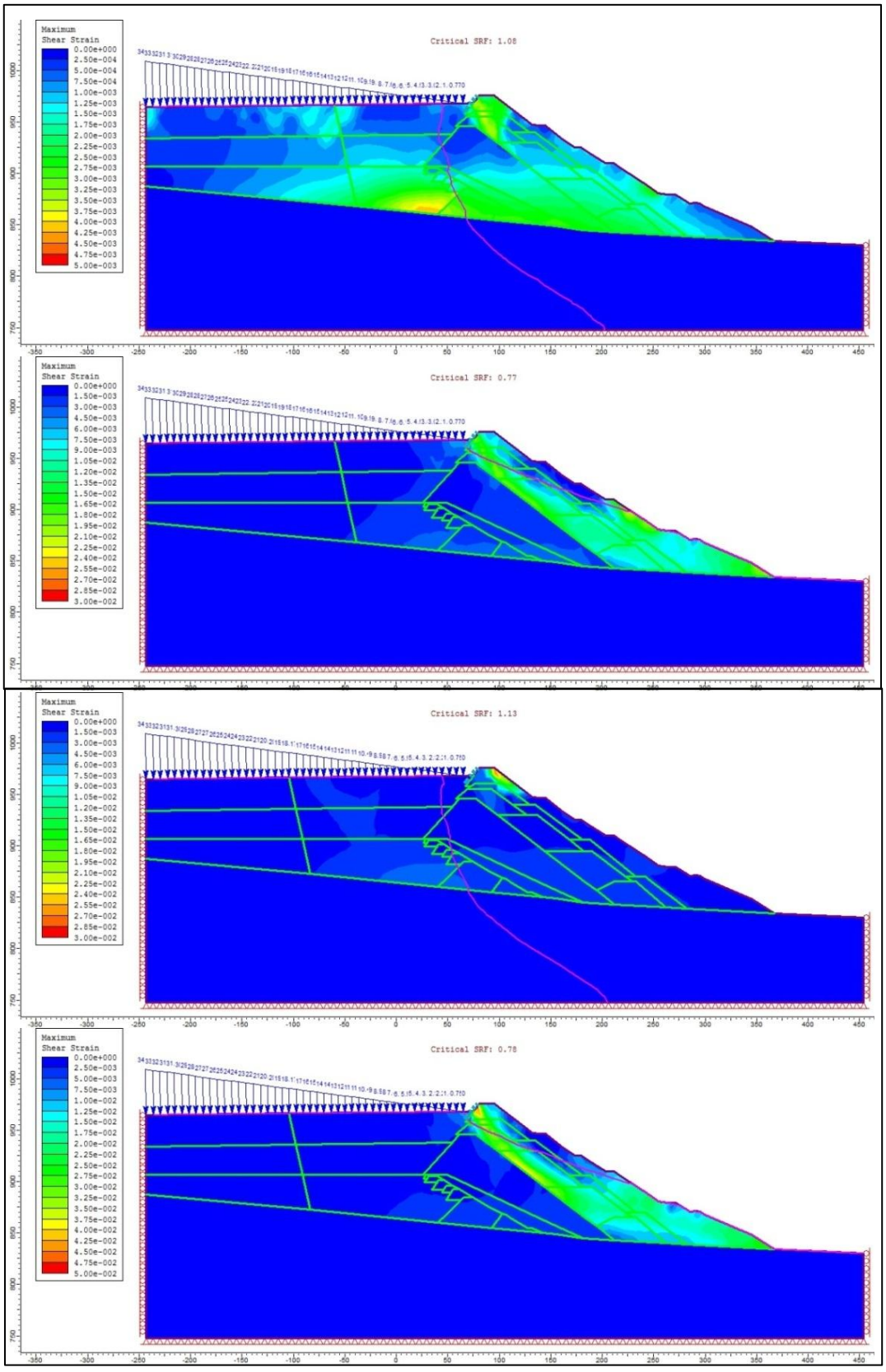

Figure 5.12 SF values for condition-1 and condition-2, ponded water 10m away from embankment

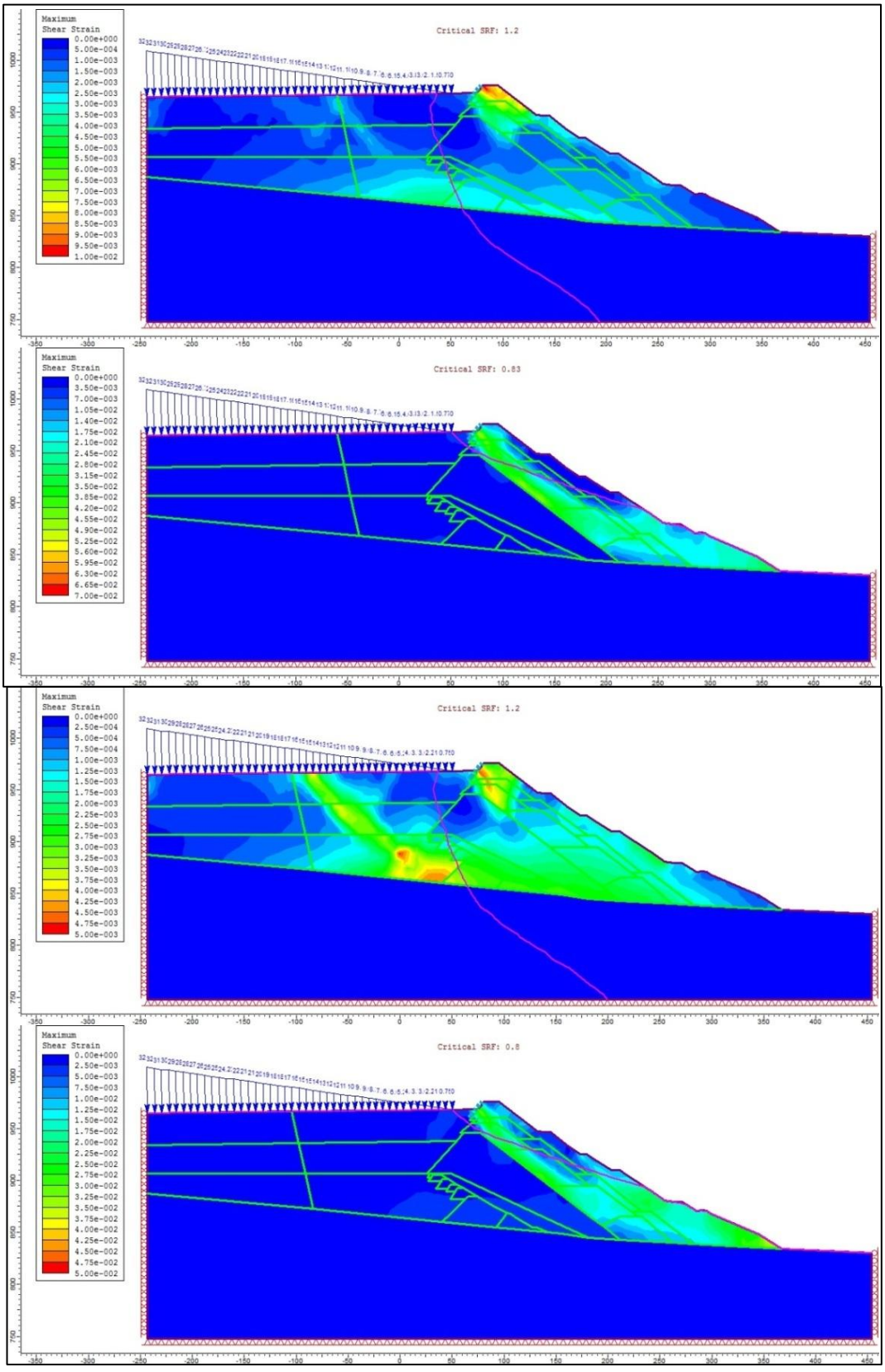

Figure 5.13 SF values for condition-1 and condition-2, ponded water 25m away from dam

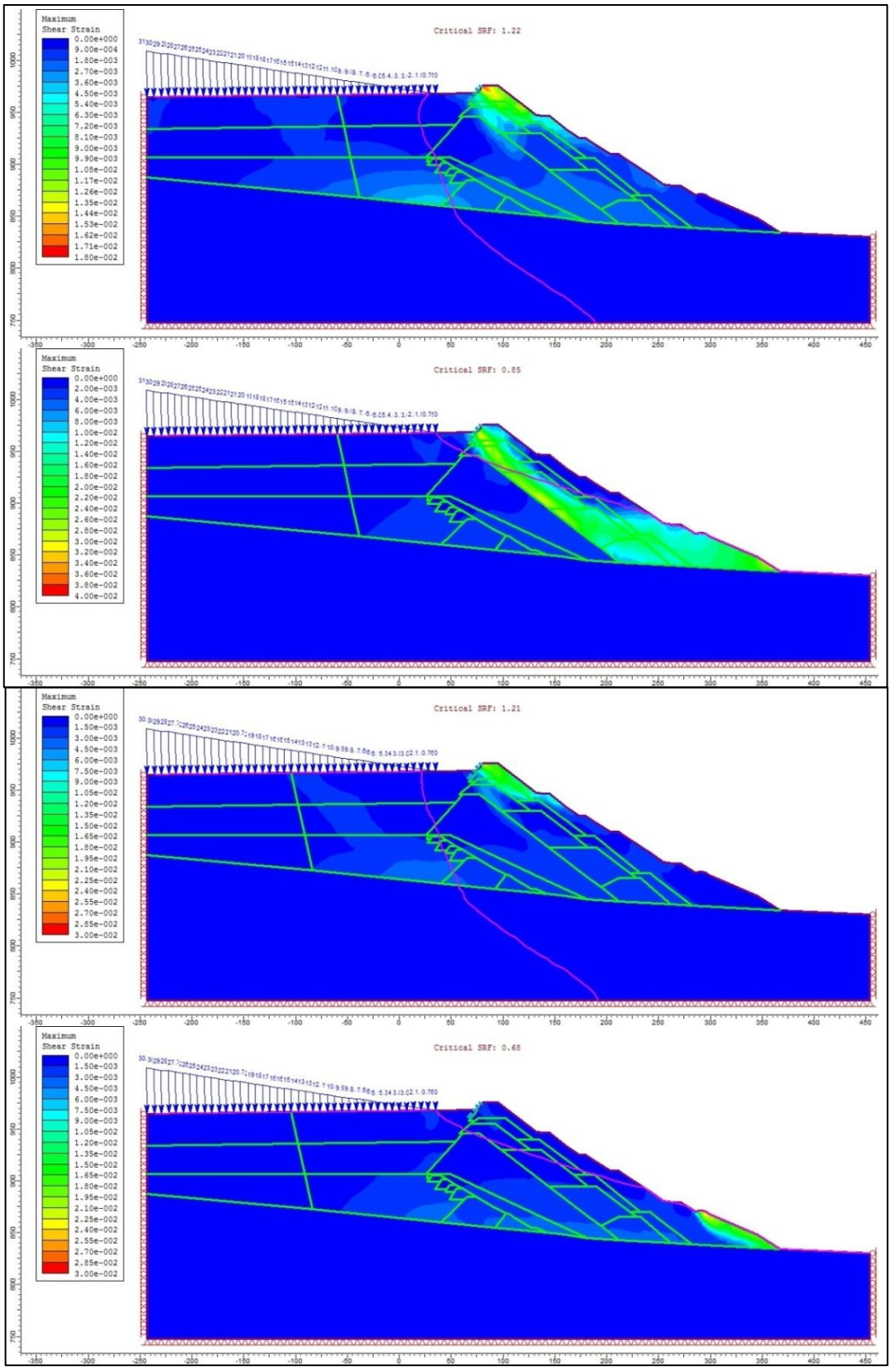

Figure 5.14 SF values for condition-1 and condition-2, ponded water 40m away from dam

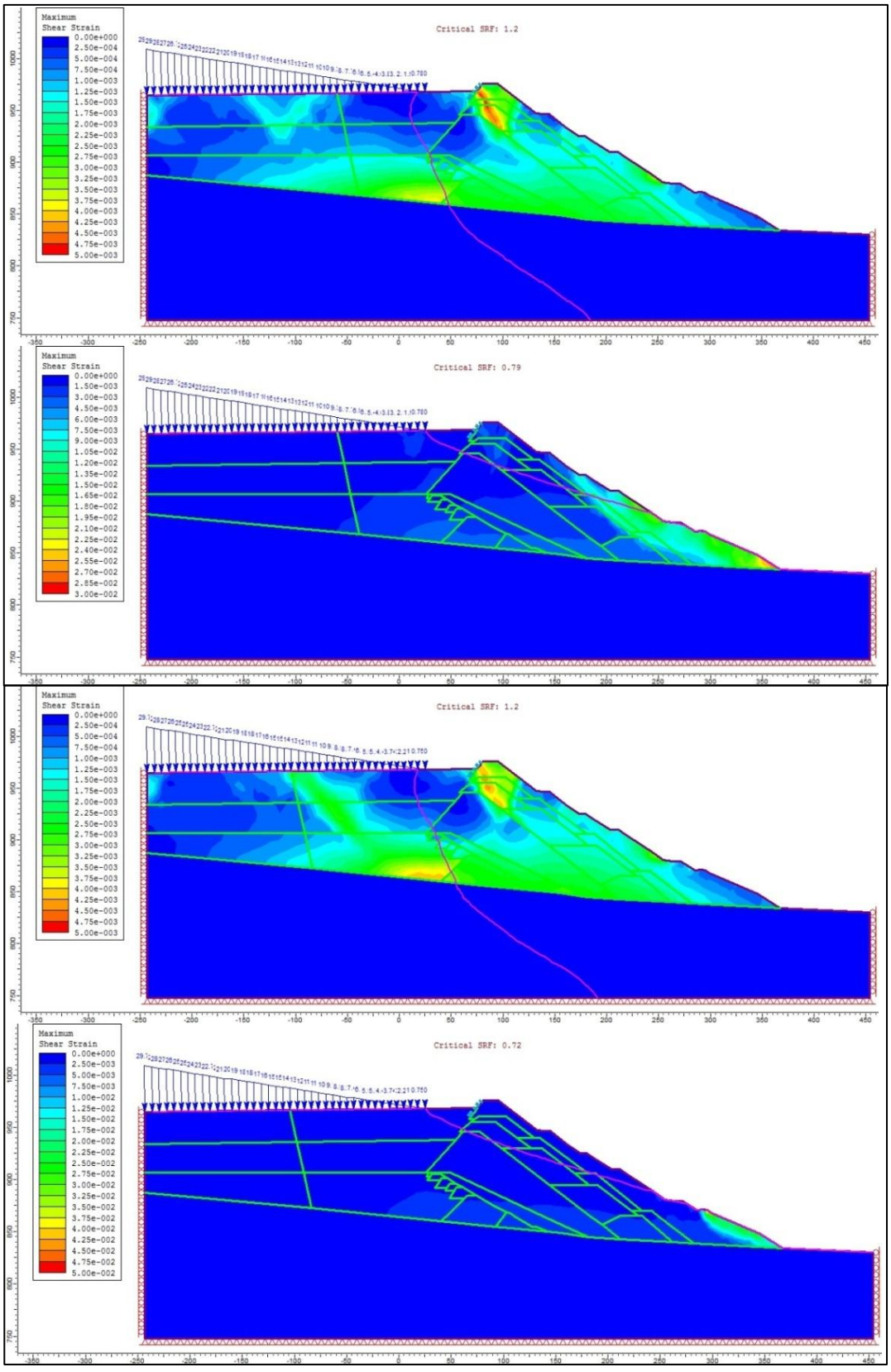

Figure 5.15 SF values for condition-1 and condition-2, ponded water 50m away from dam

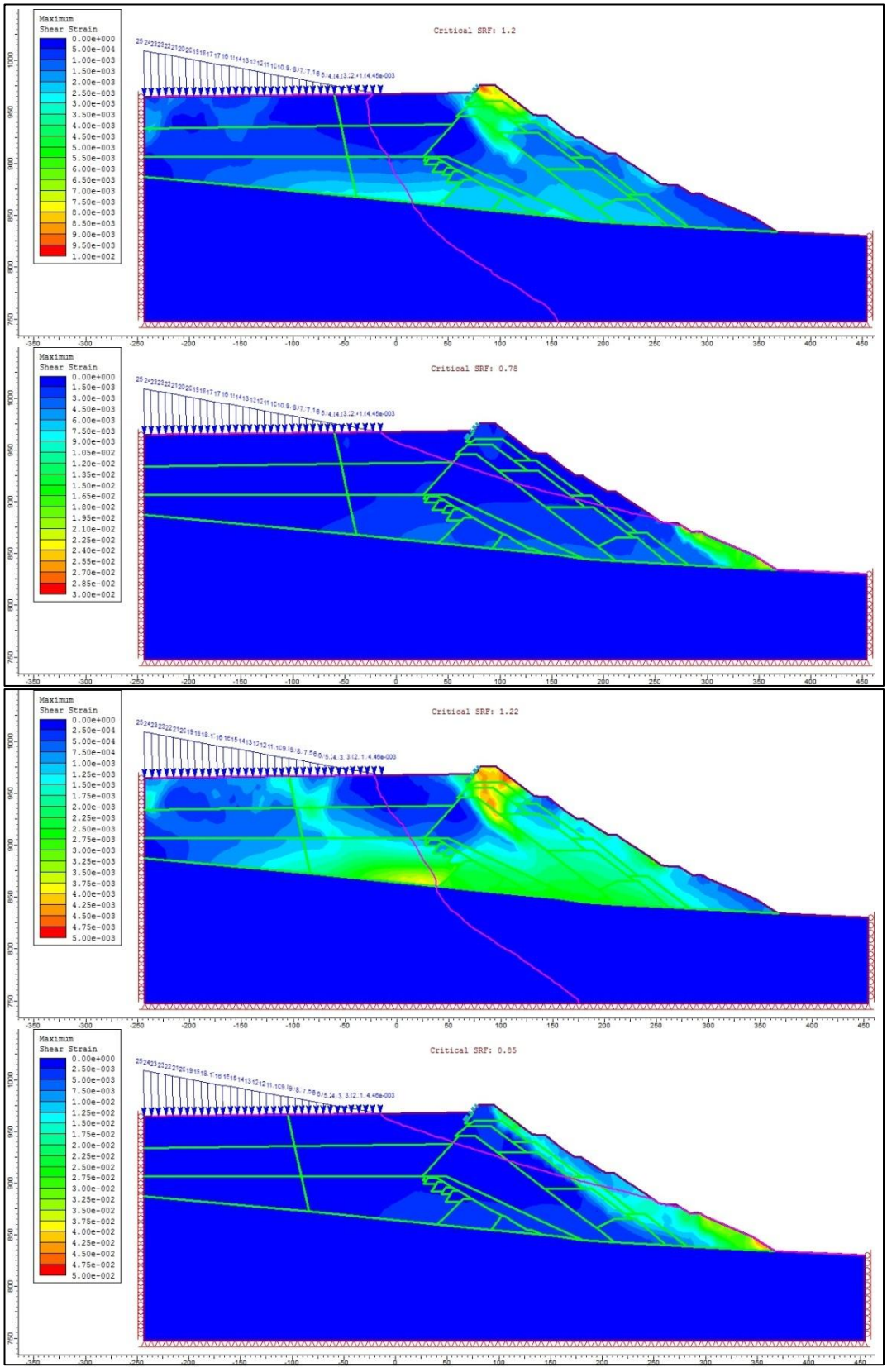

Figure 5.16 SF values for condition-1 and condition-2, ponded water 90m away from dam

Table 5.8 Significance of factor of safety (Sowers, 1979)

Factor of Safety	Significance
Less than 1.0	Unsafe
1.0-1.2	Questionable safety
1.3-1.4	Satisfactory for cuts, fills, questionable for dams
1.5-1.75	Safe for dams

Table 5.9 Maximum shear strain values for the analyses

	Maximum Shear Strain			
	Condition-1 (135m)		Condition-2 (180m)	
Slime-Sand Boundary	Boundary Conditions for Downstream Face			
Ponded-water starts from	Total head=0m	Unknown	Total head=0m	Unknown
10 m	5e-3	3e-2	3e-2	5e-2
25 m	1e-2	7e-2	5e-3	5e-2
40 m	1.8e-2	4e-2	3e-2	3e-2
50 m	5e-3	3e-2	5e-3	5e-2
90 m	1e-2	3e-2	5e-3	5e-2

Table 5.10 Total displacement values for the analyses

	Total Displacement (m)			
	Condition-1 (135m)		Condition-2 (180m)	
Slime-Sand Boundary	Boundary Conditions for Downstream Face			
Ponded-water starts from	Total head=0m	Unknown	Total head=0m	Unknown
10 m	8e-1	1	4e-1	1.4
25 m	1.4e+1	1.7e+1	8e-2	1.4
40 m	1.1e-1	1.1	5e-1	5e-1
50 m	6e-1	6e-1	8e-2	6e-1
90 m	3e-1	6e-1	1.2e-1	1.2

Maximum shear strain at the time of failure, for total head=0 at the downstream face condition instability takes place at the first slope of the dam, and for the flow through embankment condition, whole embankment slope experiences the failure. Figure 5.17 shows flow vectors, deformation contours and yielded elements for condition-1 with no flow through downstream face, which indicates the direction of groundwater flow, and the relative size of the flow vectors shows the relative velocity of the flow. Yielded elements concentrate mostly on fine tailings part and upper part of the embankment.

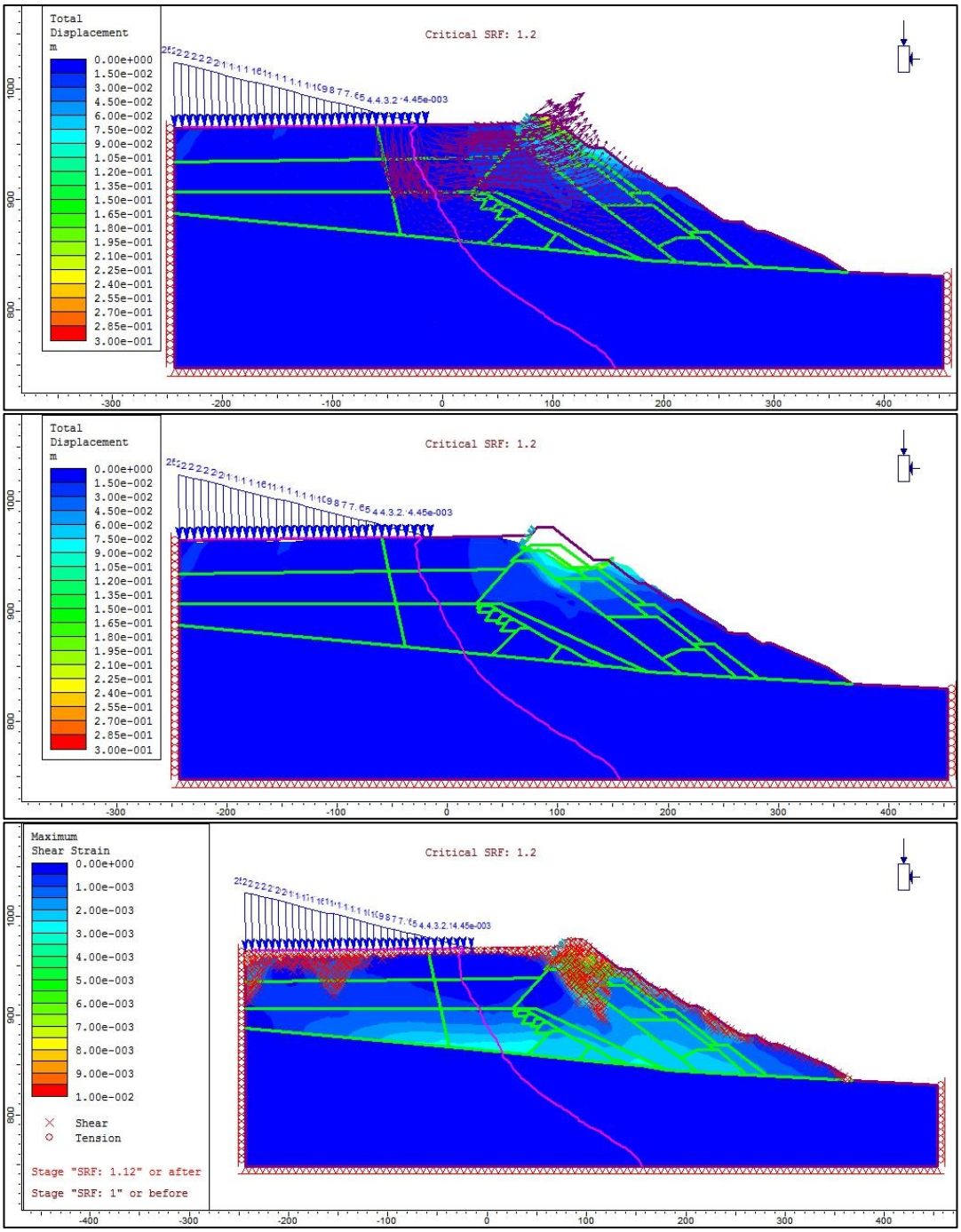

Figure 5.17 Flow vectors, deformation contours and yielded elements for condition-1 with ponded water 90m away from dam with no flow through downstream face

Figure 5.18 indicates flow vectors, deformation contours and yielded elements for condition-1 with flow through downstream face. The movement of deformation contours is in a good agreement with flow vectors for both cases. Possible shape of critical failure

surface is circular for both of the groundwater conditions. Yielded elements concentrate mostly at the bottom of the embankment, and some part at the top of the embankment.

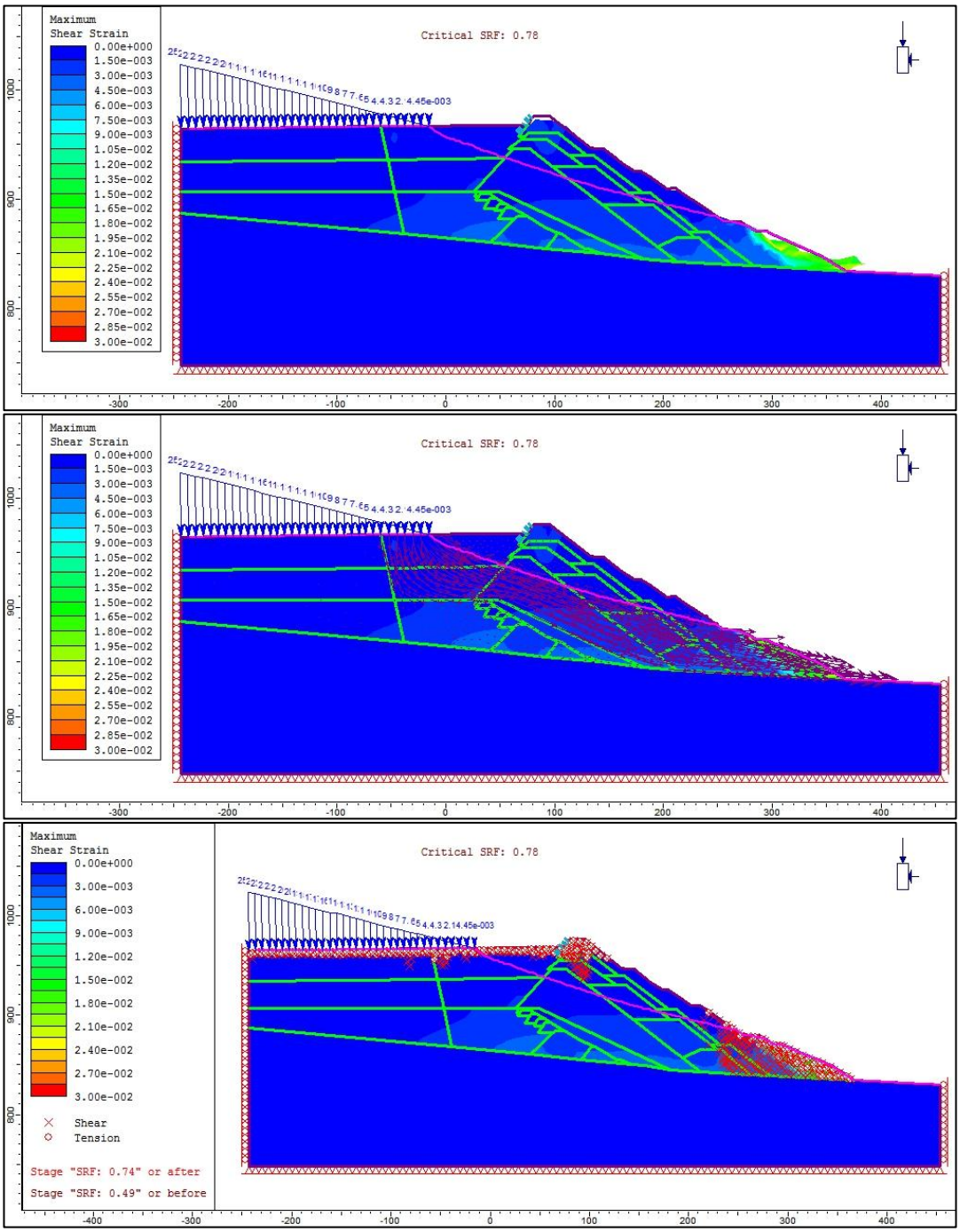

Figure 5.18 Flow vectors, deformation contours and yielded elements for condition-1 with ponded water 90m away from dam with flow through downstream face

5.4.2 Stability Analysis of Alternative Dam Geometries for Future Increases

Figure 5.19 illustrates the results of the created dam alternatives and Table 5.11 summarizes the results. The lowest safety factor was obtained for the first and the second alternatives, at which the extent of the dam body is the narrowest. The expansion of toe of the dam increases the safety factor. Widening of the dam body in the 2nd alternative increased the safety factor that is the 3rd alternative. Maximum factor of safety for the 5th option that was obtained by adding a berm to top and bottom faces of the 3rd alternative. Constituting a berm at the second face did not affect the results much. Besides, modifying the toe of the dam at the 5th model decreased the SF (7th, 8th, 9th options). Finally, further expansion of the dam body decreased SF.

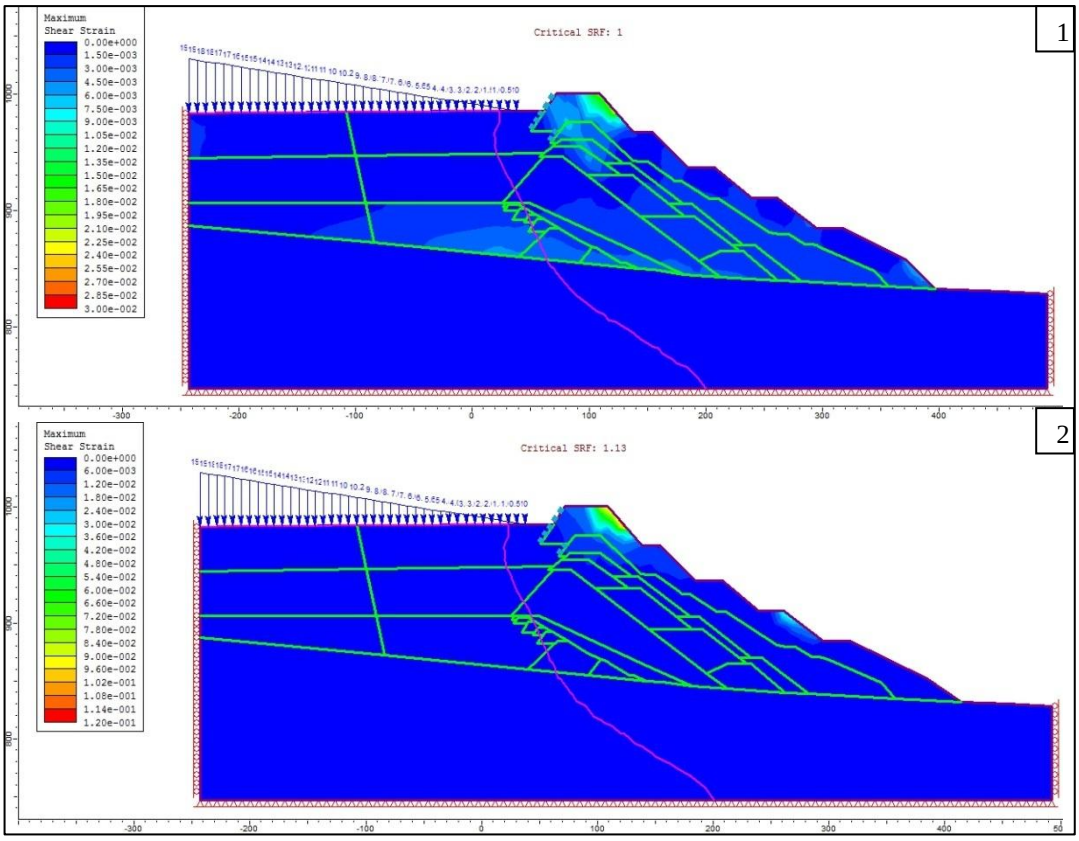

Figure 5.19 SF values for created dam alternatives

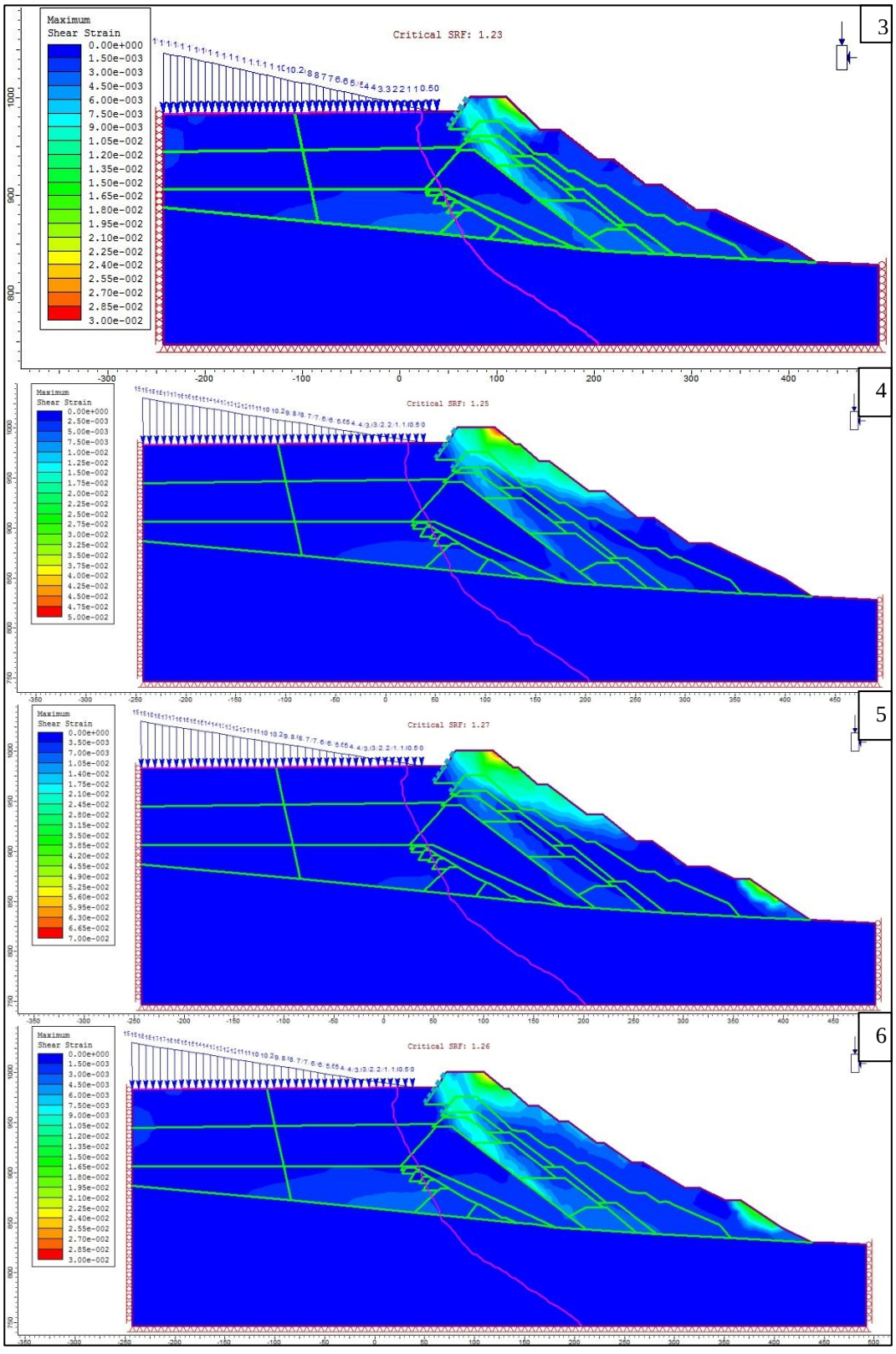

Figure 5.21 SF values for created dam alternatives (con't)

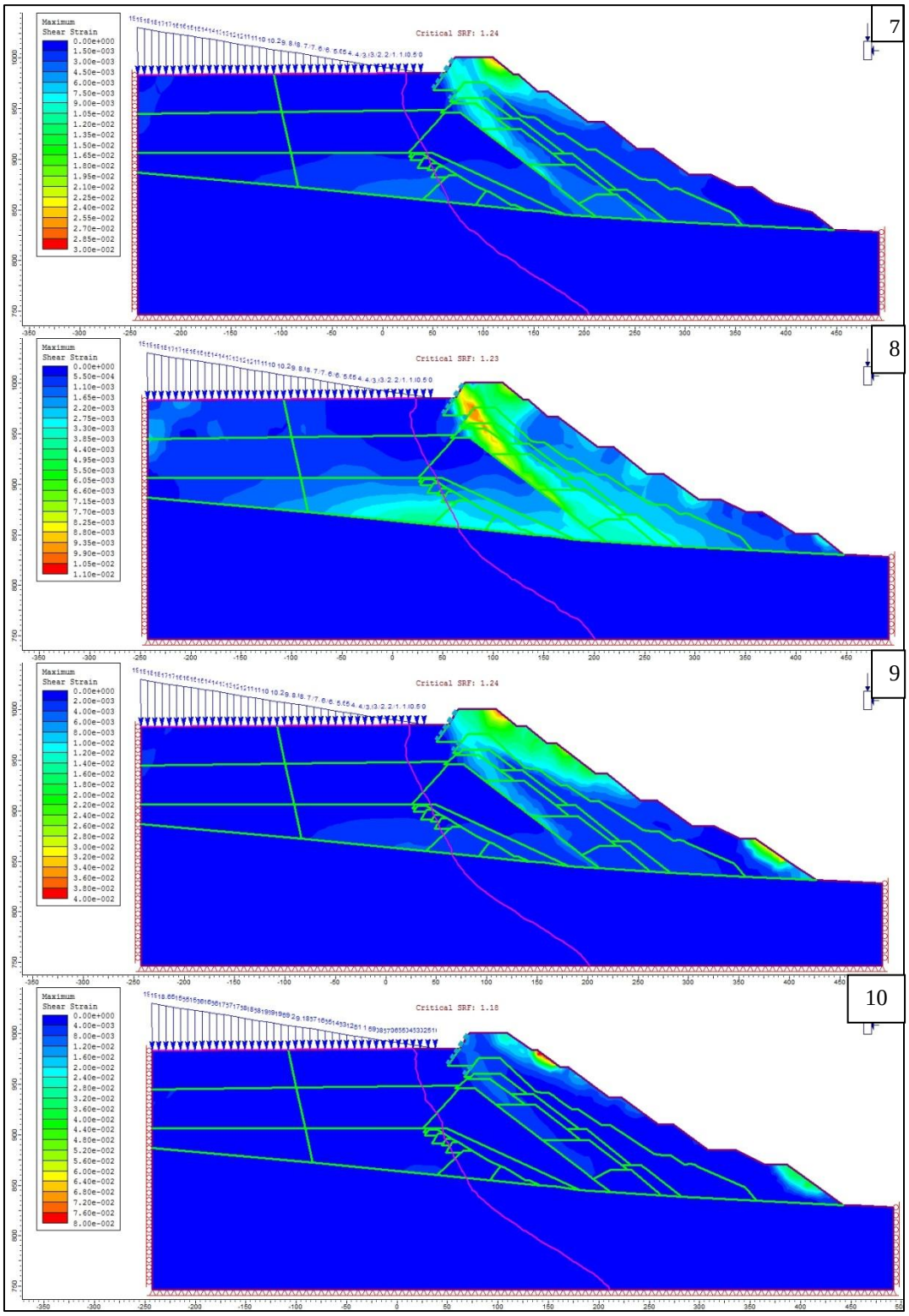

Figure 5.21 SF values for created dam alternatives (con't)

Table 5.11 SF values of the produced models

Model number	Factor of Safety Values
1	1
2	1.13
3	1.23
4	1.25
5	1.27
6	1.26
7	1.24
8	1.23
9	1.24
10	1.18

Obtained factor of safety values, presented in Table 5.11, for the generated alternatives are between 1-1.27. Consequently, the required SF could not be satisfied for the developed geometry alternatives, that is 1.5. According to Table 5.8, safety factors between 1.0 and 1.2 are classified as questionable safety. For all of the options the most critical failure model is circular failure, as it is for the existing condition of the dam.

CHAPTER 6

CONCLUSIONS AND RECOMMENDATIONS

This study covers the stability investigation of the Eti copper mine tailings dam in Kastamonu, Küre. For this purpose present dam condition and several alternatives for future raises of the dam under static loading conditions were analyzed with 2D finite element program.

According to literature survey conducted, the tailings dams constructed with upstream construction method are most susceptible to failure especially to liquefaction. Geotechnical properties of tailings, embankment and foundation used in the model were determined with laboratory tests, and then checked with the values of the materials with similar properties in the literature. The position of the water tables in the model was obtained by finite element analysis with calculated hydraulic conductivity values and water level in the pond. In this study stability analysis of the dam was conducted for only static loading conditions. A more comprehensive static stability analysis should be conducted because some simplifications were done at material properties; such as layers of tailings material and layers of embankment material have the same shear strength parameters. On the other hand, the dam has a risk of liquefaction, for this reason a stability analysis for dynamic loading conditions must be conducted. A tailings dam is a continuously changing system, however in this study the current condition of the dam was modeled, and obtained results only valid for that condition. According to the results of the analysis the following conclusions have been drawn.

1. Present condition and raised dam alternatives for future were modeled using PHASE 2 v.8.01 finite element program, and obtained safety factor values were compared with the required values given in the literature.
2. In order to analyze present condition of the dam, two positions of slime-sand boundary were analyzed with different positions of ponded water load. The

minimum SF was obtained for ponded water located 10m away from the dam for both boundary conditions. Because the position of the phreatic surface increases as the ponded water approaches to the dam. Thus special attention must be given to water level at the pond. For all of the analyses safety factor values are not satisfactory for stability, according to Sowers (1979) safety of the current condition of the dam is questionable. Thus, some remedial measures must be taken to strengthen the dam. However, according to "Küre Copper Tailings Dam Improvement and Environmental Risk Assessment Report" prepared by İTÜ Faculty of Mines the dam was found as safe with Bishop's method.

3. For future plans 10 alternative dam geometries were generated and stability analyses were conducted. All of the alternatives shows questionable safety, and obtained maximum safety factor is 1.27 for 5^{th} option. Therefore, it is not safe to raise the dam to 150 m.

According to the deduced conclusions, several recommendations are given below.

1. Flattening the slope may be the first stabilization measure. Decreasing the slope angle reduces the driving forces and increases the resisting forces because the length of the failure surface increases in base.
2. Berms generated along the the slopes of an embankment may be another measure, because it increases shear strength below the berm. However, the berms placed inappropriately may increase the driving forces below it. According to the study smaller height berms are more effective than larger height berms (Araya, 2000).
3. Deformations and seepage through dam body should be monitored during the life of the dam.
4. Geomembran application on the upstream face should continue for future increases. Moreover, soil characteritics may be improved by soil compaction for future increases.
5. For slope stabilization rockfill banks could be constituted on the downstream slopes.

REFERENCES

General Directorate of Meteorology. (1975-2008). Retrieved 12 04, 2010, from General Directorate of Meteorology: http://www.dmi.gov.tr/veridegerlendirme/il-ve-ilceler-istatistik.aspx?m=KASTAMONU

Pavement Manual. (2007, July 04). Retrieved June 02, 2012, from http://www.dot.state.mn.us/materials/pvmtdesign/docs/Chapter_3-2.pdf

IDAHO Department of Lands. (2012). Retrieved 11 1992, 16, from http://www.idl.idaho.gov/bureau/minerals/bmp_manual1992/p16-ch4.pdf

Al-Homoud, A. S., & Tanash, N. (2004). Modeling uncertainty in stability analysis for design of embankment dams on difficult foundations. *Engineering Geology, 71*(3-4), 323-342.

Alkasawneh, W., Malkawi, A. I., Nusairat, J. H., & Albataineh, N. (2008). A comparative study of various commercially available programs in slope stability analysis. *Computers and Geotechnics, 35*(3), 428-435.

Araya, B. B. (2000). Effects of Berms on the Factor of Safety of an Embankment. *Master Thesis*.

ASTM, D2435-M11. (2011). Standard Test Methods for One-Dimensional Consolidation Properties of Soils Using Incremental Loading. *ASTM Geotechnical Testing Journal*, 1-15.

ASTM, D2487 – 11. (2011). Standard Practice for Classification of Soils for Engineering Purposes (Unified Soil Classification System). *ASTM Geotechnical Journal*, 1-12.

ASTM, D3080M – 11. (2011). Standard Test Method for Direct Shear Test of Soils Under Consolidated Drained Conditions. *ASTM Geotechnical Testing Journal*, 1-9.

ASTM, D422 – 63. (2007). Standard Test Method for Particle-Size Analysis of Soils. *ASTM Geotechnical Testing Journal*, 1-8.

ASTM, D4318 – 10. (2010). Standard Test Methods for Liquid Limit, Plastic Limit, and Plasticity Index of Soils. *ASTM Geotechnical Testing Journal*, 1-16.

ASTM, D698-07. (2007). Standard Test Method for Laboratory Compaction. *ASTM geotechnical testing journal*, 1-13.

ASTM, D7012 – 10. (2010). Standard Test Method for Compressive Strength and Elastic Moduli of Intact Rock Core Specimens under Varying States of Stress and Temperatures. *ASTM Geotechnical Testing Journal*, 1-9.

Azadegan, O. (2012). Finite Element Modeling of Stability of A New Device of PLT Set Bracing. *EJGE, 17*, 511.

Babu, G. S., Srivastava, A., & Sahana, V. (2007). Analysis of stability of earthen dams in kachchh region, Gujarat, India. *Engineering Geology, 94*(3-4), 123-136.

Bagarello, V., Sferlazza, S., & Sgroi, A. (2009). Testing laboratory methods to determine the anisotropy of saturated hydraulic conductivity in a sandy-loam soil. *Geoderma, 154*(1-2), 52-58.

Bauer, G. E., & Zhao, Y. (1993). Shear Strength Tests for Coarse Granular Backfill and Reinforced Soils. *Geotech. Test. Journal, 16*, 115–121.

Bauer, G. E., Zhao, Y., & El-Shafei, M. (1990b). Direct Shear Box Tests on 'Conwed' Stratagrid 5033. *Final report submitted to Conwed*. Minneapolis.
Bishop, A. (1973). The stability of tips and spoil heaps. *Quarterly Journal of Engineering Geology & Hydrogeology, 6*, 335-376.
Bishop, A., & Bjerrum, L. (1960). The relevance of the triaxial test to the solution of stability problems. *Research conference on shear strength of cohesive soils* (pp. 437-501). ASCE, University of Colorado.
Blight, G. E., & Steffen, O. K. (1979). Geotechnics of gold mining waste disposal. *Current Geotechnical Practice in MineWaste Disposal, ASCE*, 1-52.
Brawner, C., & Campbell, D. (1973). The Tailings Structure and its Characteristics - A Soil's Engineer's Viewpoint. *Tailings Disposal Today, Proceedings of the First International Tailings.* Tucson, Arizona.
Breitenbach, A. J. (2010, April). Backfill depleted open-pit mines with lined landfills, tailings, and heap leach pads. Retrieved April 21, 2012, from http://geosyntheticsmagazine.com/articles/0410_f1_backfill.html
Brinkgreve, R. (2005). Selection of soil models and parameters for geotechnical engineering application. *In proceedings of Geo-Frontiers Conference, ASCE.* Austin, TX.
CANMET. (1977). Pit Slope Manual. In *Canada Centre for Mineral and Energy Technology Report* (p. 136). Canada: CANMET.
Chakrabarti, S., & Tabucanon, J. (n.d.). Improvement of Iron Ore Stockyard Berms Using Cementıtıous Stabilisation. Retrieved 5 10, 2012, from http://www.coffey.com/Uploads/Documents/Improvement%20of%20Iron%20Ore%20Stockyard%20Berms%20Using%20Cementitious%20Stabilisation_20110328172858.pdf
Chakraborty, D., & Choudhury, D. (2009). Investigation of the Behavior of Tailings Earthen Dam Under Seismic Conditions. *American J. of Engineering and Applied Sciences, 2*(3), 559-564.
Chang, K. (1978). *An Analysis of Damage of Slope Sliding by Earthquake on the Paiho Main Dam and its Eartquake Strengthening.* Tseng-hua Design Section, Department of Eartquake-Resistant Design and Flood Control Command of Miyna Reservoir, Peoples Republic of China.
Coulter, H. W., & Migliaccio, R. (1966). Effects of the Eartquake of March 27, 1964 at Valdez, Alaska. *Geological Survey Professional Paper No. 542-C.*
Das, B. M. (1983). Principles of Geotechnical Engineering. In B. M. Das. Sacramento: California State University.
Dawson, E., Roth, W., & Drescher, A. (1999). Slope Stability Analysis by Strength Reduction. *Geotechnique, 49*(6), 835-840.
Day, R., Hight, D., & Potts, D. (1998). Finite element analysis of construction stability of Thika Dam. *Computers and Geotechnics, 23*, 205±219.
Department of the Army U.S. Army Corps of Engineers. (1990, September 30). Engineering and Design . *Settlement Analysis*(EM 1110-1-1904). Retrieved from http://synectics.net/public/file/ShowFile.aspx?dsn=pub&category=USACE&subcategory=Engineer+Manuals&idMenu=37839&ddlDSN=SYSTM&Mode=FileImage&ID=448&Title=EM%201110-1-1904
Deprem Araştırma Dairesi. (n.d.). *Afet İşleri Genel Müdürlüğü*. Retrieved 2011, from Deprem Dairesi Başkanlığı:

http://www.deprem.gov.tr/sarbis/Shared/DepremHaritalari.aspx
Dillon, M., White, R., & Power, D. (2004). Tailings storage at Lisheen Mine, Ireland. *Minerals Engineering*, 123-130.
Duncan, J. (1996). State of the art: limit equilibrium and finite-element analysis of slopes. *Journal of Geotechnical Engineering, 122*(7), 577-596.
Durham University, Geo-Engineering Web site. (n.d.). *School of Engineering, University of Durham*. Retrieved May 14, 2012, from Durham University, Geo-Engineering Web site: http://www.dur.ac.uk/~des0www4/cal/dams/emba/seep.htm
Gens, A., & Alonso, E. (2006). Aznalcóllar dam failure Part 2: Stability conditions and failure mechanism. *Géotechnique, 56*(3), 185-201.
GeotechniCAL. (n.d.). *GeotechniCAL*. Retrieved 2012, from Educational Technology for Ground Engineering: http://environment.uwe.ac.uk/geocal/foundations/foundations.htm
Google Earth. (2011).
Grammatikopoulos, J., Manou - Andreadis, N., & Anagnostopoulos, C. (n.d.). *Determination of the modulus of elasticity Es in saturated clay-silty sand mixtures.*
Griffiths, D. V. (1999). *Stability analysis of highly variable soils by elasto-plastic finite Elements.* Rocscience Inc., Phase2 user's guide Version 2.1.
Griffiths, D., & Lane, P. (1999). Slope Stability Analysis by Finite Elements. *Geotechnique, 49*(3), 387-403.
Hammah, R., Curran, J., Yacoub, T., & Corkum, B. (2004). Stability Analysis of Rock Slopes using the Finite Element Method. *Proceedings of the ISRM Regional Symposium EUROCK 2004 and the 53rd Geomechanics Colloquy.* Salzburg.
Hammah, R., Yacoub, T., Corkum, B., & Curran, J. (n.d.). A Comparison of Finite Element Slope Stability Analysis with Conventional Limit-Equilibrium Investigation. Toronto, Canada: Rocscience Inc. Retrieved from http://www.rocscience.com/library/pdf/SSR_vs_LE.pdf
Holtz, R., & Kovacs, W. (2003). An Introduction to Geotechnical Engineering. In *Civil Engineering and Engineering Mechanics Series.* Pearson Education Taiwan Ldt.
Hough, K. (1957). *Basic Soils Engineering.* New York: The Ronald Press.
http://www.dot.state.mn.us. (n.d.). Retrieved from http://www.dot.state.mn.us/materials/pvmtdesign/docs/Chapter_3-2.pdf
http://www.stanford.edu/. (n.d.). Some Useful Numbers on the Engineering Properties of Materials. Retrieved 07 02, 2012, from http://www.stanford.edu/~tyzhu/Documents/Some%20Useful%20Numbers.pdf
Huat, B. B., Ali, F. H., & Rajoo, R. (2006). Stability Analysis and Stability Chart for Unsaturated Residual Soil Slope. *American Journal of Environmental Sciences, 2*(4), 154-160.
Hunt, R. E. (2005). 3 Measurement of Properties. In *Geotechnical Engineering Investigation Handbook, Second Edition* (pp. 165-168). United States of America: CRC Press.
ICOLD. (1996). A guide to tailings dams and impoundments-design, construction, use and rehabilitation. *Bulletin no*(106).

ICOLD and UNEP. (2001). Tailings Dams - Risk of Dangerous Occurrences, Lessons learnt from practical experiences. *Bulletin 121*.

Jewell, R. A., & Wroth, C. P. (1987). Direct shear tests on reinforced sand. *Geotechnique, 37*(1), 53-68.

Johnson, S. (1975). Analysis and design relating to embankments. In *Analysis and design in geotechnical engineering* (pp. 1-48). ASCE.

Kealy, C., & Soderberg, R. (1969). *Design of dams for mill tailings.* Washington D.C.: U.S Department of the Interior, Bureau of Mines.

Küre Dağları Milli Parkı. (n.d.). Retrieved May 21, 2012, from http://www.kdmp.gov.tr/alt_detay.asp?id=5

Ladd, C. (1991). Stability evaluation during staged construction. *Journal of geotechnical engineering, 117*(4), 540-615.

Li, A., Merifield, R., & Lyamin, A. (2009). Limit analysis solutions for three dimensional undrained slopes. *Computers and Geotechnics, 36*(8), 1330-1351.

Liang, R. Y., Nusier, O. K., & Malkawi, A. H. (1999). A reliability based approach for evaluating the slope stability of embankment dams. *Engineering Geology, 54*(3-4), 271-285.

Lighthall, P., Watts, B., & Rice, S. (1989, May 26). Deposition Methods for Construction of Hydraulic Fill Tailings Dams. *Geotechnical Aspects of Tailings Disposal and Acid Mine Drainage*.

Mendoza, F. J., & Izquerdo, A. G. (2009). Environmental risk index: Atool to assess the safety of dams for leachate. *Journal of Hazardous Materials*(162), 1-9.

Military Soils Engineering. (1997). *FM 5-410.* Washington, DC: Headquarters, Department of the Army.

Mittal, H. K., & Morgenstern, N. (1975). Parameters for the design of tailings dams. *Canadian Geotechnical Journal, 12*, 235-261.

Mowafy, Y. M. (1986). Analysis of Grid Reinforced Earth Structures. *Ph.D. thesis, Department of Civil Engineering*. Ottawa, Canada: Carleton University.

Nakao, T., & Fityus, S. (2008). Direct Shear Testing of a Marginal Material Using a Large Shear Box. *Geotechnical Testing Journal, 31*(5).

Narita, K. (2000). *Design and Construction of Embankment Dams.* Dept. of Civil Eng., Aichi Institute of Technology.

Olalla, C., & Cuellar, V. (2001). Failure mechanism of the Aznalcóllar dam. *Géotechnique, 51*(5), 399-406.

Oyanguren, P. R., Nicieza, C. G., Fernández, M. Á., & Palacio, C. G. (2008). Stability analysis of Llerin Rockfill Dam: An in situ direct shear test. *Engineering Geology, 100*(3-4), 120-130.

Priscu, C. (1999). Behaviour of mine tailings dams under high tailings deposition rates. *Doctoral Thesis*. Montreal, Canada: Department of Mining and Metallurgical Engineering, McGill University.

Psarropoulos, P. N., & Tsompanakis, Y. (2008). Stability of tailings dams under static and seismic loading. *Canadian Geotechnical Journal, 45*, 663–675.

Rico, M., Benito, G., & Díez-Herrero, A. (2008). Floods from tailings dam failures. *Journal of Hazardous Materials, 154*(1-3), 79-87.

Rico, M., Benito, G., Salgueiro, A., Diez-Herrero, A., & Pereira, H. (2008). Reported tailings dam failures A review of the European incidents in the worldwide context. *Journal of Hazardous Materials*, 846–852.

Rocscience Inc. (2001-2004). Application of the Finite Element Method to Slope Stability. Toronto, Ontario, Canada.
Rocscience Inc. (2004). A New Era in Slope Stability Analysis: Shear Strength Reduction Finite Element Technique. *RocNews*.
Rocscience Inc. (2005). Phase2 Version 6.0. *Finite Element Analysis for Excavations and Slopes*. Toronto, Ontario, Canada: www.rocscience.com.
Rocscience Inc. (2005). Phase2 Version 6.0 Tutorial Manual. *Importing Slide Files / SSR Analysis*. Toronto, Ontario, Canada: Rocscience Inc.
Rolston, J. W., & Lade, P. V. (2009). Evaluation of Practical Procedure for Compaction Density and Unit Weight of Rockfill Material. *Geotechnical Testing Journal, Volume. 32*(No.5), 1-8.
Saad, B., & Mitri, H. (2011). Hydromechanical Analysis of Upstream Tailings Disposal Facilities. *Journal Of Geotechnıcal And Geoenvıronmental Engıneerıng, 137*, 27-42.
Sarsby, R. (2000). *Environmental Geotechnics.* London: Thomas Telford Publishing.
Shamsai, A., Pak, A., Mohyeddin Bateni, S., & Amir Hossein Ayatollahi, S. (2007). Geotechnical Characteristics of Copper Mine Tailings:A Case Study. *Geotech. Geol. Eng., 25*, 591–602.
Sherman, W. C. (1977, April). Soil Foundations-Design Concepts. *Unpublished paper presented at Station, Unpublished paper presented at Construction of Earth and Rockfill Dams Training Course at Waterways Experiment Station*. Vicksburg, Missisipi.
Shulz, L. (1979). Recommendation for estimation of the spigotted tailings dams physical characteristics. Mechanobr, Leningard.
Singh, B., & Varshney, R. (1995). *Engineering for Embankment Dams.* Rotterdam: A.A Balkema.
Sowers, G. F. (1979). *Introductory soil mechanics and foundations.* Macmillan.
Steiner, C. (. (2006, April). *The Alternative Energy EMagazine*. Retrieved April 21, 2012, from http://www.altenergymag.com/emagazine.php?issue_number=06.04.01&article=gold
Swan, C., & Seo, Y. (1999). Limit State Analysis of Earthen Slopes Using Dual Continuum/FEM Approaches. *Int. J. Numer. Anal. Meth. Geomechanics, 23*, 1359-1371.
The Soil Liquefaction web site. (2000, January). *University of Washington*. Retrieved May 15, 2012, from The Soil Liquefaction Web site: http://www.ce.washington.edu/~liquefaction/html/what/what1.html
Thiel, R. (2012). *Thiel Engineering.* Retrieved 04 12, 2012, from Peak vs Residual Shear Strength for Landfill Bottom Liner Stability Analyses: http://www.rthiel.com/
Turkey's State Institute for Statistics. (n.d.). *Turkey's State Institute for Statistics*. Retrieved from Turkey's State Institute for Statistics.
U.S. Army Corps. of Engineers. (2003). *Engineering and Design, Slope Stability* (Vol. Engineer Manual). Washington, DC: Department of Army Corps. of Engineers.
U.S. Environmental Protection Agency. (1994). *Design and Evaluation of Tailings Dams.* Special Waste Branch. Washington, DC: U.S. Environmental Protection Agency Office of Solid Waste.

Vardar, M., Avcı, İ., Karagüzel, R., & Esin, N. (2010). *ETİ BAKIR A.Ş. Küre Bakır İşletmesi Atık Barajı Geliştirilebilirlik ve çevresel Risk Değerlendirmesi Sonuç Raporu.* İstanbul: İTÜ Maden Fakültesi Uygulamalı Jeoloji Mühendislik Jeolojisi ve Kaya Mekaniği Çalışma Grubu.

Vick, S. G. (1983). *Planning, Design and Analysis of Tailings Dams.* New York: Wiley.

Vick, S. G. (1990). Planning, Design and Analysis of Tailings Dams. *BiTech Publishers Ltd.*

Volpe, R. (1975). Geotechnical engineering aspects of coppertailings dams. *ASCE, Pre-print 2696*, 1-30.

Volpe, R. (1979). Physical and engineering properties of copper tailings. *Current geotechnical practice in mine wastedisposal, ASCE*, 242-260.

Wahler, W. (1974). *Evaluation of mill tailings disposal practices and potential dam stability problems in Southwestern United States.* Washington, D.C.: U.S Department of the Interior, Bureau of Mines.

Walker, W. L. (1984, December). Earth Dams: Geotechnical Considerations in Design and Construction. Oklahoma, United States of America.

Weishui, F., & Yangyang, Z. (n.d.). Analysis on the Stability of Tailing Dam Under Earthquake. China: Faculty of Architecture Engineering, Kunming University of science and Technology.

Wheeler, S., Näätänen, A., Karstunen, M., & Lojander, M. (2003). An anisotropic elastoplastic model for soft clays. *Canadian Geotechnical Journal, 40*(2), 403-418.

Witt, K. J., Schönhardt, M., Saarela, J., & Frilander, R. (2004). *Sustainable Improvement in Safety of Tailings Facilities.* TAILSAFE.

Wolff, T. F. (1985, May). Analysis and Design of Embankment Dam Slopes: A Probabilistic Approach. *PhD Thesis*, 17. Purdue University.

Wood, D. (1990). *Soil behaviour and critical state soil mechanics.* Cambridge University.

www.tailings.info. (2012). Retrieved May 10, 2012, from Tailings info web site: http://www.tailings.info/accidents.htm

www.wise-uranium.org. (2008). *WISE Uranium Project*. Retrieved 12 5, 2012, from http://www.wise-uranium.org

Youd, T. L., Harp, E. L., Keefer, D. K., & and Wilson, R. C. (1984). Liquefaction Generated by the 1983 Borah Peak, Idaho Earthquake. *Proceedings of Workshop XXVIII On the Borah Peak, Idaho Earthquake. Volume A*, pp. 625-634. U.S. Geological Survey, Menlo Park, CA.

Zandarín, M. T., Oldecop, L. A., Rodríguez, R., & Zabala, F. (2009). The role of capillary water in the stability of tailing dams. *Engineering Geology,, 105*(1-2), 108-118.

Zardari, M. A. (2011). Stability of Tailings Dams, Focus on Numerical Modelling. Luleå, Sweden: Luleå University of Technology, Division of Mining and Geotechnical Engineering.

APPENDIX A

MATERIAL PROPERTIES IN THE LITERATURE

Table A.1 Typical Elastic Moduli of soils based on soil type (modified from U.S. Army Corps of Engineers, 1990)

Soil	E_s (kPa)
very soft clay	478.8-4788
soft clay	4788-19152
medium clay	19152-47880
stiff clay, silty clay	47880-95760
sandy clay	23940-191520
clay shale	95760-191520
loose sand	9576-23940
dense sand	23940-95760
dense sand and gravel	95760-191520
silty sand	23940-191520

Table A.2 Typical modulus of elasticity values for soils (http://www.stanford.edu/)

Soil	Young's modulus E_s
Clay soil (soft to stiff)	10-200 MPa
Sandy soil (loose to compact)	10-50 MPa
Gravel soil (loose to compact)	70-170 MPa
Soft clay	1-3 MPa
Hard clay	6-14 MPa
Loose sand	10-28 MPa
Dense sand	35-69 MPa

Table A.3 Typical Poisson's ratio values for soils (http://www.stanford.edu/)

Soil	Poisson's Ratio, υ
Sandy Soil	0.25-0.4
Gravel soil	0.15-0.35
Granite	0.1-0.3
Sandstone	0.21-0.38
Shale	0.2-0.4

Table A.4 Poisson's ratio range and typical values for soils (Pavement Manual, 2007)

Soil	Range for Poisson's Ratio, υ	Typical Value
Loose sand or silty sand	0.20-0.40	0.30
Dense sand	0.30-0.45	0.35
Fine-grained soils	0.30-0.50	0.40
Saturated soft clays	0.40 – 0.50	0.45

Table A.5 Typical values of Poisson's ratio (GeotechniCAL)

Soil	Poisson's Ratio, υ
Undrained saturated clays/silts	0.50
Stiff sandy or silty clays	0.2 - 0.4
Medium to loose sands	0.40
Dense sands	0.2 - 0.45